SCUOLA NORMALE SUPERIORE DI PISA

Ph. D. Thesis

Molecular Biology

High-throughput RNA interference screening identifies human genes regulating AAV transduction

Rudy Ippodrino

Advisor:

Prof. Mauro Giacca

2015

Index

Abbreviations

% percent

+/+ wildtype

-/- knockout

°C degree Celsius

AADC aromatic l-amino acid decarboxylase

AAV adeno-associated virus

Ad Adenovirus

A adenine

Ago Argonaute

Ala alanine

APS ammonium persulphate

Arg arginine

bp base pairs

BSA bovine serum albumin

C cytosine

cDNA complementary DNA

CDS coding sequence

Chr chromosome

DAPI 4′,6-diamidino-2′-phenylindol-dihydrochloride

DDR DNA damage response

DNA deoxyribonucleic acid

dNTP deoxynucleotide triphosphate

dpc days post coitum

ds double-stranded

DSBs double strand breaks

DTT dithiothreitol

E. coli Escherichia coli

eGFP enhanced green fluorescent protein

Eri1 enhanced RNAi1

ETS external transcribed spacer

FACS fluorescence-activated cell sorting

FCM flow cytometry

FCS fetal calf serum

FDR false discovery rate

g gramm

G guanine

gDNA genomic DNA

h hour

HET heterozygous

HRP horse radish peroxidase

HU hydroxyurea

Ig immunoglobulin

IRES internal ribosome entry site

ITS internal transcribed spacer

kb kilo base pairs

kDa kilo Dalton

KO knockout

LB media Luria-Bertani media

Lys lysine

M molar

MEF mouse embryonic fibroblasts

min minute

miR microRNA

miRNA microRNA

mM millimolar

moi multiplicity of infection

mRNA messenger RNA

ms millisecond

ncRNA non-coding RNA

nt nucleotide

PAGE polyacrylamide gel electrophoresis

PBS phosphate buffered saline

PCR polymerase chain reaction

pH potentia hydrogenii

PMSF phenylmethylsulfonyl fluoride

pre- precursor

pri- primary

PVDF polyvinylidene fluoride

rAAV recombinant AAV

rDNA ribosomal DNA

RIP RNA immunoprecipitation

RISC RNA-induced silencing complex

RNA ribonucleic acid

RNAi RNA interference

RNA-Pol RNA polymerase

RNase ribonuclease

rpm rounds per minute

rRNA ribosomal RNA

RT room temperature

RT-PCR reverse transcription-PCR

scAAV self complemetary AAV

s second

S Svedberg units

SDS sodium dodecyl sulfate

shRNA small hairpin RNA

siRNA small interfering RNA

SLBP stem-loop binding protein

snoRNA small nucleolar RNA

snRNA small nuclear RNA

tRNA transfer RNA

U uracil

UTR untranslated region

v/v volume per volume

wtAAV wild-type AAV

WT wild-type

w/v weight per volume

Synopsis

In vivo gene replacement for the treatment of inherited pathologies is one of the most compelling concepts in modern medicine and recombinant adeno-associated virus vectors (rAAV) offer nowadays a real promise for gene therapy of several diseases. Recombinant adeno-associated virus vectors definitely possess a large number of properties that render them suitable for clinical gene therapy, including being based upon a virus that is not related to any human known pathology and shows natural propensity to persist in human post mitotic cells in an episomic form. Given the molecular simplicity of AAV vector particles, all the determinants of permissivity to vector transduction appear to reside among the molecular features of the host cell. For this reason, the identification of the cellular proteins that regulate vector transduction is an essential requisite to improve *in vivo* transduction, expand the number of permissive tissues and achieve AAV-mediated gene correction at a clinically applicable level.

The aim of this PhD thesis was to study and understand the cellular mechanisms that regulate Adeno-associated virus transduction. This work was performed exploiting high throughput screening technologies. Taking advantage of genome-wide siRNA libraries it was possible to identify some relevant cellular factors that mediate rAAV2 transduction. Differences in AAV transduction in HeLa cells were assessed using a recombinant ssAAV2 vector expressing the firefly Luciferase reporter gene. Analysis of the results obtained from this primary screening identified 1528 genes affecting transduction by AAV vectors by more than 4-fold (184 genes by more than 8-fold). Of these genes, 993 are inhibitors of AAV transduction, whereas 535 are required for efficient transduction by AAV vectors.

The work described in this thesis is divided in two sections. The first part focuses on the characterization of the top-10 siRNAs identified in the screening that were able to increase rAAV transduction in HeLa cells from 19 up to 50 folds and therefore targeting factors inhibitory on rAAV transduction. This part of the

research highlights new mechanisms that describe the correlation between AAV infection and cellular checkpoint activation. The second part of the thesis focuses on the study of factors required for rAAV infection. In particular, we characterize the mechanism of action of Eri1, a 3′-exoribonuclease known to degrade endogenous miRNAs and histone mRNAs, on AAV transduction. We determined that Eri1 is essential for ssAAV but not scAAV transduction and that effect is specifically exerted by changing the AAV genome chromatin composition through the modulation of the cellular histone dosage.

The findings described in this thesis may foster the development of druggable siRNA molecules or pharmacological strategies specifically aimed at improving AAV transduction in vitro and vivo.

1. Introduction

The development of suitable vectors for gene therapy has been a challenging goal over the past decade; the enormous potential of this approach has attracted the attention of an increasing number of researchers. To date, several classes of viral and non-viral vectors are being exploited as tools for delivering therapeutic genetic information into cells for the treatment of a wide variety of inherited disorders in clinical and pre-clinical trials (**Figure 1.1**). One of the most promising virus vectors being studied for human gene transfer is derived from the adeno-associated virus (AAV), a single-stranded, non-pathogenic DNA virus that is ubiquitous in humans. Recombinant AAV (rAAV) vectors, indeed, represent today one of the most popular viral vector systems for gene transfer applications. The favourable characteristics of these vectors include broad tropism, simplicity of their genome devoided of any gene of viral origin, limited capacity to induce immune responses after *in vivo* administration, capacity to transduce postmitotic cells and to drive persistent, virtually life-long-lasting expression of the encoded genes. Due to these favorable characteristics, recombinant AAV (rAAV) vectors offer a valuable tool that permits *in vivo* phenotypic assessment of gene function and pre-clinical disease modeling in small and large size experimental animals. Recombinant AAVs have being developed for an ever-growing variety of therapeutic applications. Among the clinical successes obtained using rAAV there is gene therapy for the Leber's congenital amaurosis diseases, which is an inherited blinding disease caused by mutations in the RPE65 gene (Buch et al., 2008). The results of first clinical trials have been promising, showing an increase in vision and most importantly the lack of side effects in treated patients (Cideciyan et al., 2009). Currently, a clinical trial administering an AAV vector by intraocular administration for the expression of the RPE65 gene, has reached phase III (Simonelli et al., 2010). Moreover, an AAV1 vector coding for the lipoprotein lipase (LPL) for the treatment of patients with familial LPL deficiency, has been the first gene medicinal product approved for marketing in the Western world, authorized by the European

Commission in 2012 under the commercial name of Glybera (Salmon et al., 2014). Promising results using rAAV technology have been obtained also for the treatment of Duchenne muscular dystrophy (DMD) and Parkinson's disease (PD). The first clinical gene therapy trial for DMD began in March 2006 (Rodino-Klapac et al., 2007). This was a Phase I study in which an AAV vector was used to deliver micro-dystrophin to the biceps of boys with DMD. Recently, two phase I clinical trials on PD were conducted at the University of California San Francisco (UCSF) and Jichi Medical University (JMU) to evaluate the safety and potential efficacy of AAV vector–mediated gene delivery of aromatic l-amino acid decarboxylase gene (AADC) to the bilateral putamen. Alleviation of motor symptoms associated with PD was observed in both trials (Christine et al., 2009) (Muramatsu et al., 2010). CERE-110 is another therapeutic based on adeno-associated virus technology to deliver nerve growth factor gene (NGF) into the brain of patiences with Alzheimers disease (AD). The study is evaluating whether CERE-110 (AAV-NGF) is a safe and effective treatment for AD. Approximately fifty people with AD are participating in this study; data from this phase II trial will be available in 2015 (Mandel, 2010). Hemophilia B is another attractive target disease for rAAV gene therapy applications but a potential complication of a gene-based treatment is the development of neutralizing antibodies (NAb) against the therapeutic transgene. There are now three ongoing trials based on AAV-mediated gene transfer in haemophilia B all aiming to express the factor IX gene from the liver (High et al., 2014).

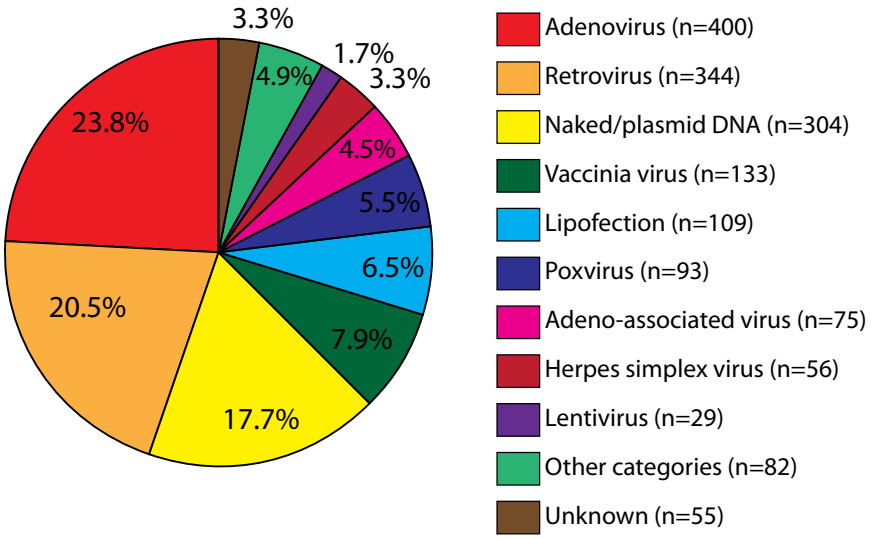

Fig 1.1 : Vectors used in Gene Therapy clinical trial. Adapted from (Sheridan, 2011).

1.1. Overview of Adeno-associated vectors

1.1.1 Wild type AAV virus

Adeno-associated viruses belongs to the family of parvoviridae that comprises viruses with a linear, single-stranded DNA genome of approximately 5 kb and a non-enveloped, icosaedrical capsid with a diameter of 18-30 nm (Siegl et al., 1985). These features make parvoviruses the smallest DNA viruses in nature. Within this group, the adeno-associated viruses are classified in the genus of the Dependovirus (Lat. dependere: to depend), because they require exogenous factors for their replication, and this distinguishes them from autonomous parvoviruses. Dependoviruses and autonomous parvoviruses infect vertebrates. Another group of parvoviruses, the densoviruses, infects insects and replicates autonomously (Galev et al., 1989). AAV-2 was the first serotype discovered in 1965 as contaminant of adenovirus preparations hence its name (Atchison et al., 1966). Previous studies indicated that the presence of adenovirus infection was required

for AAV-2 to replicate its genome and generate a productive viral infection (Casto et al., 1967). Later, studies demonstrated that other viruses such as herpesviruses, vaccinia and papillomaviruses were also able to boost AAV-2 replication, as well as several chemical, physical factors and carcinogenic compounds, genotoxic agents, UV or γ-irradiation (Johnson et al., 2011; McPherson et al., 1985) (Yakobson et al., 1989). The wild type AAV viral genome contains two open reading frames (orf) and three promoters regulate the gene expression. From the first orf, four different RNAs are generated through alternative splicing; these code for the non structural Rep proteins (**Figure 1.2**). The two major forms of Rep (Rep78 and Rep68) bind specific sites within the inverted terminal repeats (ITRs), and are required for both viral DNA replication and site-specific integration (Senapathy et al., 1984). In addition, the AAV Rep proteins participate in the regulation of gene expression. In particular, Rep induces the up-regulation of the homologous AAV promoters in the presence of adenovirus infection, while it exerts an inhibitory effect when adenovirus is absent (Trempe and Carter, 1988). Rep is also able to down regulate other heterologous promoters, including viral and proto-oncogene promoters, suggesting a pleiotropic effect exerted by this protein on gene expression (Marcello et al., 2000). The mRNAs coding for Rep78 and its splicing variant Rep 68 start at the p5 promoter and are 4.2 and 3.9 kb long respectively. The Rep52 mRNAs and its splicing variant Rep40 start at promoter p19 and are 3.6 and 3.3 kb long respectively (Marcus et al., 1981). Proteins Rep78, 68, 52 and 40 consist of 621, 537, 397 and 313 amino acids respectively (Mendelson et al., 1986). The CAP open reading frame, located at the 3' end, codes for the three structural capsid proteins VP1, VP2 and VP3 that are transcribed from the p40 promoter and expressed at a ratio of 1:1:8 respectively (Kronenberg et al., 2001). Translation efficiency is regulated by the alternative splicing of the VP1 coding intron and by the use of an unusual initiation codon (ACG) for VP2 that leads to a 10-fold reduced translation of the protein in comparison to the AUG initiation codon of VP3 (Becerra et al., 1988). AAV capsid proteins VP1, VP2 and VP3 use the same stop codon and have molecular weights of 90, 72 and 60 kDa respectively. The viral protein half life is

around 15 hours while its mRNAs are degraded within 4-6 hours (Senapathy and Carter, 1984).

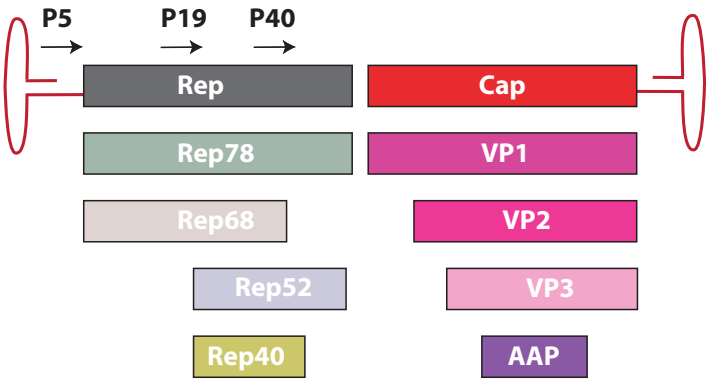

Figure 1.2 Genomic organization of the wtAAV genome. Rep transcripts are non-structural proteins – Rep40, Rep52, Rep68 and Rep78 – they are involved in gene regulation, viral DNA encapsidation and genome integration. VP1,2,3 are transcribed from the Cap gene, they are the structural proteins that compose the AAV capsid.

Some authors recently showed that AAV encodes a protein required for capsid formation by means of a nested, alternative ORF in the Cap gene. This protein, which was named assembly-activating protein (AAP), localizes in the host cell nucleolus, where AAV capsid particles assembling occurs. AAP targets newly synthesized capsid proteins to this organelle and, in addition, fulfills a function in the assembly reaction itself (Sonntag et al., 2010). It is important to underline that the mechanism of assembly of AAV particles is not known in detail. The whole coding region of AAV genome is flanked by two 145 bop ITRs (**Figure 1.3**), which show complementarity within the first 125 bp and form a T-shaped hairpin at both ends of the genome. This palindromic sequence is the only *cis*-acting element required for all the major functions of AAV (Ashktorab and Srivastava, 1989) .

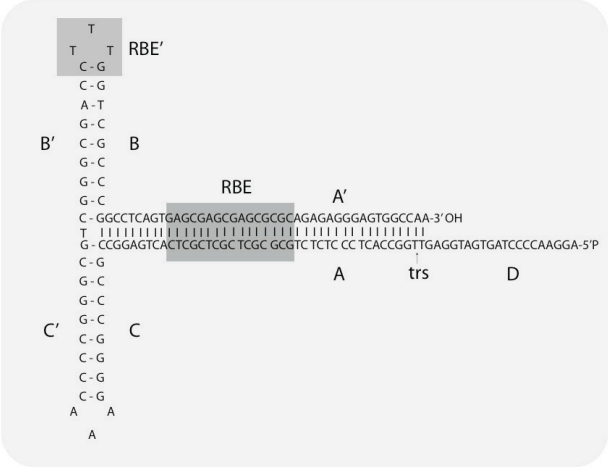

Figure 1.3 : AAV genome resides between inverted terminal repeat (ITRs), symmetric DNA sequences of 145 bases. They contain the Rep-binding element (RBE) and the terminal resolution site (trs) that are required for wtAAV genome replication process.

wtAAV life cycle depends on the presence of a helper virus superinfecting the host cells. Under non-permissive conditions (i.e. without helper virus), the AAV genome establishes a latent infection mainly integrating into a specific sequence of human chromosome 19q13.3, designated as AAVS1 (Berns and Linden, 1995). A crucial role in latency persistence is played by Rep 68/78, which is synthesized at basal levels and negatively regulates AAV gene expression and DNA synthesis. The latency state, although not altering cell viability, does affect the phenotype as well as the expression of specific cellular genes, conferring more sensitiveness to UV-light, genotoxic agents and heat, enhancing serum requirement and reducing the cellular growth rate. It is assumed that all these effects are somehow related to a low-level production of the Rep protein (Marcello et al., 2000). Under the presence of helper virus, the regulation of AAV gene expression becomes rather complex, depending upon both the foreign virus and the presence of Rep68/78 proteins. In these circumstances, it could happen that the AAV integrated genome undergoes an excision process from the host cell DNA and is packaged into infectious

particles. The mechanism underlying the integration process, depending on the specific recognition between AAV sequences and the AAVS1 region on chromosome 19, is not yet fully understood. Some evidence indicates that this region is located close to the human troponin T gene, displaying an overall GC content of 65%, a 35-mer minisatellite tandemly repeated for 10 times and a putatively transcribed ORF; the possible role of these features in the integration process still remains unclear (Dutheil et al., 2000). A pivotal role in the integration and rescue mechanisms is exerted by the viral ITRs, and, in particular, by two short sequences (Rep Binding Element, RBE and Terminal Resolution Site, TRS) in the stem of the T-shaped structure. These sequences drive the binding of Rep 68/78 and the subsequent nicking of the viral DNA, a process essential for viral DNA replication. Since the same RBS and TRS are also present within the AAVS1 sequence, a model was proposed that suggests the involvement of an oligomeric complex of Rep to juxtapose the RBS and TRS from the cellular and viral DNAs. Some studies reported that a portion of wtAAV can also integrate randomly into the genome; more specifically, experiments performed in the mouse liver demonstrated that 53% of wtAAV integrations are within genes, 27% within 1 kb of a transcription start site, and 25% within a CpG island (Ohashi et al., 2005). Analysis of integration patterns in primary human fibroblasts transduced with rAAV2, disclosed that 38% of the integrations are within the genes, and 4% within a CpG island (Inagaki et al., 2007). Studies in which rAAV2 and rAAV8 were used, revealed that, in addition to these regions, AAV vectors display a preference for integration into ribosomal DNA repeats, and near palindromes with arms being at least 20-bp long (Miller et al., 2005). The AAVS1 hotspot represents about 10% of the total events of integration; novel hotspots near consensus RBSs were identified distributed all over the human genome (Huser et al., 2014). Other hotspots are in chromosome 5p13.3 and chromosome 3p24.3 (Huser et al., 2010). **(Figure 1.4)** It should be emphasized that integration of the AAV genome is strictly dependent on the Rep gene, or at least on one of its products, the Rep68 or Rep78 proteins. Recombinant AAV vectors, devoid of Rep genes, are unable to integrate into the

host genome, neither site-specifically nor in a random manner, and their genomes persist almost exclusively in the form of single and/or concatameric circular episomes.

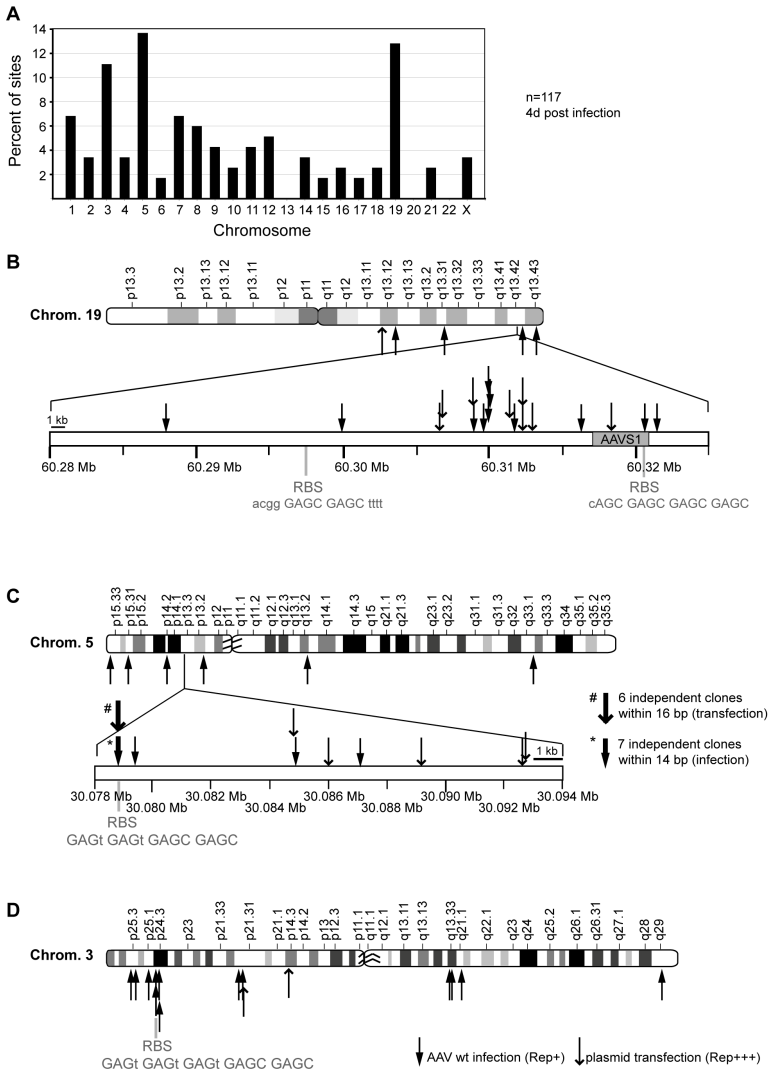

Figure 1.4 : Integration hotspots of wtAAV. AAVS2 site is on chr. 5 and AAVS3 on chr. 3. The sites display RBS similarly proficient for Rep-binding as AAVS1, the standard site that resides on chr. 19 (adapted from Huser et al., 2010).

1.1.2 Construction and production of recombinant AAV vectors

The characteristics of AAV life cycle, including its defectiveness and ability to persist in infected cells as a latent viral genome, early suggested that this virus could be an excellent tool for *in vivo* gene transfer. Since the AAV genome cloned into a plasmid is still infectious and able to produce viral particles, any exogenous gene (less than 4.5 kb in length) can theoretically be placed within the two 145 bp ITRs to obtain a circular backbone suitable for vector production (Gao et al., 1998). Unlike other delivery systems that have evolved into several generations, the original composition of the AAV vector plasmid (a transgene expression cassette flanked by the two ITRs) is essentially the same as in the current version. The traditional method for rAAV production is based on co-transfection in adherent HEK293 cells of the vector plasmid together with a second plasmid, supplementing the rep and cap gene functions, into helper-infected cells, typically Adenovirus or Herpesvirus (**Figure 1.5**) (Laughlin et al., 1983) (Samulski et al., 1982). To avoid the problem of residual presence of contaminating helper virus in purified recombinant AAV stocks, current improved protocols entail the use in the production of rAAV of a helper plasmid carrying a few adenovirus genes known to be necessary for full AAV amplification (E4, VA and E2a) but lacking the Ad structural and replication genes (Gao et al., 1998) (Grimm et al., 2003) (Grimm et al., 1998). In this way, it is now possible to obtain rAAV preparations free of contaminating helper virus and unwanted adenoviral protein at a yield even higher than that achieved by using infectious helper virus.

AAV vector particles are then harvested and purified from cell lysates by biochemical procedures and repeated density gradient (typically cesium chloride or iodixanol); a purification using ion-exchange chromatography is often used to obtain a pure rAAV preparation with the aim to increase its infectivity (Hermens et al., 1999; Zolotukhin et al., 2002). Recently, Guo and co-workers developed a simplified method using PEG/(NH(4))(2)SO(4) aqueous two phase partitioning that claims to be quick and not expensive (Guo et al., 2013).

To overcome the dependency on transient transfection, many efforts have been put in the establishment of packaging cell lines, similar to those already developed for retroviral and adenoviral vector production, but stably containing multiple copies of the rep and cap genes. Expression of these genes would be moderate in basal conditions, but could be triggered by infection with adenovirus. Nonetheless, these efforts have met very limited success so far, mainly due to the toxicity of the constitutive expression of Rep, which, even at very low levels, is very badly tolerated by proliferating cells (Holscher et al., 1994). Therefore, transient transfection still remains the method of choice to obtain AAV vector preparation for both investigation and gene therapy purposes.

An alternative procedure, which has gained significant momentum over the last few years, is based on a baculovirus expression vector system in non-adherent insect cells grown in bioreactors, with significant methodological simplification (Mietzsch et al., 2014). This system appears stable and particularly useful for scaling up and production of clinical grade vectors.

Packaging efficiency seems to depend principally on the cellular system used and on the size of the packaged genome. A "head-full" mechanism appears to be used by the packaging machinery, with upper and lower limits of 4.9 and 4.1 kb respectively for optimal packaging, even if constructs up to 5.2 kb are tolerated.

(Grimm et al., 1998). Production titers within $1x10^4$ and $1x10^5$ AAV particles per cell (as measured by quantifying the number of viral genomes) represent current, consistent and probably limiting values, still amenable to scaling up to a certain extent by increasing the number of cultured cells.

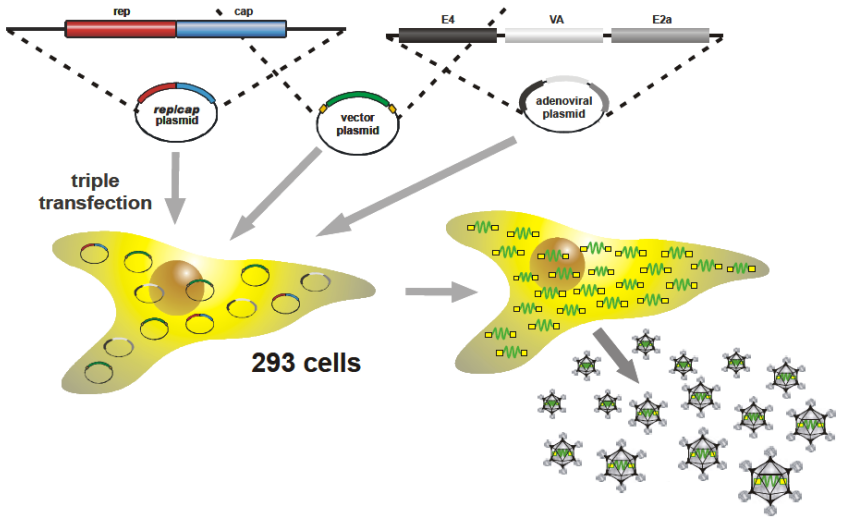

Fig 1.5. AAV production, triple transfection protocol. The is co-transfected a vector plasmid encoding the transgene cassette between the ITRs, an AAV packaging plasmid carrying the rep-cap genes and an adenovirus helper plasmid, the rAAV vectors are produced very efficiently.

1.1.3 AAV serotypes

Nowadays more than one hundred distinct primate AAV capsid sequences have been found. Each of the AAV types has unique serological profiles and has been named as a particular AAV particle (Gao et al., 2005). To date, 13 primate serotypes (AAV1–13) have been described. The AAV1 and AAV6 capsids differ by only six amino acids and, subsequent to their naming, they have been found to be serologically indistinguishable. The capsids for which the crystal structures have been determined so far are AAV2, AAV4, and AAV8 (Gao et al., 2002).

Previous work has compared AAV serotypes characterizing their transduction efficiency in tissues *in vivo* (Fig 1.6). In striated muscle, early studies achieved high transduction efficiency with AAV1, AAV6, and AAV7. More recently, AAV8 and AAV9 have been found to transduce striated muscle with efficiencies at least as high. rAAV8 and rAAV9 are considered to have the highest level of hepatocyte transduction (Ohashi et al., 2005). In the pulmonary system, rAAV6 and rAAV9 transduce much of the entire airway epithelium, while rAAV5 transduction is limited to lung alveolar cells. With respect to transduction of the central nervous

system, rAAV serotypes 1, 4, 5, 7, and 8 have been found to be efficient transducers of neurons in various regions of the brain (Zabner et al., 2000).

rAAV1 and rAAV5 have also been reported to transduce ependymal and glial cells. In the eye, rAAV serotypes 1, 4, 5, 7, 8, and 9 efficiently transduce retinal pigmented epithelium, while rAAV5, rAAV7, and rAAV8 transduce photoreceptors as well. rAAV1, rAAV8, and rAAV9 have shown the highest reported transduction in pancreas tissue, primarily in acinar cells (Inagaki et al., 2006). Kidney seems to be a less permissive organ, although proximal tubule cells have been transduced by rAAV2 at low levels, and glomeruli were targeted by rAAV9. rAAV1 has been shown to transduce adipose tissue, although with the help of a nonionic surfactant (Mizukami et al., 2006). The adult heart is one of the tissues most permissive to transduction with various AAV serotypes, including AAV1, AAV2, AAV6, AAV8 and AAV9. It is noteworthy that AAV1 expressing the SERCA2a gene, a sarco/endoplasmic reticulum Ca^{2+}-ATPase**,** was used to successfully reversed cardiac dysfunction in several large animal models. Moreover, AAV1 SERCA2a gene therapy revealed an excellent safety profile in a phase I clinical trial and the results from a phase II trail have further established the clinical efficacy of type of therapy (Bish et al., 2008) (Lyon et al., 2011).

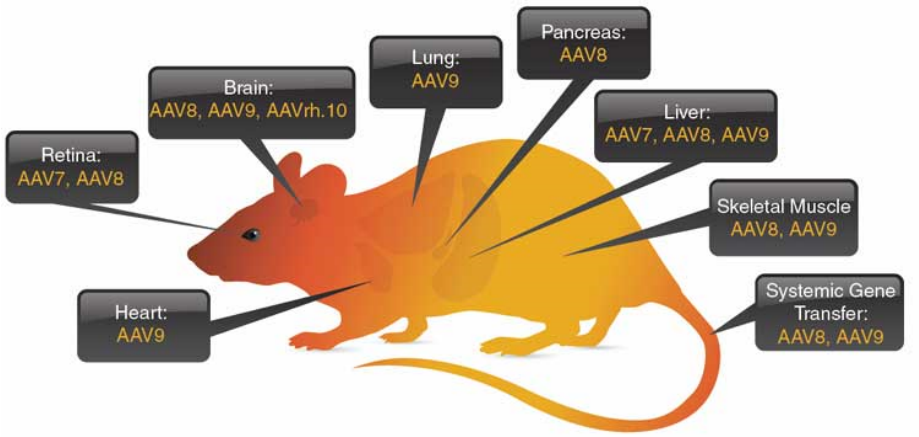

Figure 1.6. AAV serotypes allow *in vivo* targeting of different tissues and organs. AAV tropism depend on the capsid composition, these favorable characteristics make AAV a versatile vector for gene therapy approaches. (adapted from nature methods 7, 2010).

1.1.4 Self-complementary AAV

Self-complementary adeno-associated virus (scAAV) is a viral vector engineered from the naturally occurring AAV virus. scAAVs have been designed to overtake the single stranded AAV second-strand synthesis, that represent a rate-limiting step for efficient transduction (Ferrari et al., 1996). scAAV vector genomes are capable to self-hybridize by folding back upon release from the capsid into the infected cells, producing an immediate double-stranded (ds) AAV genome (**Figure 1.7**).

This class of vectors has also been reported to result in higher level transduction and more rapid onset of transgene expression in several tissue types, including liver, retina, brain and muscle (Petersen-Jones et al., 2009) (Fu et al., 2003) (McCarty et al., 2001). The scAAV vector genomes are created by removing the TRS site (terminal resolution site) from one of the ITRs. When the vector DNA is replicated by the rolling hairpin method, the replication machinery binds at a site present in the wt ITR and continues towards the mutated ITR. In the absence of a TRS or a break in DNA, second strand synthesis continues throughout the mutated ITR and back again along the genome using the opposite strand as template. The synthesis continues to the end of the wt ITR, which is then resolved at the TRS, resulting in a dimeric genome with a mutated ITR in the middle (McCarty et al., 2003). The scAAV DNA inside the AAV capsid is compacted in a single-stranded forms (McCarty et al., 2003). After the viral uncoating, the single-stranded genome is released into the nucleus, and the palindromic wild-type ITRs pair up forming a double-stranded genome that is immediately ready for transcription.

Due to its characteristics, the packaging capacity of the scAAV vector is limited to approximately 2.1 kb. There are some evidences that indicate that the fate of scAAV genome differs from that of ssAAV. The genome conversion step involves DNA damage related proteins that collocate scAAV in different DDR related pathway, some authors showed that ATR (ataxia telangiectasia and Rad3-related protein) blocks the conversion of ssAAV to dsDNA but it does not affect scAAV

genomes (Cataldi and McCarty, 2010). Despite the fact that the scAAV genome processing is not fully clear and needs further investigation, the potential of scAAV vectors at clinical level has been shown in several studies (Wu et al., 2008).

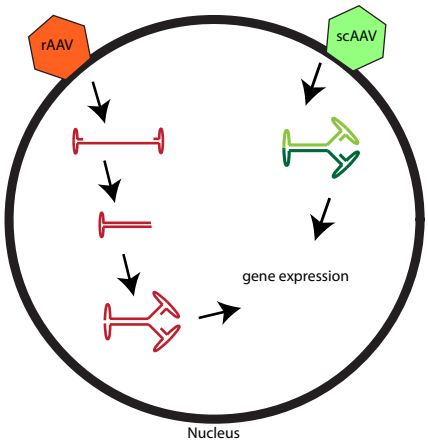

Fig 1.7 Scheme of ssAAV and scAAV genome processing step. rAAV need the DNA second strand synthesis step. scAAV genome is capable to do self-annealing becoming immediately double stranded and ready to transcribe.

1.2 Infection Biology of rAAV vectors

The adeno-associated virus infects the host cell through a mechanism that involves these principal steps, represented in **Figure 1.8** :

1. - Binding of the virion to the cellular membrane
2. - Internalization of the virion through clathrin coated pits endocytosis
3. - Escaping from late endosome
4. - Passage through the nuclear pore complex
5. - Uncoating from capsid inside the nucleus
6. - Genome processing
7. - Gene expression

The first step of the infection process is mediated by two different classes of cellular receptors. A primary receptor is responsible for the recognition of the target cell and the binding of the virus to the cell membrane. In addition, binding to a secondary receptor triggers a cascade of events that cause endocytosis and internalization of the AAV particles. Heparan sulfate proteoglycan (HSPG) has been identified as the primary receptor for AAV2 (Summerford and Samulski, 1998). This molecule is present in a wide range of human cell types, explaining the broad tissue range of AAV serotype 2. The $\alpha_v\beta_5$ integrin, human Fibroblast Growth Factor Receptor (hFGFR1) have been described as secondary receptors for AAV2 (Mizukami et al., 1996). While integrin is involved in endocytosis, hFGFR1 seems to enhance the attachment process. However, the contribution of these co-receptors to AAV2 infection is not completely understood yet (Summerford et al., 1999). A summary of AAV receptor and co-receptor described for the different serotypes is reported in **Table1**.

Virus	***Glycan receptor***	***Co-receptor/other***
AAV1	N-linked sialic acid	Unknown
AAV2	HSPG	FGFR1, HGFR, LamR, CD9 tetraspanin
AAV3	HSPG	FGFR1, HGFR, LamR
AAV4	O-linked sialic acid	Unknown
AAV5	N-linked sialic acid	PDGFR
AAV6	N-linked sialic acid, HSPG	EGFR
AAV7	Unknown	Unknown
AAV8	Unknown	LamR
AAV9	N-linked galactose	LamR
BAAV	Ganglioside GM1	Unknown

Table 1. AAV receptors and preferential tissue tropism. Abbreviations: AAV, adeno-associated virus; EGFR, epidermal growth factor receptor; FGFR1, fibroblast growth factor receptor 1; HGFR, hepatocyte growth factor receptor; HSPG, heparan sulfate proteoglycan; PDGFR, platelet-derived growth factor receptor. Adapted from (Nonnenmacher and Weber, 2012)

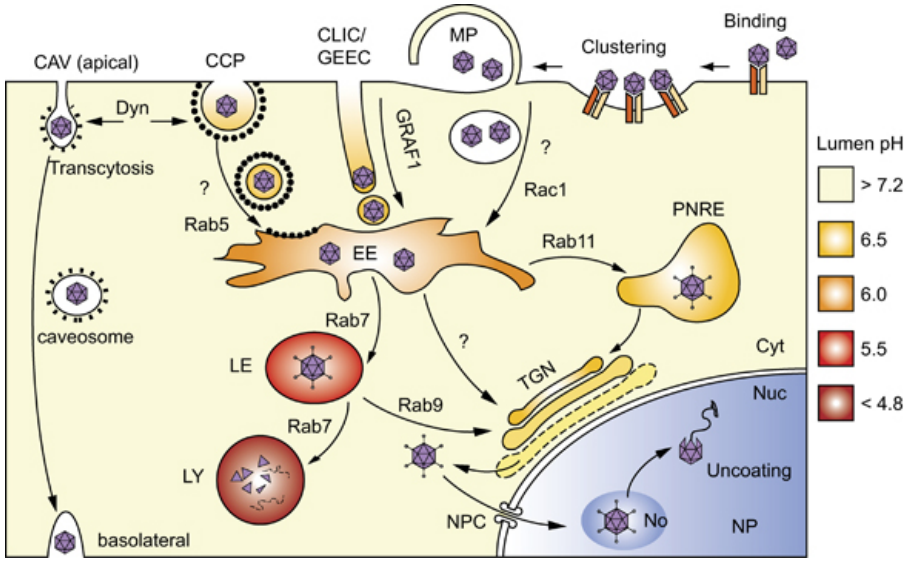

Figure 1.8. AAV entry steps into HeLa cells. Following attachment to HSPG, AAV is rapidly internalized via clathrin-coated pits through a process involving $\alpha_v\beta_5$ integrin. Once inside the cell, an acidic environment allows the penetration of the virus into the cytoplasm. Following endosome release, AAV accumulates perinuclearly and slowly penetrates through the NPC into the nucleus where viral uncoating occurs. (Adapted from T Weber, 2012)

After binding to the cell membrane, AAV virons are internalized through clathrin-coated pits mediated endocytosysis that seems to be the predominant, although not the exclusive mechanism followed by the virus to traffic to the nucleus.

Interestingly, there is a conserved region inside the AAV VP1 capsid protein, found also in other parvoviruses, which contains a phospholipase A2 (PLA2) motif (HDXXY). Little is known about the functional properties of this moiety, but some authors suggest that the phospholipase A2 activity of VP1 may be required for viral escape from endosomes (Girod et al., 2002). Relatively fewer data describe the trafficking of the virus to the nucleus and where and how viral uncoating occurs. Several studies have observed a perinuclear accumulation and subsequent slow nuclear entry of fluorescent labeled viral particles (Bartlett et al., 2000). Using a single molecule imaging technique, Seisenberger and colleagues described a very quick transfer of viral particles to the nuclear area and a very rapid and efficient

AAV nuclear entry compared to what was previously reported in the literature (Seisenberger et al., 2001). Some experiments showed that AAV transport across the nuclear membrane does not seem to depend on active transport through nuclear pore complexes (NPC) (Xiao et al., 2002). Recent data, however, demonstrate that AAV enters into the nucleus through an active importin-β related mechanism (Nicolson and Samulski, 2014). Interestingly, all cellular determinants required for viral uncoating and second-strand synthesis are contained within the nucleus (Hansen et al., 2001). Some experiments reported that nuclear injection of antibody against intact capsids dramatically reduces transduction demonstrating that viral uncoating may be a rate-limiting step of transduction, dependent in part on AAV serotype (Sonntag et al., 2006). After uncoating, AAV genomes have to become double-stranded in order to be transcribed. The mechanism by which the single-stranded rAAV genome becomes double-stranded is not fully understood. It was generally assumed that host-cell polymerases would be involved in second-strand synthesis, due to the fact that, in vitro, cells in S-phase are transduced at a rate 200 times higher than non-dividing cells. However, agents that damage DNA (such as ultraviolet or γ-radiation) or agents that inhibit DNA synthesis (such as hydroxyurea or topoisomerase inhibitors) were also reported to increase rAAV2 transduction in vitro (Russell et al., 1995), suggesting that DNA repair mechanisms may be involved in transduction (Jurvansuu et al., 2005). Previous studies described AAV genome second-strand synthesis as a rate-limiting step for the viral transduction (Ferrari et al., 1996). Experiments performed in vitro and *in vivo* put in evidence the requirement of host cell-mediated second strand synthesis for AAV genome processing, demonstrating that a mutant rAAV2 vector genome of single-polarity (obtained by mutating the AAV ITR D segment) was proficient for transduction with the same efficiency as a standard rAAV2 vector, composed of equal amount of packaged genomes of either polarity (Zhou et al., 2008). However, this does not exclude the existence of other mechanisms for ssAAV processing. Indeed, there is experimental evidence describing that self-annealing of complementary AAV (+) and (-) single

stranded genomes also contributes to the generation of double-stranded AAV genomes (Nakai et al., 2000).

1.2.1 Factors that increase AAV transduction

Experimental evidence from different laboratories has demonstrated both in vitro and *in vivo* the existence of several barriers that may affect AAV transduction, including virus internalization, trafficking to the nucleus and genome conversion. Early studies have shown that several classes of chemical and physical agents are able to enhance AAV transduction (Yalkinoglu et al., 1988). There is experimental evidence, for example, that different classes of proteasome inhibitors increase transduction by multiple AAV serotypes, both in vitro and *in vivo*, enhancing the rate of viral translocation to the nucleus (Yan et al., 2002). It is likely that the viral capsid undergoes a ubiquitination process, since the inhibition of ubiquitin ligase E3 is able to induce an enhancement of rAAV2 transduction (Yan et al., 2002). Although the mechanisms by which these drugs increase transduction have not been fully elucidated, these findings suggest that proteasome-mediated degradation may represent a significant limitation of AAV-mediated transduction (Yan et al., 2004). Work from different laboratories has demonstrated that genotoxic agents that lead to a DNA damage response (DDR) in the host cell, such as hydroxyurea (HU), doxorubicin (DOXO), and camptothecin (CAMPTO), are also capable to increase AAV transduction (Russell et al., 1995). Previous findings from our laboratory showed that DNA repair proteins belonging to the MRN complex, Rad50, NBS1, MRE11, are able to inhibit AAV infection (Cervelli et al., 2008); furthermore, a collaborative work with the M. Weitzman group demonstrated that the adenovirus protein E4-orf6 helps AAV transduction triggering the degradation of MRE11, a crucial protein of the MRN complex (Schwartz et al., 2007). One hypothesis is that the DDR proteins block incoming single stranded AAV genomes and that an induced massive DDR diverts the inhibitory proteins away from viral

DNA to other damaged host genome sites (Cervelli et al., 2008). Samulski and co-workers proposed an additional model to explain HU enhancing effect, showing that cell treatment with this drug increases the mobilization into the nucleoplasm of AAV virons initially accumulated into nucleoli; the release of viral particles may accelerate the un-coating process. Interestingly, some HDAC inhibitors were also able to increase AAV transduction. It was demonstrated that the acetylated histones associated with the AAV genome could play a role in AAV transgene expression, while other experiments demonstrated that rAAV promoter methylation state does not influence viral transduction (Okada et al., 2006) (Leger et al., 2011).

1.3 Chromatin

1.3.1 Histone octamer

Histones are the primary proteins associated with the DNA in eukaryotes. The key unit of chromatin is represented by the nucleosome, which is composed of a histone octamer wrapped around with a 147 bp DNA in 1.65 left-handed super-helical turns (Luger et al., 1997). Core histones are four proteins called H2A, H2B, H3 and H4 that compose the histone octamer. The histones H1 and H5 are known as the linker histones, which bind the nucleosome at the entry and exit sites of the DNA, thus locking the DNA into place and allowing the formation of higher order structure (Allan et al., 1981). The sequence similarity is low between the core histones, but each of the four proteins has a conserved structure consisting of three α-helix called the histone fold motif (Arents et al., 1991).

The role of histones in packaging the chromosomal DNA was described the first time in 1974 (Kornberg, 1974); these proteins are responsible for the 40,000 times

compaction of a DNA molecule, necessary to fit the large eukaryotic genomes inside the cell nuclei. The histone octamer interacts with the DNA minor groove and this interaction is prevalent with A:T enriched regions than G:C enriched regions (Shrader and Crothers, 1990).

During that last decade, different laboratories have contributed to the characterization of many post-translational modifications of histone proteins, such as methylation, acetylation, phosphorylation, ubiquitination, SUMOylation, citrullination, ADP-ribosylation; these modifications seem to play key roles in the modulation of chromatin folding and regulation of the accessibility of the DNA to factors involved in transcription, replication, recombination and repair (Ito, 2007). The discovery of the histone post-translational modifications has supported the so-called "histone code" hypothesis that the genetic information could be partially regulated by the chemical variations of histones (Jenuwein and Allis, 2001).

Despite their resistance to DNA dissociation due to their positive electrical charge, nucleosomes are not static factors but can shift along DNA. Access to nucleosomal DNA is governed by two major classes of protein complexes: the covalent histone-modifying enzymes and the ATP-dependent chromatin remodelling factors. Chromatin remodelling is defined as the enzyme-assisted process to facilitate access to nucleosomal DNA by remodelling the chromatin structure, it has a role in crucial biological processes, like apoptosis, chromosome segregation, transcription, DNA replication and repair (Teif and Rippe, 2009).

1.3.2 Histone deposition

Nucleosome assembly following DNA replication, DNA repair and gene transcription is critical for the maintenance of genome stability and epigenetic information. All four core histones (H2A, H2B, H3, H4) contain about one forth of

positive charged residues such as lysine and arginine, and this characteristic endows these proteins with great DNA affinity and binding capacity. For these reasons, the process that couples histones to DNA is tightly regulated by the cell in order to avoid their potential toxicity due to their strong affinity to negatively charged nucleic acids. Work performed in vitro showed that the first event in the nucleosome assembly on replicating DNA is the deposition of an H3–H4 tetramer, which is rapidly followed by deposition of two H2A–H2B dimers (Smith and Stillman, 1991). Histone chaperones are key proteins that act at multiple steps of nucleosome formation. H3 histone is deposited onto DNA by the histone chaperone CAF-1. CAF-1 is the major factor that orchestrates replication-coupled nucleosome assembly and is composed of p150, p60, and p48 subunits (Marheineke and Krude, 1998). The histone H3 variant H3.3, differing from canonical H3 by four or five amino acids, is deposited, together H4 histone, by the HIRA histone chaperones in replication-independent manner (Tagami et al., 2004).
There is some evidence that indicates that chromatin restoration after DNA damage cannot rely simply on histone recycling and that new histone incorporation at repair sites should be present. Polo and co-workers showed, for example, the occurrence of a CAF-1 mediated new histone deposition upon UV irradiation in human cells (Polo et al., 2006).

1.3.3 Histone gene expression and mRNA metabolism

The organization of histone genes into clusters is evolutionary conserved from yeast to humans. Histone gene clusters in mammals are heterogeneously organized and contain one or more copies of the five histone subtypes. The 74 known human histone genes can be found within the major and minor clusters located on chromosomes 6p21 and 1q21, respectively (Schaffner et al., 1978). In the mouse, there are 65 distinct canonical histone mRNAs, which code for the five types of canonical histone proteins (Marzluff et al., 2002). These histone mRNAs are

the only known metazoan mRNAs that are not polyadenylated but contain a unique 3′ end stem-loop structure. Transcriptional activation of histone subtypes is co-ordinately regulated and tightly coupled with the onset of DNA replication during the S-phase, when histone gene transcription is induced approximately 5-fold (DeLisle et al., 1983). It was reported that the E-Cdk2 substrate NPAT plays an essential role in the transcriptional activation of histone genes at the G1/S-phase transition (DeRan et al., 2008). In the same way, after S-phase completion, histone mRNAs encoded by replication-dependent histone genes must be rapidly degraded. Conversely, the transcripts of the replication-independent histone variants are polyadenylated and their synthesis persists also outside S-phase.

The genes encoding metazoan canonical histones lack introns, and thus one endonucleolytic cleavage reaction is the only processing event necessary to form mature histone mRNA. Cleavage requires binding of the stem-loop binding protein (SLBP) and is carried out by a multi-component machinery containing U7 snRNP (Mowry and Steitz, 1987). SLBP remains bound to the histone mRNA as it relocates to the cytoplasm, where histone mRNA is circularized through a complex of proteins including at least SLBP, SLBP-interacting protein 1 (SLIP1) and eukaryotic translation initiation factor 4-γ (EIF4G). Subsequently, translation of histone mRNA takes place. At the end of S-phase, a short U-tail is added to histone mRNA in the cytoplasm. The LSM1–7 ring complex binds the oligo(U) histone structure to cooperate with a conserved complex of 3′ to 5′ exonucleases that degrade the histone mRNA. The 3'-5' exoribonuclease 1 or Eri1 has been characterized for its ability to bind the 3'-end of histone mRNAs and to degrade them, after replication (Herrero and Moreno, 2011) (Hoefig et al., 2013). In addition, the cyclin A/cyclin-dependent kinase 1 complex (CycA/CDK1) phosphorylates SLBP to trigger its degradation; this event avoids the accumulation of histone mRNAs and, eventually, histone proteins (Marzluff et al., 2008).

1.3.4 Chromatin remodeling in DNA double strand break repair

The role of chromatin in the responses to DNA double strand breaks represent today one of the most intriguing fields of basic research investigation. An efficient DNA double strand breaks repair system requires a complex organization of chromatin, since the nucleosome structure represents a huge obstacle to the efficient detection and repair of DNA lesions.

A DNA double strand break can be repaired through two main mechanisms: non-homologous end-joining (NHEJ), which is error-prone, and homologous recombination (HR) (Lukas and Bartek, 2009) (Huertas, 2010).

NHEJ requires the Ku70/80 DNA-binding complex and the DNA-PK catalytic subunit (DNA-PKcs), which allows the non-homologous and quick junction of the DNA ends. This system is the predominant double-stranded DNA break repair pathway in mammalian cells. Some authors showed that the NHEJ pathway in yeast is favoured by H3K36 methylation; this histone modification reduces chromatin accessibility, decreasing the DNA end-resection process that belongs to the HR pathway (Pai et al., 2014). Homologous recombination is more complex and requires the processing of single-stranded DNA (ssDNA) intermediates, which is used to search for the homology within adjacent sister chromatids. The production of ssDNA requires the initial nuclease activity of the MRN complex (Sartori et al., 2007) followed by further DNA end-processing by additional nucleases to produce ssDNA intermediates (Symington and Gautier, 2011).

The MRN complex, consisting of the MRE11, RAD50, and NBS1 proteins, is the first sensor of double strand breaks (DSBs)., which functions to recruit and activate the ATM/ATR complex (Paull and Lee, 2005). Activated ATM/ATR then phosphorylates, through a cascade, several target proteins, including factors involved in checkpoint activation (p53 and chk1/chk2) and DNA-repair proteins such as BRCA1 and 53BP1 (Chen and Poon, 2008). A critical target for ATM is phosphorylation of the C terminus of the histone variant H2AX, one of the most common histone modification signature characterizing the DDR.

In 1998, the group of Rogakou described for the first time the involvement of the histone variant H2AX and its phosphorylation at the serine139 residue in the DDR process (Rogakou et al., 1998). Subsequently, phosphorylation of H2AX by ATM spreads away from the DSB, creating γ-H2AX domains that extend for hundreds of kilobases along the chromatin from the DSB (Rogakou et al., 1999).

Histone acetylation is another common histone modification related with both transcription and DNA damage. Histone acetylation neutralizes positively charged lysine residues, thus altering histone-histone interactions to promote chromatin decondensation favouring the access to nucleosomal DNA (Kouzarides, 2000). Acetylation at the H3 and H4 tails, such as ac-H3K56, plays a critical role in DNA metabolism involving DNA replication, genomic stability and in the binding of the chromatin assembly factor (CAF1)-PCNA complex (Chen and Tyler, 2008). Literature reports that acetylated H3 and H4, induced by CBP and p300, cooperate with the SW1/SNF complex to facilitate recruitment of NHEJ proteins such as Ku70/80 (Ogiwara et al., 2011). During HR, a number of acetylation events occur on histones H3 and H4 involving a large number of factors such as GCN5, NuA4 and HAT1 (Murr et al., 2006).

Histone methylation on lysine and arginine was discovered more than fifty years ago (Murray, 1964). Histone methylation is often related with transcriptionally repressed chromatin but an histone methylation code associated with DNA damage was also described. During DDR, methylation occurs at multiple sites on H3 and H4 (mono- di- and trimethyl groups per residue) including K4, K9, K27, K36, K79 and R2, R8, R17, R26 for H3 and K20 and R3 for H4 (Ferrari and Pasini, 2013). The source of the methyl group required by histone methyl-transferases is S-adenosyl-methionine; presence of a SET domain characterizes several proteins belonging to this class of enzymes (Trievel et al., 2002). In mammals, dimethylation of histone H4 lysine 20 (H4K20me2), is induced by the MMSET enzyme and this process seems to be critical for the recruitment of 53BP1 in vicinity to DSBs. Interestingly, MMSET methyl-transferase depletion significantly decreases H4K20 methylation at DSBs, as well as 53BP1 accumulation at damaged DNA sites (Pei et

al., 2011). SETD8, an enzyme that mono-mehtylates lysine H4 residue K20 is also present on the double strand break sites; H4K20me1 is enriched during mitosis and represents a specific tag for epigenetic transcriptional repression (Dulev et al., 2014). Metnase is another methylase that dimethylates histone H3 residue K36 (H3K36me2) at the DNA DSB site; the levels of H3K36me2 were found to correlate positively with DSB repair efficiency (Povirk, 2012). Another histone modification, H3K4me3, induced by SET1 methyltransferase has been found at DNA DSBs, and the absence of this modification was associated with defective DNA DSB repair (Faucher and Wellinger, 2010).

Similar to other conserved DNA repair mechanisms, ubiquitylation is also a tightly regulated event involving the enzymatic activity of E1, E2 and E3 proteins (Hershko and Ciechanover, 1998). Ubiquitination of nuclear histones occurs after DBS induction by RNF8, and RNF168, two E3 ubiquitin-protein ligases, which catalyse formation of lysine 63 linked polyubiquitination chains on histones H2A and H2AX (Doil et al., 2009). Another important ubiquitination event during DDR is induced by the BRCA1 E3 ligase, which promotes BRCA2 binding that subsequently triggers RAD51 recruitment during DNA strand resection in the DNA HR repair pathway (Qing et al., 2011). Moreover, some authors reported that the UBC13 E3 ligase is required for HR itself. In particular, Zhao and co-workers showed that cells lacking UBC13 are defective in break resection as determined by RPA recruitment to DNA DSBs (Zhao et al., 2007).

The histone code describing the interplay between chromatin and the DDR is complex and each molecular signature is not univocal. Histone modification after the DDR induced by DSBs reflects changes in chromatin composition and compaction. For example, some experiments showed that DNA DSBs can induce chromatin decondensation and that this is an actively regulated process (Ziv et al., 2006). A global increase in chromatin accessibility in response to UV damage was also reported (Carrier et al., 1999). On the other hand, DSBs can lead to a repressive chromatin state; heterochromatin displays specific histone modifications, such as di- or tri-methylation of histone H3 at lysine 9, and the

subsequent recruitment of chromatin association proteins such as heterochromatin protein1 (Hp1) (Cheutin et al., 2003). Some authors showed that a complex containing the suv39h1 methyltransferase is rapidly recruited to DSBs, where it directs H3K9 methylation on large chromatin domains adjacent to the DSB (Ayrapetov et al., 2014).

There is also multiple evidence indicating that CAF-1, the major H3/H4 histone chaperone, plays a role in setting up a repressed chromatin state after a DNA damage signal. Some authors reported that propagation of silenced chromatin is intimately linked to the histone deposition process, moreover, loss of CAF-1 function causes heterochromatin abnormalities and loss of viability during development in mouse, Xenopus and Drosophila (Quivy et al., 2001) (Moggs et al., 2000). However, the precise effect that the overall compaction status of chromatin exerts on the access, signaling, and repair of DNA damage is not known. Understanding the chromatin changes during the DDR still remains a central topic for investigation.

As far as the DDR is concerned, the most common histone modifications are depicted in **Figure 1.9.**

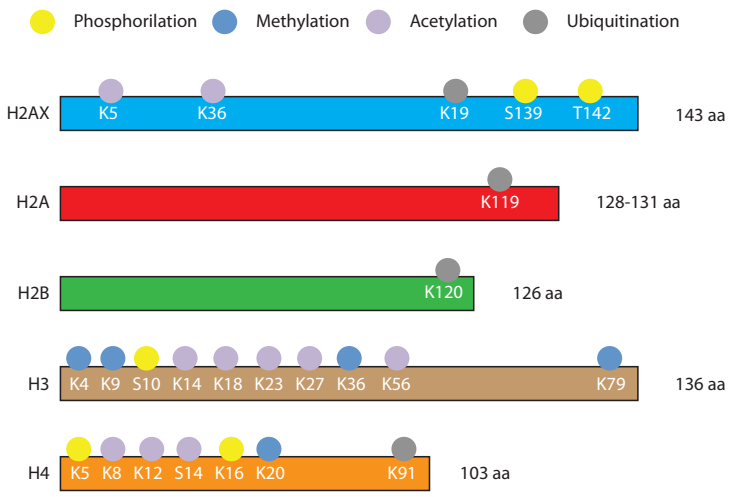

Figure 1.9 The most common histone modifications following DNA DSBs.

1.3.5 Chromatin as an anti-viral defense mechanism

In recent years, several investigations have highlighted the importance of chromatin during viral infection. It is now clear that the chromatinization of viral genomes should be considered part of the host defense to invading pathogens. The interplay between viral and host chromatin determines the outcome of viral infection and regulates viral latency and reactivation by modulating gene expression, impeding genome conversion or inducing epigenetic repression.

For example, it is known that treatment with HDAC inhibitors stimulates transcription from many viral promoters, including the CMV promoter (Murphy et al., 2002). This mechanism was also described for the reactivation of Herpes simplex 1 and Epstein-Barr viruses from latency, suggesting a role for HDACs in the silencing of latent viral genomes.

Cells have also developed mechanisms against retroviruses that act through creating a repressive chromatin state on the viral genome. For example, the host positive transcription elongation factor p-TEFb triggers the methylation of histone H3 Lys4 and Lys36 during reactivation of latent HIV genomes. This event suggests that the P-TEFb kinase activity plays an important role in regulating downstream chromatin modifications, such as histone methylation during HIV-1 transcription elongation (Zhou et al., 2004). Thus, quite paradoxically, this represents a cellular defense mechanism that contributes to HIV viral latency and persistence.

More recently, several experiments have demonstrated the pivotal role that chromatinization exerts in HIV viral gene expression. Protein complexes involved in chromatin remodeling, including histone acetyltransferases, can activate HIV-1 gene expression both *in vitro* and *in vivo*. Agents such as polyamides, which interacts with the HIV promoter by blocking HDAC-1 recruitment, and trichostatin A, a HDAC inhibitor, have striking positive effects on HIV gene activation (Ylisastigui et al., 2004) (Quivy et al., 2002).

Also Adenovirus (Ad) does not escape the chromatinization process. Indeed, six hours post infection approximately 50% of adenoviral DNA is associated with

nucleosomes (Ross et al., 2011), which control gene expression and stability. In chromatin immunoprecipitation studies, helper-dependent adenovirus (hdAd), both E1-deleted adenovirus and wild type adenovirus DNA are associated with H3.3, a histone variant that marks open chromatin. H3.3 association with the adenoviral genomes occurs after four hours after infection, which suggests that a replication-independent mechanism is responsible for the assembly of chromatin on the viral DNA (Ross et al., 2011). Recent work performed by Komatsu *et al.* (Komatsu and Nagata, 2012) showed that the silencing of CAF-1, the main cellular histone chaperone, does not affect histone deposition on the adenovirus genome. This finding supports the idea that H3.3 is overrepresented on the Ad viral genome. Recent studies have suggested that the rapid deposition of H3.3 mediated by the HIRA histone chaperone may be an evolved mechanism to protect "naked" DNA from damage (Schneiderman et al., 2012) and that this strategy might be exploited by adenovirus to avoid the inhibition that DNA repair proteins can impose on the incoming viral genomes.

Infection of cells with wild-type adeno-associated virus was able to trigger pan-nuclear activation of γ-H2AX, but not of recombinant AAV vectors. This effect indicated that the phosphorylation was due to a component of the wild-type AAV genome and not the viral capsid (Schwartz et al., 2009) (Fragkos et al., 2008). The phosphorilation of γ-H2AX by wild-type AAV was detected onto the p5 promoter region, which acts as a potential viral origin of replication (Schwartz et al., 2009). Other experiments showed that the DDR response during wt AAV infection was much more intense in the presence of helper Adenovirus (Fragkos et al., 2008). R.O. Snyder and co-workers demonstrated that the episomal AAV genomes can assimilate into chromatin with a typical nucleosomal pattern *in vivo* (Penaud-Budloo et al., 2008). Their work suggests that the AAV chromatin structure is important for episomal maintenance of AAV genome and, consequently, for prolonged transgene expression and persistence of the vector in quiescent tissues. Okada and colleagues demonstrated that an histone deacetylase inhibitor, FR901228, increased AAV transduction both in *vitro* and *in vivo*. These results

suggest that the superior AAV transduction obtained following HDAC inhibitor treatment may be related to the histone-associated chromatin form of the AAV genomes in transduced cells; a cellular immunity defense mechanism aimed to inhibit single stranded DNA viruses at the chromatin level might thus be postulated to exist (Okada et al., 2006).

It is also interesting to consider that one of the major obstacles to success in non-viral gene therapy is the transcriptional silencing of the naked DNA vector. Some evidence showed that changes in the pattern of histone modifications were related to the observed transcriptional silencing of exogenous DNA vectors (Riu et al., 2007). The mechanisms underlying gene silencing/repression of exogenous DNA in mammalian cells appear complex and definitely need further investigation.

1.4 The Eri1 exoribonuclease

Eri1 is a protein of 349 residues with an amino-terminal SAP domain and a carboxy-terminal 3' exonuclease domain able to degrade RNA.

The SAP domain is composed of 35 residues containing an invariant glycine and a conserved distribution of hydrophobic, polar and bulky amino acids. The SAP domain is present in a number of eukaryotic proteins in conjunction with other domains that link these proteins with the RNA or DNA metabolism (Aravind and Koonin, 2000). Eri1 elicits its nuclease activity in the presence of riboadenine-5'-monophosphate and Mg2+ ions (Cheng and Patel, 2004) (**Figure 1.10**).

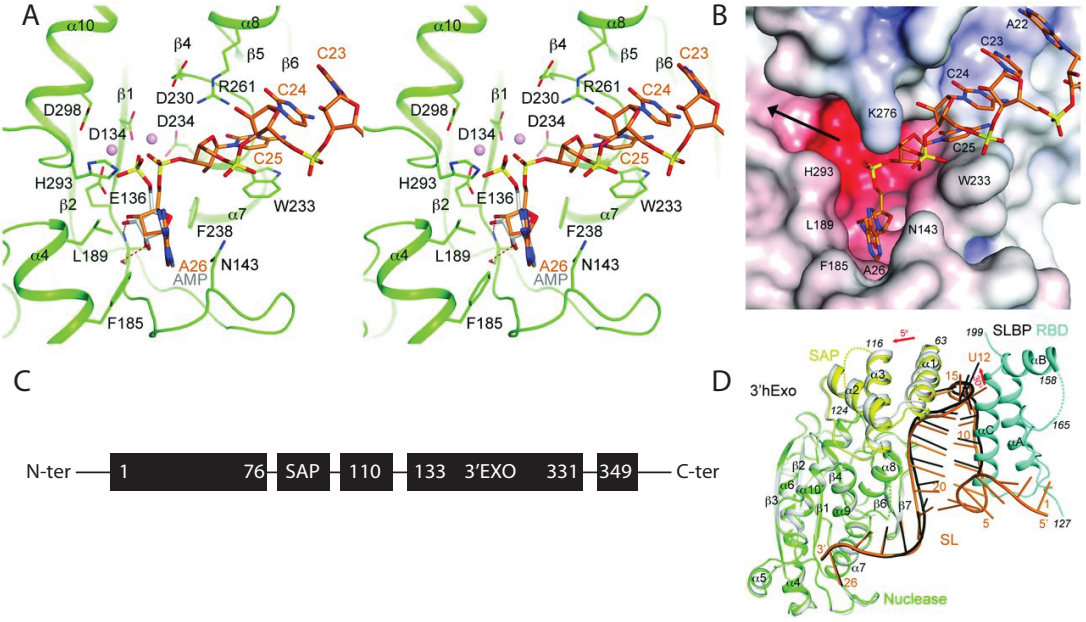

Figure 1.10 Eri1 structure. Eri1 binds the 3'-end of histone mRNAs in a stem-loop structure containing the "ACCCA" consensus sequence. Eri1 degrades histone RNAs and small RNAs through its carboxy-terminal 3′ exonuclease domain. The 3′ flanking sequence of the SL RNA is located in the 3′hExo active site. (**A**) Stereopair showing interactions of the 3′ flanking sequence of the SL RNA (orange) with the active site of the Eri1 nuclease domain (green). The bound positions of AMP (gray) and two metal ions (pink spheres) to the nuclease domain of Eri1, as observed earlier, are also shown (21). (**B**) Molecular surface of the active-site region of Eri1 colored according to electrostatic potential. The SL RNA is shown as a stick model (orange). The black arrow indicates another opening from the active site, through which Eri1 may accommodate longer RNA molecules. (**C**) Eri1 protein domain composition (**D**) Overlay of the structures of the ternary (SL-SLBP-Eri1, in color) and binary (gray for Eri1 and black for SL) complexes. (Adapted from (Tan et al., 2013)).

The Eri1 nuclease domain shows an α/β globular fold conformation. In the active site, residues D134, E136, D234 and D298 and H293 define the core responsible for the hydrolytic RNA cleavage in the 3′-5′ direction (Cheng and Patel, 2004). The nuclease domain is similar to that found in the 3′ exonucleases of the DEDD-family, including both DNA- and RNA-specific enzymes, and is characterized by the presence of these four invariant acidic amino acids from which the family name originated (Zuo and Deutscher, 2001). Eri1 exoribonuclease binds the 3'-end of histone mRNAs and degrades them, suggesting that it plays an essential role in histone mRNA decay after replication (Hoefig et al., 2013). A 2' and 3'-hydroxyl

groups at the last nucleotide of the histone 3'-end is required for efficient degradation of RNA substrates. Eri1 is also able to process the 3'-overhangs of short interfering RNAs (siRNAs), suggesting a possible role as regulator of RNA interference (RNAi), (Kennedy et al., 2004). Some experiments demonstrated that Eri1 also binds the 5.8s ribosomal RNA and it is required for 5.8S rRNA 3'-end processing (Ansel et al., 2008).

1.4.1 Eri1 regulates RNA interference

Another described function of Eri1 is to bind and degrade the 3'-overhangs of short interfering RNAs and to function as a negative regulator of the endogenous RNA interference (RNAi) machinery (Kennedy et al., 2004). In support of this activity, G. Ruvkun and colleagues showed that worms with Eri1 mutations accumulated more siRNAs after exposure to dsRNA or siRNAs than wild-type animals. Moreover, mass-spectrometry data revealed that Eri1 is present in the DICER complex, and that it is required for the generation of endogenous siRNAs in C. elegans (Duchaine et al., 2006). In the model proposed by Kennedy and co-workers, Eri1 is able to recruit endogenous RNAs and lead to the cleavage of 3' end of them; after this step, an RNA-dependent RNA polymerase is involved in the synthesis of double stranded RNA species that will be cleaved by DCR-1 and subsequently introduced into the RNAi-pathway. This model implies that the lack of Eri1 impedes the endogenous siRNA production; indeed, exogenously introduces siRNAs showed an increased effect in worms with inactive Eri1 (Kennedy et al., 2004). Consistent with these observations, other studies have documented the involvement of the protein in limiting the heterochromatin assembly mediated by RNAi in fission yeast by degradation of nuclear siRNAs (Iida et al., 2006). More recently, Eri1 was also described to limit the expression of global, mature miRNAs in mouse T and NK cells (Thomas et al., 2012).

1.4.2 Eri1 processing of ribosomal RNA

Ribosomal RNA (5.8S rRNA) is one of the conserved targets of Eri1. Although most ribosome processing happens in the nucleolus, Eri1-mediated 5.8S rRNA trimming is likely to occur in the cytoplasm (Gabel and Ruvkun, 2008) (Ansel et al., 2008). Although the function of 5.8S rRNA30 trimming is poorly understood, it is likely to be important because it is conserved even in Saccharomyces cerevisiae, in which an unrelated endonuclease, Ngl2, performs the same function (Faber et al., 2002). One hypothesis is that Eri1 binds intact cytoplasmic ribosomes as a way to home to the basal translation machinery its enzymatic functions, such as the inhibition of RNAi. Interestingly, Eri1 is just one of the several ribosomal RNA processing proteins recruited into regulatory small RNA pathways. Alternatively, the function of Eri1 in ribosome maturation and miRNA turnover may be purely coincidental, because 3'-end trimming is a relatively common post-transcriptional modification required for the biogenesis of many unrelated non-coding RNAs. To date, a connection between Eri1-dependent rRNA processing and altered epigenetic gene regulation remains purely speculative.

1.4.3 Eri1 binds the stem loop of histone mRNAs

Histone mRNAs contain a highly conserved 26-nucleotide sequence that forms a 6-nucleotide stem and a 4-nucleotide loop structure, characterized, among vertebrates, by the presence of the "ACCCA" sequence (Yang et al., 2006).

Dominski and colleagues showed that Eri1 could bind oligos mimicking this 3' stem loop of canonical histone mRNAs in vitro (Dominski et al., 2003). Subsequent studies have demonstrated that Eri1 targets histone mRNA sequences through its SAP domain (Yang et al., 2006). In 2006, Cheng and co-workers solved the crystal structure of Eri1 in complex with stem loop RNA; their data suggested that the SAP domain is indispensable for binding histone RNA (Cheng and Patel, 2004).

Functional assays supported this evidence, showing that, by mutating the SAP domain, it is possible to abolish the binding of Eri1 to stem loop-RNA structure (Yang et al., 2006).

Aim of the thesis

The aim of this PhD thesis was to study and understand the cellular mechanisms that regulate Adeno-associated virus transduction. This work was performed exploiting high throughput screening technologies. Taking advantage of genome-wide siRNA libraries it was possible to identify some relevant cellular factors that mediate rAAV2 transduction. The work described in this thesis is divided into two sections. The first part focuses on the characterization of the top-10 siRNAs identified in a screening, performed in HeLa cells, for siRNAs increasing rAAV efficiency and therefore targeting factors inhibitory on rAAV transduction. This part of the research highlights the mechanisms underlying a correlation between AAV infection and cellular checkpoint activation. The second part of the thesis focuses on the study of factors required for rAAV infection. In particular, we characterize the mechanism of action of Eri1, a 3'-exoribonuclease known to degrade endogenous miRNAs and histone mRNAs, on AAV transduction. We determined that Eri1 is essential for ssAAV but not scAAV transduction and that this effect is specifically exerted by changing the AAV genome chromatin composition through the modulation of the cellular histone dosage.

The findings described in this thesis may foster the development of druggable siRNA molecules or pharmacological strategies specifically aimed at improving AAV transduction in vitro and vivo.

2. Results I

2.1 High-throughput, genome-wide siRNA screening reveals cellular factors critical for AAV transduction

Over the last few years, viral vectors based on AAV have gained increasing popularity due to several favourable characteristics, including the excellent safety profile, lack of inflammatory response, prolonged transgene expression, relative genetic simplicity and high efficiency of transduction of post-mitotic tissues such as muscle, heart, brain and retina. Nonetheless, it has become evident that significant improvements need to be achieved before attaining broader clinical application. Given the molecular simplicity of AAV vector particles, all the determinants of permissivity to vector transduction appear to reside among the molecular features of the host cell. For this reason, the identification of the cellular proteins that regulate vector transduction is an essential requisite to improve *in vivo* transduction, expand the number of permissive tissues and achieve AAV-mediated gene correction at a clinically applicable level (Carter, 2005).

To systematically identify the host cell factors involved in the internalization, intracellular trafficking, processing of AAV genome and, eventually, AAV gene expression, either positively or negatively, we have performed a high-throughput screening using a genome-wide siRNA library (18175 human gene targets). We assessed differences in AAV transduction in HeLa cells; 48 h after transfection with the siRNA library cells were infected using a recombinant single-stranded (ss) AAV2 vector expressing the firefly Luciferase reporter gene. Cells were transduced at a multiplicity-of-infection (moi) of 2500 viral DNA genomes (vg)/cell, since it was estimated that this allows one to achieve a sub-saturating levels of transduction optimal for the detection of both positive and negative regulators (**Figure 2.1**).

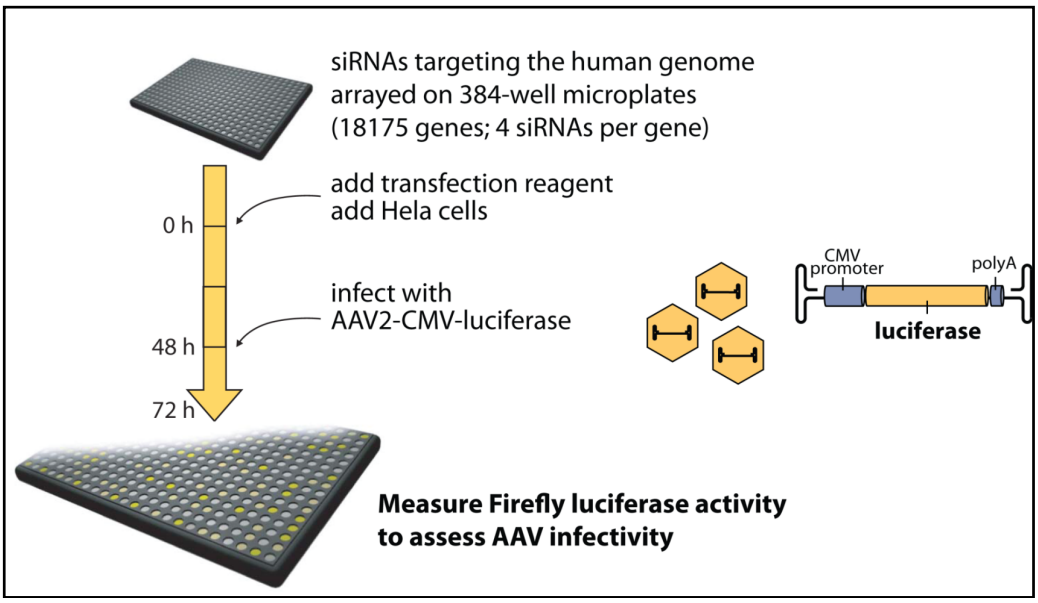

Figure 2.1 AAV transduction high-throughput screening setup. The screening was performed in HeLa cells, using human a genome-wide siRNA library; each siRNA mixture was composed by a pool 4 siRNAs targeting each single gene of human genome. Cells were silenced for 48 h and subsequently infected with an AAV expressing the firefly luciferase gene for 24 h. The measure of luciferase activity was used to quantify AAV infectivity. Finally, the luciferase readout was normalized for cell viability.

Analysis of the results obtained from this primary screening identified 1528 genes affecting transduction by AAV vectors by more than 4-fold (184 genes by more than 8-fold).

Of these genes, 993 were inhibitors of AAV transduction, whereas 535 were required for efficient transduction. Short interfering RNA pools decreasing cell viability to less than 75% were considered toxic, and were thus excluded from further analysis; these included siRNAs against well-known, essential genes (e.g. UBB, UBC, COPB1, PLK1). Remarkably, the 10 top scoring siRNA pools increased or decreased ssAAV2 transduction by as much as 50- and 10-fold, respectively.

The effect of these genes on AAV transduction was further confirmed in a secondary screening based on high-content microscopy analysis using siRNAs against the 1,486 genes that affected ssAAV2 transduction by more than 4-fold in the primary screening. In this case, HeLa cells stably expressing EGFP under the

CMV promoter were transfected with the siRNAs of interest and transduced, 48 h later, with a ssAAV2 vector expressing the red fluorescent protein DsRed (ssAAV2-DsRed). This validation strategy was designed in order to recognized the siRNAs affecting expression from the CMV promoter rather than AAV transduction itself.
We selected the siRNA pools that increased or decreased the percentage of DsRed positive cells of more than 4-fold, when compared to cells treated with a control siRNA. The siRNAs that decreased EGFP expression were removed from our candidate list .

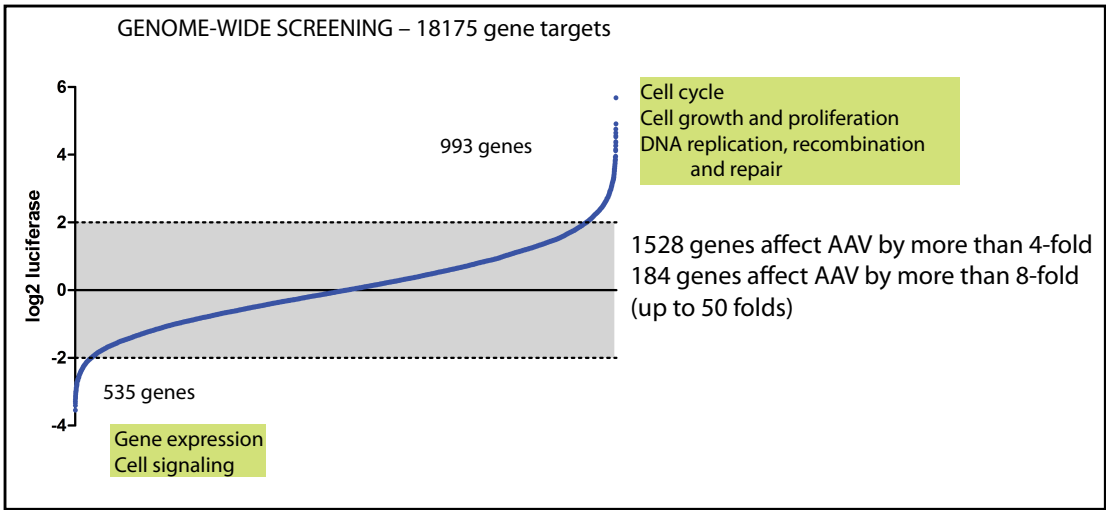

Figure 2.2 Distribution of the effects of siRNAs regulating AAV transduction. The screening identified 993 genes inhibitory of AAV transduction, the knockdown of which increased transduction from 4 up to 50 folds.

Gene ontology analysis of the inhibitory genes revealed a clear overrepresentation of genes related to DNA recombination and repair and cell cycle control, whereas the subset of genes required for infection were enriched in genes involved in endocytosis, intracellular trafficking and transcription (**Figure 2.2**). Consistent with our previous results, among the genes that restricted AAV transduction, we found members of the MRN complex and other genes involved in the cellular DDR, as well as genes involved in the ubiquitin-proteasome system. In addition, a significant number of genes were identified, which had not previously been

associated with AAV transduction.

The 10 siRNAs that were most effective at increasing AAV transduction genes belonging to different families. Interestingly, seven out of ten of these factors are involved in cell cycle regulation and DNA repair and have a nuclear localization. In addition, some of them (SETD8, CASPBAP2, NPPAT and CAF-1) are involved in chromatin remodeling pathways (Congdon et al., 2010) (Hummon et al., 2012) (DeRan et al., 2008) (Houlard et al., 2006) (**Figure 2.3**).

N°	Gene	Entrez gene name	Efficiency of transduction (fold over control)
1	SETD8	SET domain containing (lysine methyltransferase) 8	51.4
2	CASP8AP2	Caspase 8 associated protein	30.2
3	SOX15	SRY (sex determining region Y)-box 15	27.0
4	TROAP	Trophinin associated protein (tastin)	25.1
5	NPAT	Nuclear protein. ataxia-telangiectasia locus	23.6
6	PHC3	Polyhomeotic homolog 3 (Drosophila)	23.1
7	CHAF1A	Chromatin assembly factor 1 subunit A (p150)	20.9
8	SF3B1	Splicing factor 3b. subunit 1 155kDa	20.5
9	RTBDN	Retbindin	19.3
10	BOMB	WW and C2 domain containing 2	19.2

Figure 2.3 List of the top 10 siRNAs increasing AAV transduction discovered in the screening. The right column number shows efficiency of AAV infection (fold increase over control) following siRNA treatment.

2.2 Correlation between rAAV infection and DNA damage

Long standing evidence indicates that viral DNA can be recognized inside the host cell by the DDR machinery and that genotoxic damage increases cellular permissivity to AAV (Yalkinoglu et al., 1988) (Russell et al., 1995). In addition, different laboratories, including our own, have previously shown that proteins of the DDR, in particular those of the MRN (MRE11-RAD50-NBS1) (Zentilin et al., 2001), inhibit AAV transduction in both cell culture (Cervelli et al., 2008) and primary cells *in vivo* (Lovric et al., 2012).

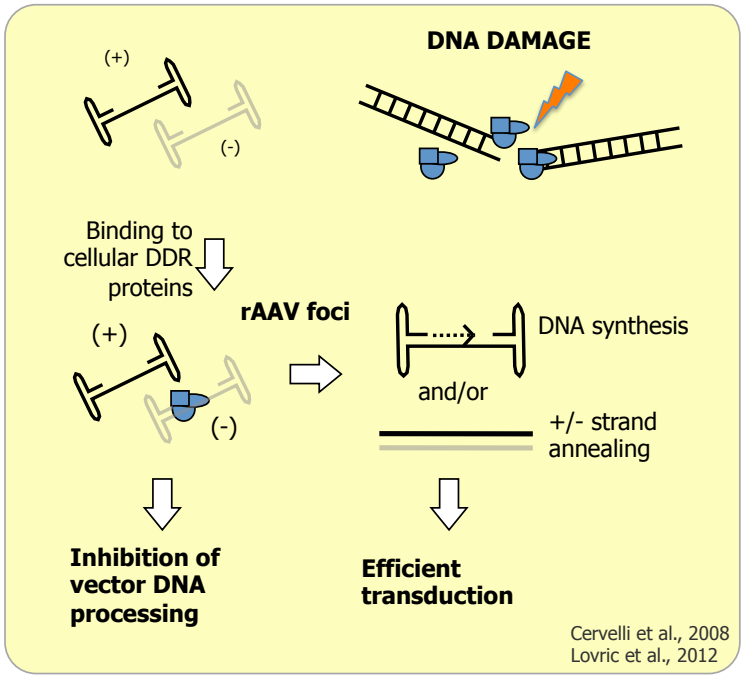

Figure 2.4 The "titration model" to explain AAV permissivity. This model proposes that genome DNA double strand breaks are capable to engage and sequester a large amount of nuclear DNA repair proteins, leading to a context in which the single-stranded AAV genome is converted more efficiently to double-stranded DNA.

Following these considerations, we decided to investigate whether the top ten siRNAs of our primary screening exerted any effect on cellular DNA damage, in the absence of viral infection.

We first analyzed the phosphorylation of histone H2AX at serine 139 (ɣ-H2AX), a hallmark of cellular DNA damage (Rogakou et al., 1998), in HeLa cells treated with the selected siRNAs. Remarkably, downregulation of six of these genes, at a different extent, was able to increases ɣ-H2AX phosphorylation, with SETD8, CASP8AP2 and BOMB being the most effective. (**Figure 2.5**). In the same experimental conditions, a non-targeting siRNA was not able to induce any ɣ-H2AX activation (western blot not shown). Immunofluorescence experiments using an antibody against ɣ-H2AX also confirmed the formation of nuclear foci after cell treatment with selected siRNAs from the top 10 inducing AAV transduction (**Figure 2.6**).

Taken together, these results indicate that several of the siRNAs inducing cellular permissivity to AAV can do so by inducing DNA damage.

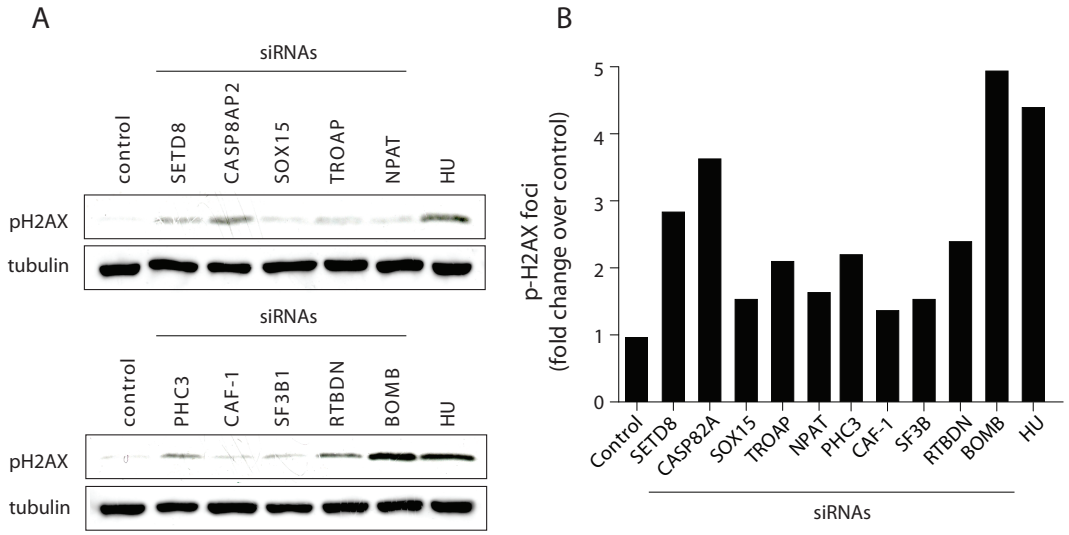

Figure 2.5. (Panel A) The top 10 siRNAs increasing AAV transduction determine DNA damage, as revealed by ɣ -H2AX histone positivity. The western blot demonstrates that, at a different extent, six out of the top10 siRNAs induce the phosphorylation of H2AX histone variant. Hydroxyurea (HU) was used as positive control. (Panel B) Quantification of the immunoblot shown in panel A. The experiment is representative of at least three experiments giving analogous results. Band quantification indicated a statistically significant difference between control and all the analyzed siRNAs (P>0.05).

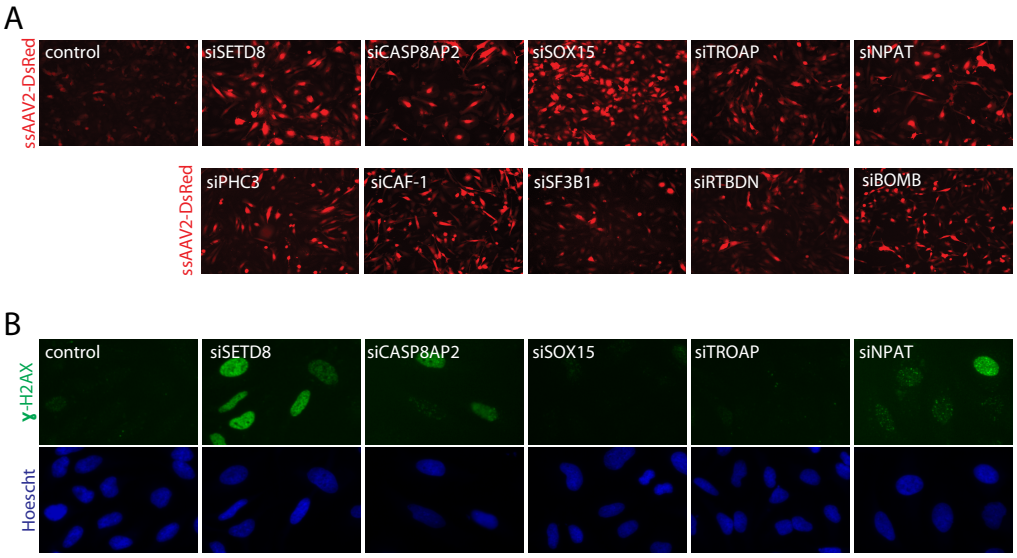

Figure 2.6. (Panel A) Top 10 siRNAs treatment increases AAV transduction in HeLa cells. Immunofluorescence images show AAV2-DsRed infection (red color) after silencing. Cells were silenced for 48 h and then infected for 24 h, using an moi of 2500 vg/cell. (Panel B) The immunofluorescence shows that, at a different extent, six out of the top 5 siRNAs are able to trigger the phosphorylation of H2AX histone variant; the nuclear γ-H2AX foci are visible in green.

These results raised the possibility that it was the recognition of DNA damage, induced by top-10 siRNAs in the screening, to activate AAV transduction. A reasonable assumption was that DDR acted as a decoy for MRN or other DNA damage recognition proteins, or that even γ-H2AX itself could be involved in determining AAV permissivity.

To address these possibilities experimentally, we devised an experimental strategy exploiting short DNA oligonucleotides that could act as decoys for the DDR response proteins and activate H2AX histone phosphorylation. The rationale of this approach was based on the demonstration that small DNA oligonucleotides transfected into the cells could mimic DNA double-strand breaks and thus act by acting a decoys for the DDR proteins. A similar approach was successfully used to inhibit DNA repair in cancer cells and to increase the efficacy of chemotherapy in colorectal cancer (Quanz et al., 2009).

We designed double-stranded DNAoligonucleotides differing in length and in 3' or

5′ overhang conformation and also included a ssDNA oligonucleotide, capable of self-annealing and mimicking the hairpin structure of the AAV ITR (**Figure 2.7**).

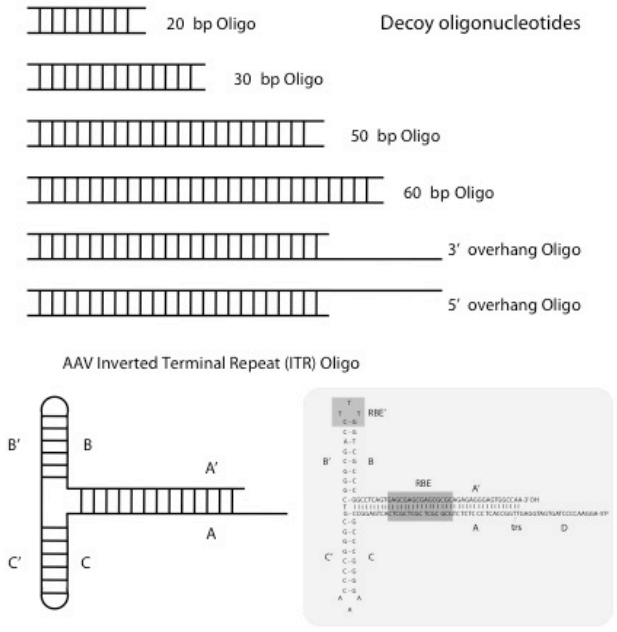

Figure 2.7 DNA decoys. Types of DNA oligonucleotides designed to mimic a double-stranded DNA break. We generated oligonucleotides of 20, 30, 50, 60 base pairs, oligonucleotides ending with 5′ and 3′ overhangs and an oligo that mimics the hairpin structure of the AAV ITR .

Twenty four hours after transfection of the different type of oligonucleotides we analyzed phosphorylation of ϒ-H2AX by immunofluorescence staining in HeLa cells. Only oligos having a length longer than 30 bp were able to induce nuclear ϒ-H2AX foci.

We decided to compare the effects produced by the synthetic oligonucleotides with those elicited by the siRNA against SETD8, the most effective inducer of permissivity to AAV transduction in our primary screening. SETD8 silencing lead to activation, this confirmed the data that we previously observed by immunoblotting (**Figure 2.8**). We observed that the transfection of 30, 50 and 60

base pairs oligonucleotides were able to induce H2AX activation, and hence a DDR response, at levels comparable to SETD8 knock down or hydroxyurea treatment (**Figure 2.8**).

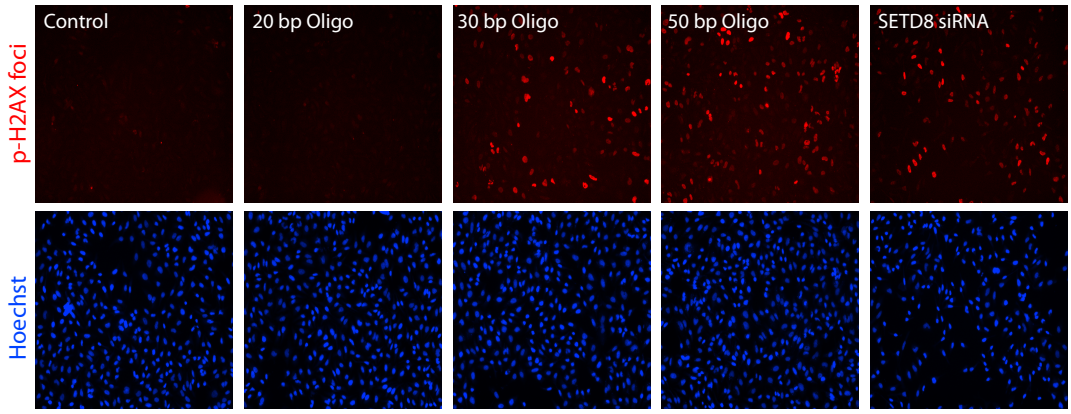

Figure 2.8 Nuclear foci after oligonucleotide treatment. HeLa cells were transfected with double stranded DNA oligonucleotides. Immunofluorescence shows che appearance of nuclear foci in the cells treated with oligos longer than 20 bp. The siRNA against SETD8 is here used as a positive control.

Then we assessed whether the oligonucleotides activated AAV transduction. Contrary to our expectations, analysis of transduction of the oligonucleotide-treated cells with either AAV2-EGFP or AAV2-Luciferase, using an moi of 2500 vg/cell, revealed that none of the transfected oligonucleotides was able to increase levels of marker transgene expression above untreated infected control (**Figure 2.9**) (**Figure 2.10**).

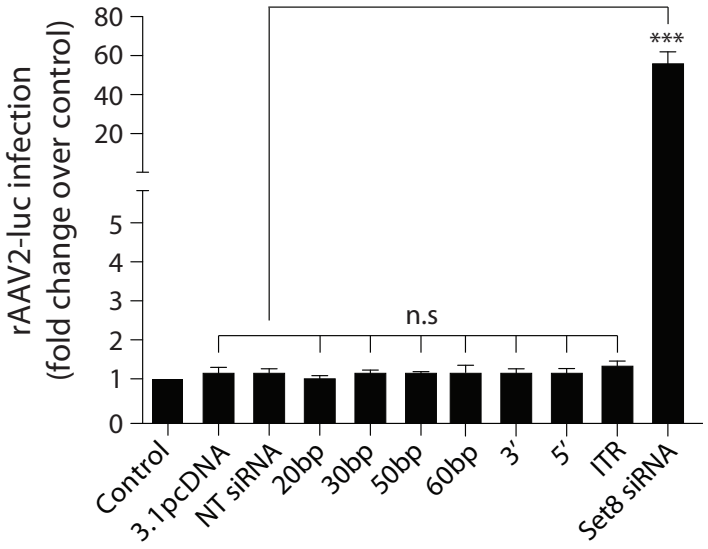

Figure 2.9 Oligonucleotide transfection has no effect on AAV transduction. HeLa cells were transfected with oligonucleotides that differ in length and end conformation for 24 h and then infected with AAV2-luc for 24 h. Luciferase activity has been used to measure AAV infectivity. All samples were normalized over untreated cells (control). Differences of siRNAs treated samples vs NT siRNA and oligos treated samples vs pcDNA3.1 treated cells were analyzed by one-way ANOVA test followed by Tukey post-hoc test. Star code for statistical significance (A): *** P<0.001; n.s. = not significant.

.

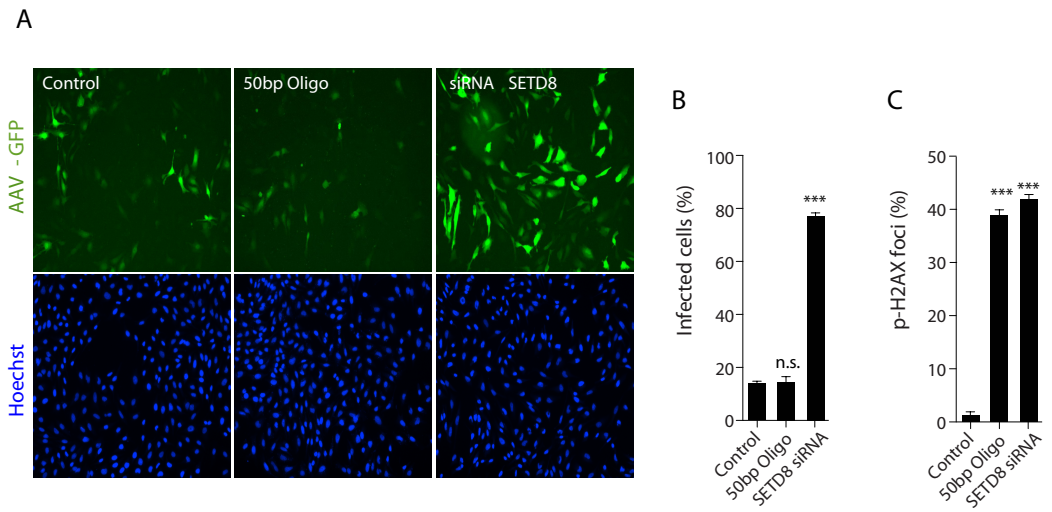

Figure 2.10 (Panel A) Oligonucleotide transfection determines formation of γ-H2AX DNA foci without increasing AAV infection. HeLA cells were transfected with a 50 bp oligonucleotide for 24 h and then infected with AAV-EGFP for 24 h. The immunofluorescence panel shows that the

percentage of GFP-positive cells is comparable between the oligo-treated cells and the control. SETD8 silencing was used as positive control. (Panel B-C) Quantification of the results of three different 96 well-plate replicates (mean ± sem) showing nuclear foci (C) and AAV infection (B). Differences of treated samples vs control were assessed by ANOVA test followed by Tukey post-hoc test. Star code for statistical significance *** P<0.001; n.s. = not significant.

2.3 Correlation between rAAV infection and cellular checkpoint activation

Considering that formation of γ-H2AX foci does not positively correlate with AAV infection, we decided to evaluate in more details the actual relationship between the downstream level of the DDR response and AAV transduction.

It is well recognized that the phosphorylation of NBS1 serine 343 is a marker of DNA damage, specifically indicating the activation of the MRN complex, one of the earliest respondents to DNA DBSs. This activation initiates a cell-cycle checkpoint signaling cascades through the phosphorylation of ATM and ATR, which in turn also represent master sensors of DNA damage. The cellular kinases Chk1 and Chk2 are the downstream effectors of this signaling pathway, activated through phosphorylation by ATM and ATR (Chaturvedi et al., 1999) (Walworth and Bernards, 1996).

We therefore analyzed phosphorylation of ATM, ATR, NBS1, Chk1 and Chk2 proteins following treatment of HeLa cells with the different oligonucleotide decoys (**Figure 2.11**). Again, results from immunoblots showed that only SETD8 knockdown was able to activate proteins involved at different levels in the DNA DSB repair pathway. Oligonucleotide decoys were only able to trigger the phosphorylation of H2AX (**Figure 2.11**). We confirmed these data also by confocal microscopy analysis, by which we observed the formation of p-NBS1 foci only after SETD8 knockdown or hydroxyurea treatment, but not treatment with the oligonucleotides (**Figure 2.12**).

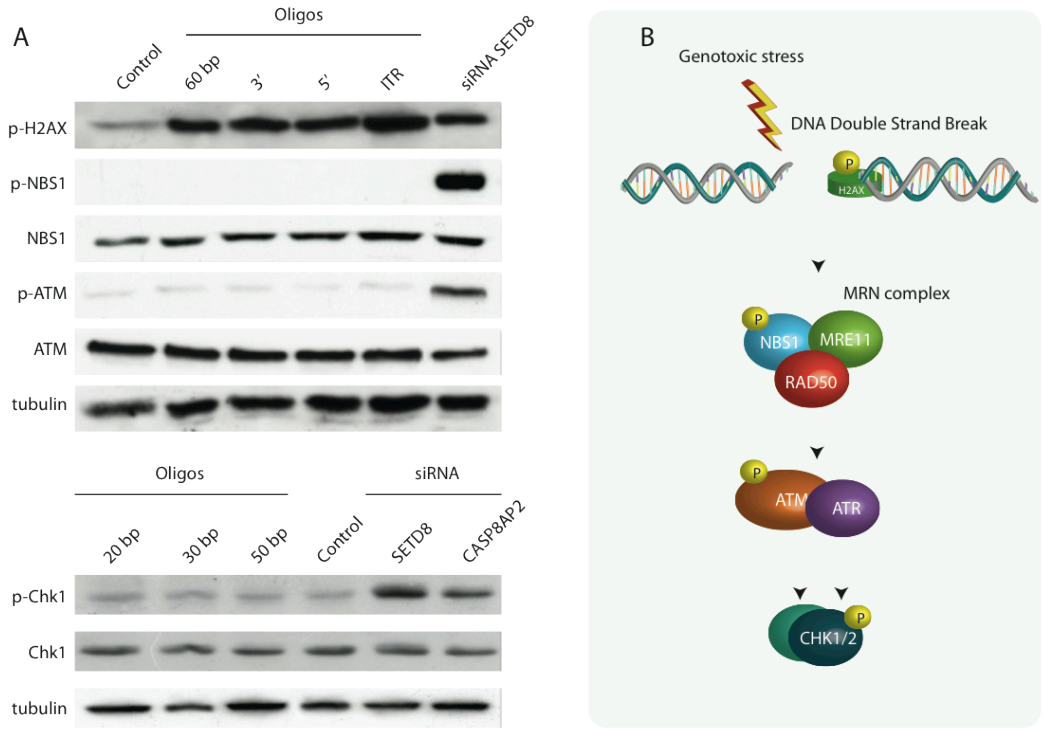

Figure 2.11 (Panel A) Immunoblotting analysis showing the activation of p-NBS1, p-ATM and p-Chk1 in HeLa cells following transfection of DNA oligonucleotides decoys or SETD8 and Casp gene silencing. The immunoblotting results show that only the SETD8 knockdown was able to induce the phosphorylation of ATM, NBS1 and Chk1. Chk1 phosphorylation was also induced by the Casp knock-down (Panel B) Cartoon representing the DNA DBS signaling response pathway.

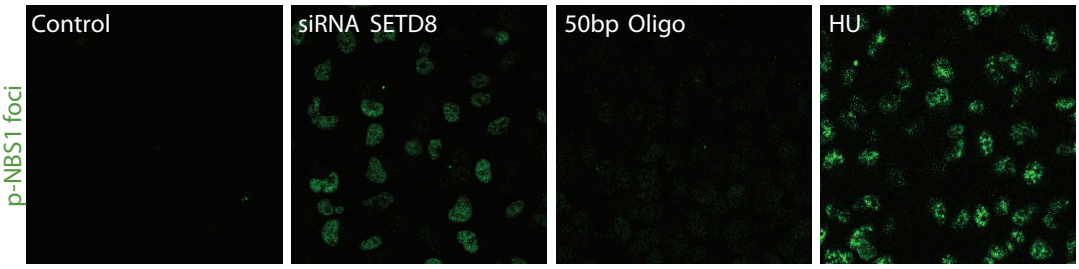

Figure 2.12 Confocal microscopy of p-NBS1 foci. HeLa cells were transfected with a 50-bp oligonucleotide for 24 h or silenced with SETD8 siRNAs for 48 h or treatment with HU overnight. HeLa cells were stained with anti p-NBS1ser(343) antibody. The images show that only HU treatment or SETD8 silencing were able to induce NBS1 phosphorylation.

2.4 Effect of the top 10 siRNAs from the AAV screening on cellular checkpoint activation

From the results described above, it is evident that the synthetic oligonucleotides tested, although recognized as DNA damage, are not able to trigger the DDR signaling cascade, and that the sole activation of γ-H2AX is not sufficient to enhance cell permissivity to AAV vector transduction.

On the other hand, the downregulation of SETD8, which produces a strong effect on AAV transduction, appeared not only to trigger the phosphorylation of γ-H2AX, but also of NBS1, ATM and Chk1 (**Figure 2.11**).

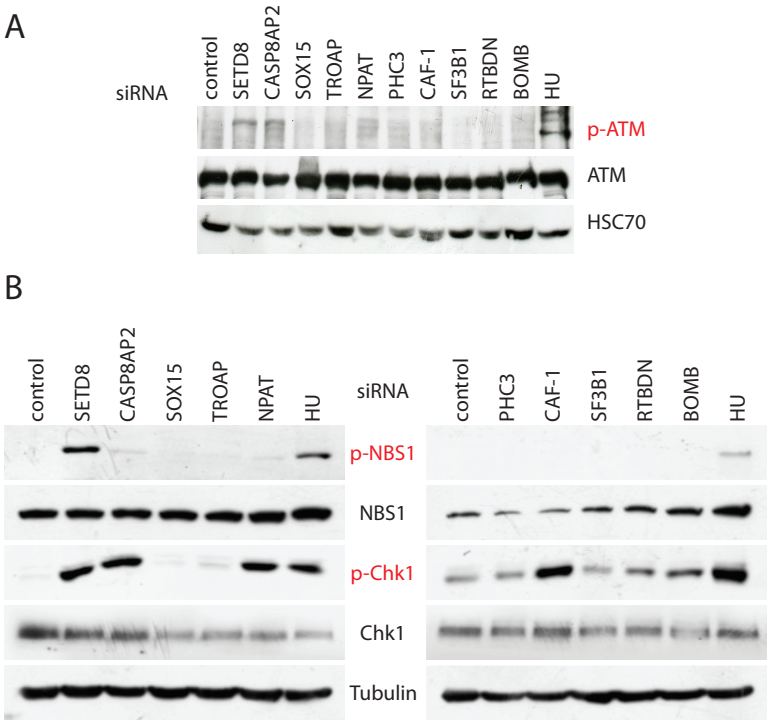

Figure 2.13 Immunoblot showing the effect of the top 10 siRNAs on cellular DSB checkpoint activation. The analysis reveals that six out of ten siRNAs were able to trigger the phosphorylation of Chk1 (SETD8, CASP, NPAT, RTBDN, BOMB, CAF-1). The western blot also shows that changes in the total amount of the non-phosphorylated proteins were negligible. SETD8 and CASP82AP2 silencing lead to a strong activation of the DNA DBS repair pathway. The two most effective siRNAs from the AAV transduction screening triggered he phosphorylation of ATM (Panel A), NBS1 and Chk1 (Panel B) respectively. Lysates of HU treated cells were used as positive controls.

Further analysis, extended to the effects of all top 10 siRNAs, revealed that at least

six of them (SETD8, CASP8AP2, NPAT, CAF-1, BOMB and RTBDN) induced a remarkable aberration of the cell cycle profile and phosphorylation of Chk-1, indicating the activation of a cell cycle checkpoint. In addition to what was observed with the siRNA against SETD8, silencing of CASP8AP2 also induced the phosphorylation of NBS1 and ATM (**Figure 2.13**). Taken together, these results indicate that ,mimicking the induction of DNA damage on its own is not sufficient to induce permissivity to AAV transduction. Instead, the phosphorylation of Chk1, one of the downstream effectors of the DDR signaling cascade, following cell treatment with the top-10 siRNAs, appears to be a common signature that correlates with enhanced AAV transduction.

Summary Results I

The results described in this Chapter show that the down-regulation of all the top-10 siRNAs that increase AAV transduction, identified in the high-throughput screening, was also able to increase, at different extents, phosphorylation of γ-H2AX (a hallmark of cellular DNA damage), with siRNAs against SETD8, CASP8AP2 and BOMB being the most effective.On the other hand, we observed that although the transfection of short DNA oligonucleotides in HeLa cells can efficiently mimics a cellular DDR response with induction of γ-H2AX histone phosphorylation to levels comparable to those exerted by most of the top-10 siRNAs, this was not sufficient to increase AAV infection. Indeed, we demonstrated that the sole synthetic oligonucleotide treatment was not able to trigger a complete DDR signaling cascade. Contrary, the down-regulation of SETD8, the most potent siRNA at inducing AAV transduction, appeared not only to cause phosphorylation of γ-H2AX, but also of NBS1, ATM and Chk1. The phosphorylation of Chk1, one of the downstream effectors of the DDR signaling cascade, following cell treatment with the top 10 siRNAs, appears to be the prevalent, although not indispensable, common signature that correlates with enhanced AAV transduction.

3. Results II

The second part of the work is focused on the identification and characterization of cellular factors required for efficient AAV transduction. The screening identified 535 siRNAs that decreased AAV infection without affecting cell viability, thus targeting factors that positively regulate AAV transduction. These siRNAs were re-screened for their efficiency to also increase transduction of self-complementary AAV (scAAV) vectors, with the ultimate goal of detecting cellular proteins differentially involved in the processing of the AAV ssDNA or dsDNA genomes. This screening was performed by simultaneously infecting cells, treated with the 535 siRNAs, with a standard ssAAV2 expressing Ds-Red and a scAAV2 expressing EGFP. The results of this screening are shown in **Figure 3.1**.

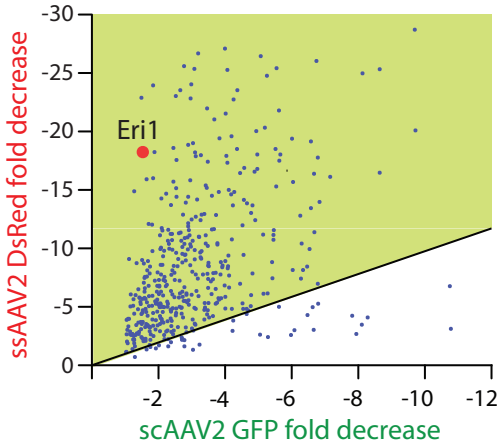

Figure 3.1. Results of the screening of 535 siRNAs previously found to decrease ssAAV2 transduction on the simultaneous infection of HeLa cells with ssAAV2-DsRed and scAAV2-GFP. The siRNA against Eri1 was one of the most effective in selectively impairing ssAAV (almost 20-fold reduction over control) but having marginal effect on scAAV (1.7 fold reduction).

3.1 Cellular factors selectively required for ssAAV infection.

We concentrated our attention on 7 factors (**Table 2**). The siRNAs against 4 of these selectively impaired ssAAV but not scAAV transduction. The targeted factors were C6ORF146, of unknown function; the exoribonuclease Eri1, involved in the regulation of the histone dosage and degradation of endogenous microRNAs (details shown in **Figure 3.1**); RDBP, a factor implicated in the RNA metabolism; and SCGB1D1, a factor predicted to be secreted. Other 3 factors instead appeared required for both ssAAV and scAAV transduction. These were BCCIP, a protein involved in DNA repair and interacting with BRCA2 and p21; MSH5, a protein acting in the DNA HR pathway; and PIK4CA, a cytoplasmic kinase.

	1st screening	2nd screening	
	AAV2 luc /ctrl	AAV2-dsRED /ctrl	scAAV2-GFP /ctrl
C6ORF146	0.20	0.10	0.90
ERI1	0.24	0.05	0.65
RDBP	0.16	0.10	0.63
SCGB1D1	0.15	0.06	0.60
BCCIP	0.24	0.04	0.23
MSH5	0.19	0.04	0.12
PIK4CA	0.12	0.15	0.03

Table 2. Factors required for cell permissivity to AAV transduction. The 7 factors listed were all identified in a primary screening testing AAV2-luciferase transduction of HeLa cells (the fold reduction in luciferase activity compared to control is reported in the first column). Short interfering RNAs against the 7 factors were then used in a secondary screening simultaneously assessing transduction with ssAAV2-DsRed and scAAV2-GFP (results in columns 2 and 3 respectively); siRNAs against the factors boxed in green selectively impaired ssAAV, those against the factors boxed in orange both ssAAV and scAAV.

We rescreened the selected siRNAs in cultured cell lines derived from different histological type of cancers, including as HeLa (cervical cancer), Huh7 (epatocarcinoma), U2OS (osteosarcoma), T98G (glioblastoma). Forty-eight hours after siRNA administration cells were infected simultaneously with ssAAV2-DsRed and a scAAV2-EGFP at an moi of 2500 vg/cells. As shown in **Figure 3.2**, the only siRNAs found to selectively inhibit ssAAV but not scAAV in a consistent manner without affecting cell viability **(Figure 3.2)** in all the cell lines was the one against

Eri1.

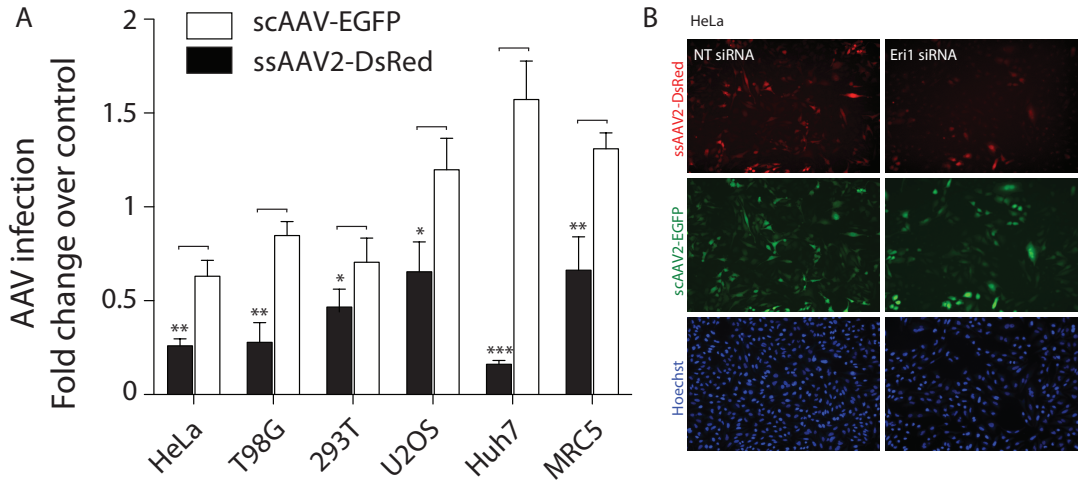

Figure 3.2. Eri1 silencing leads to a selective decrease of ssAAV infection in different cell lines (panel A). Representative immunofluorescence images in HeLa cells showing Eri1 silencing affects selectively ssAAV trasduction; the cells were coinfected simultaneously with ssAAV2 ds-Red and scAAV EGFP using a moi of 2500 vg/cell (panel B). Results represent mean and s.e.m. from 3 independent experiments. The percentage of infected cells was first normalized over untreated cells, and then we compared the ssAAV2-DsRed over the scAAV-EGFP values through t-test. Star-code for significance: *** $P<0.001$, ** $P<0.01$, * $P<0.05$.

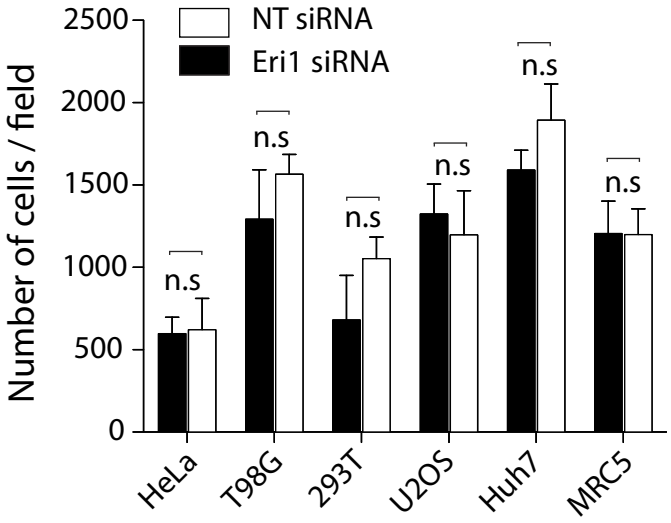

Figure 3.3. Eri1 silencing decreases ssAAV infection without affecting cell viability in different cell lines. Results represent mean and s.e.m. from 3 independent experiments. No statistically significant difference between NT siRNA- and Eri1 siRNA treated cells was observed (t-test).

Interestingly, Eri1 silencing also decreased ssAAV infection in highly permissive cells. Previous work from our group showed that the ATM–/– fibroblasts (AT5), a cell line lacking the ataxia-telangectasia mutated factor, one of the master regulators in the DDR pathway, are highly permissive to AAV transduction (Zentilin et al., 2001) . We silenced Eri1 with its specific siRNA for 48 hours in AT5 fibroblasts, and then we infected the cells with rAAV2-EGFP for 24 hours. The results indicated that the absence of Eri1 in AT5 cells totally abolishes the high permissivity to AAV, suggesting that Eri1 regulates AAV infection independently from or upstream the DDR pathway (**Figure 3.4**).

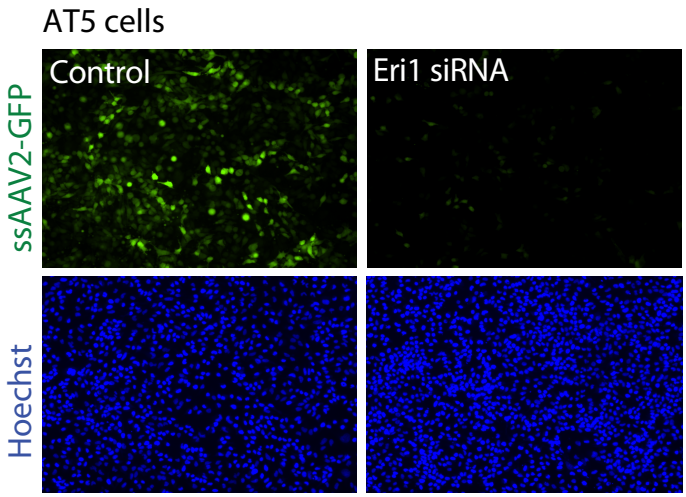

Figure 3.4. Representative immunofluorescence images showing that Eri1 silencing also decreases AAV transduction in ATM -/- fibroblasts (AT5 cells), which are highly permissive to AAV infection.

The siRNA used for the Eri1 knockdown experiments is a commercial pool of 4 individual siRNAs against the Eri1 mRNA. To exclude off-target effects, we deconvoluted this pool by testing the effects of the individual siRNAs separately. Three out of the four siRNAs composing the Eri1 silencing pool (siRNAs #1, #2, #3, #4) significantly decreased AAV-luciferase infection (Fig. 3.5A). We also tested the levels of the Eri1 mRNA in cells treated by the siRNA pool, and found that this was reduced over 5 times (Fig. 3.5B).

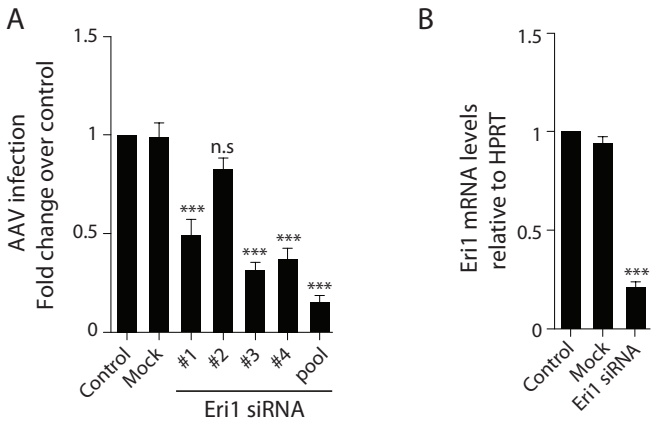

Figure 3.5. siRNA deconvolution experiment. Panel A: Three individual siRNAs out of the four composing the Eri1 silencing pool used in the screening (#1, #2, #3, #4) were able to significantly decrease AAV infection. After normalization over control, data were compared to mock by ANOVA test followed by Tukey post-hoc test.
Panel B: RT PCR analysis revealed that Eri1 siRNA was able to significantly decrease ER1 mRNA. The values derived from siRNA treated cells were first normalized against untreated cells (control), and then compared with mock by t-test.
Star-code for statistical significance: *** $P<0.001$, n.s. not significant.

3.2 Eri1 stimulates rAAV transduction

Our data indicate that Eri1 is required for efficient AAV transduction, since the knock down of its mRNA significantly decreased it. We thus wanted to test whether, on the contrary, the overexpression of the protein might increase transduction. To this end, we transfected a plasmid encoding recombinant Eri1 fused to GFP under the control of the CMV promoter in different cell lines (HeLa, T98G, 293T, U2OS, Huh7, MRC5). Twenty-four hours after transfection cells were infected with AAV2-DsRed (moi, 2500 viral particles per cell). The quantification, by high-content fluorescence microscopy, of the percentage of GFP positive cells allowed measuring the number of transfected cells, whereas the count of Ds-Red positive cells indicated the extent of AAV infection. We observed that AAV transduction increased following Eri1 overexpression, from 2 up to 7 times depending on the cell type (**Figure 3.6);** this effect was prominent also in cells

showing low permissitivity, such as MRC5 (**Figure 3.7**).

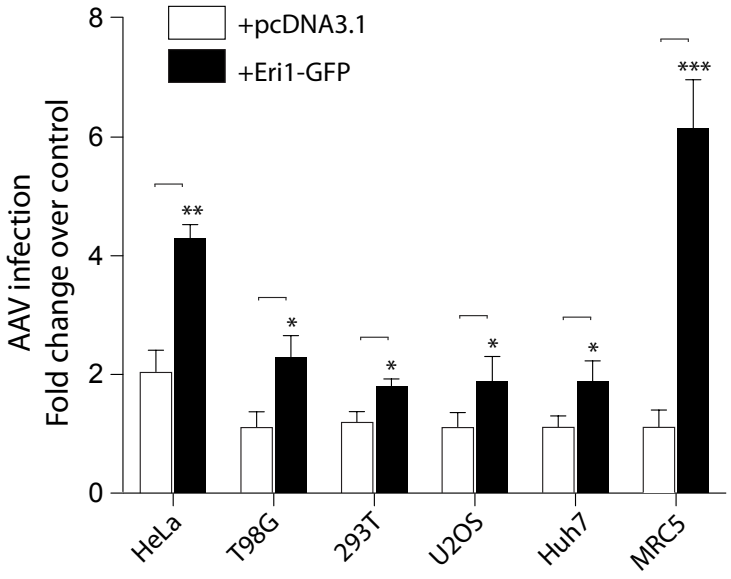

Figure 3.6. Effect of Eri1 overexpression on AAV transduction in different cell lines. Results show mean and s.e.m. from three independent experiments. The values derived from Eri1 transfected cells were first normalized against untreated cells, and then we compared the results obtained in Eri1-GFP transfected cells with those in pcDNA3.1 transfected cells, by t-test. Star-code for statistical significance: *** $P<0.001$, ** $P<0.01$, * $P<0.05$.

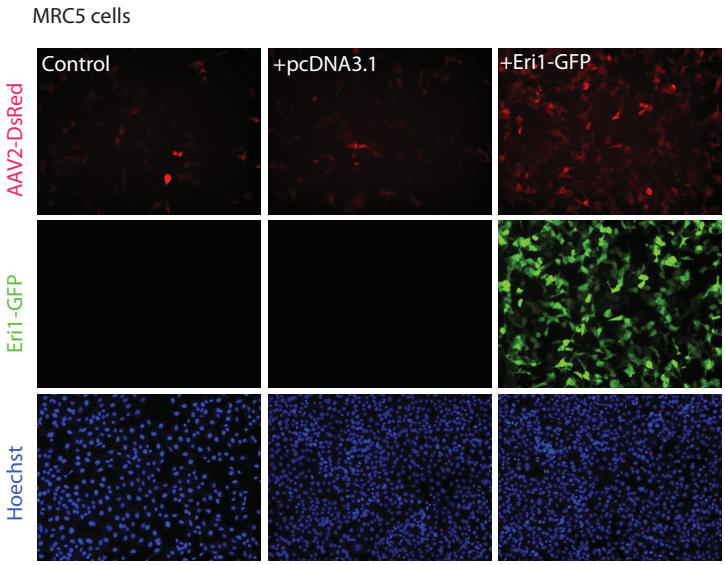

Figure 3.7. Representative immunofluorescence images in MRC5 cells showing AAV infection after Eri1-GFP overexpression. MRC5 cells were transfected with a plasmid expressing an Eri1-GFP fusion protein for 24 h and then infected with AAV2-DsRed using a moi of 2500 viral particles per cell.

Consistent with the screening results, Eri1 overexpression did not significantly modify the levels of scAAV transduction, confirming that this factor is crucial for ssAAV transduction **(Figure 3.8** panel A**).** The enhancing effect on rAAV2 transduction increased linearly with the amount of transfected plasmid, as shown for HeLa cells infected with AAV2-Luciferase reporter vector (**Figure 3.8** panel B**)**. The bell shaped dose-response curve is probably consequent of toxicity of the protein at high doses.

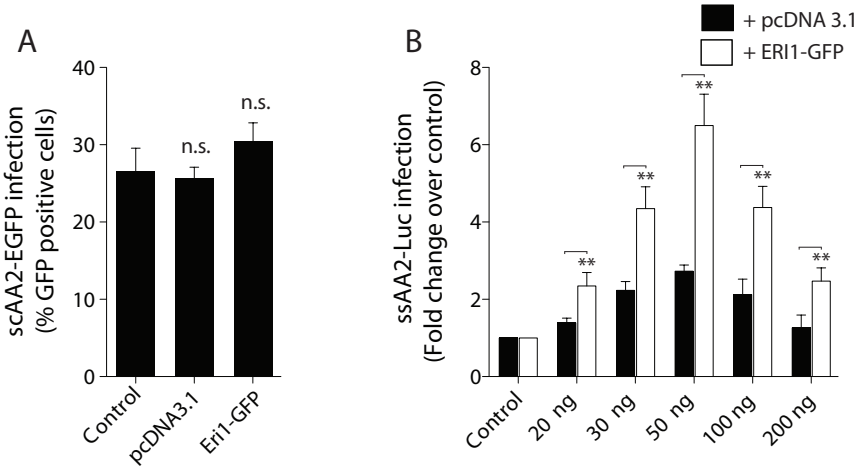

Figure 3.8. Panel A **:** The effect of Eri1 overexpression on scAAV transduction in not significant. Treated samples were compared to the control using one-way ANOVA followed by Tukey post-hoc test; N.s. = not significant . Panel B : the graph shows a dose response curve that correlates transfected Eri1 DNA and ssAAV transduction efficiency in HeLa cells. Results show mean and s.e.m. from three independent experiments. The infection of ssAAV2 of transfected cells was first normalized against control; then we compared the Eri1-GFP transfected cells over the pcDNA3.1 transfected cells. For each different amount of DNA, *P*-values were < 0.01, calculated by Student t-test.

3.3 Mechanism of action of Eri1 on AAV transduction

3.3.1 Eri1 levels do not correlate with the amount of AAV DNA inside the cell nucleus.

Eri1 is an evolutionarily conserved 3'-5' exoribonuclease, which participates in end-processing and turnover of replication-dependent histone mRNAs (Dominski et al., 2003). Over the course of evolution, Eri1 has also been recruited into a variety of conserved and species-specific regulatory small RNA pathways, which include the regulation of endogenous small RNAs (Kennedy et al., 2004). Eri1, as other stem-loop binding proteins, localizes predominantly in the nucleus at the G1/G2 phases and at the beginning of S phase of the cell cycle. Throughout the S phase, Eri1 is partially redistributes to the cytoplasm. Binding to histone mRNA is necessary for cytoplasmic localization (Yang et al., 2006). Since Eri1 shuttles between the nucleus and the cytoplasm, we wanted to verify whether Eri1 silencing or overexpression could somehow interfere with AAV nuclear entry. We performed experiments either silencing Eri1 for 48 hours or overexpressing the protein for 24 hours. After treatment, the cells were infected for 24 hours with AAV2-Luc, using a moi of 2500 vg/cell. We quantified, by real time PCR, the number of rAAV genomes present in the HeLa nuclear fraction in order to measure the extent of viral DNA nuclear entry. Eri1 levels did not correlate with the amount of AAV DNA inside the cell nucleus (**Figure 3.9**).

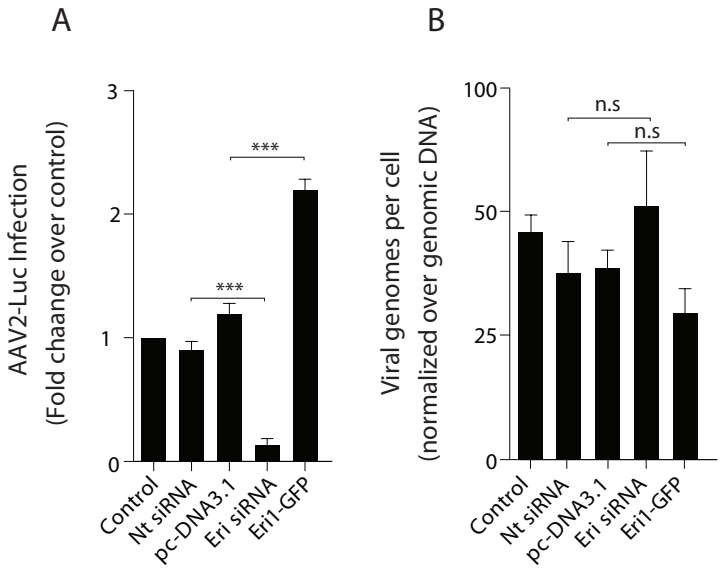

Figure 3.9. Efficiency of AAV transduction (panel A) and amount of viral DNA in the nucleus (panel B) in HeLa cells in which Eri1 was either knocked out or overexpressed. Results show mean and s.e.m. from three independent experiments. Statistical significance was assessed by t-test comparing samples with their respective relative mock : *** P <0.001, n.s. not significant.
.

3.3.2 The effect of Eri1on ssAAV transduction is independent from the RNAi pathway.

It has also been demonstrated that Eri1 physically interacts and cooperates with the Dicer complex for miRNA precursor processing (Kennedy et al., 2004). Thus we wanted to ascertain whether the effect of the protein on AAV transduction were mediated by interference with the miRNA pathway. We knocked out Dicer and Drosha in HeLa cells by specific siRNA transfection; after 48 hours, cells were infected with AAV-luc, at a moi=2500 vg/cell (**Figure 3.10**). Changes in AAV infection after Drosha silencing were negligible, while the Dicer knock-down exhibited an opposite effect on AAV transduction compared to treatment with the Eri1 siRNA. These data suggest that Eri1 does not exert its effect on the modulation of AAV transduction through the RNAi pathway.

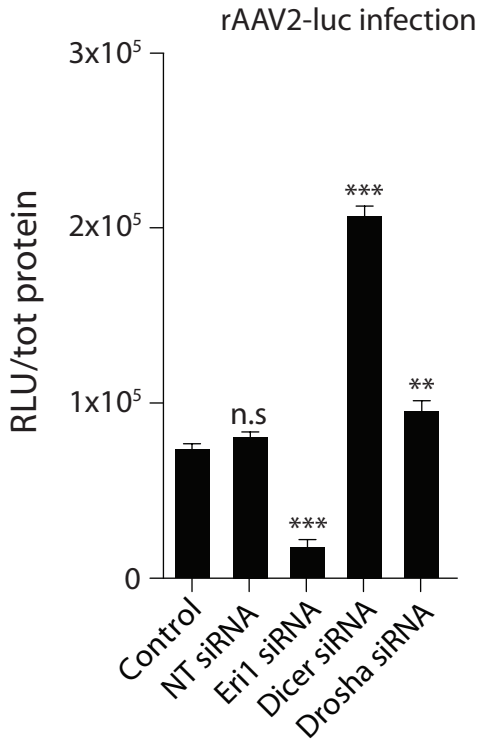

Figure 3.10. Effect of Dicer and Drosha knockout on AAV transduction. HeLa cells were silenced for 48 hours using siRNAs against Dicer or Drosha and then infected with AAC-luc. The mean ± sem of three independent experiments is shown. Differences between siRNAs treated samples over the control were assessed by using one-way ANOVA test followed by Tukey post-hoc test. Code for statistical significance: ** $P<0.01$, *** $P<0.001$, n.s. not significant.

3.3.3 Eri1 mutants

To start exploring the molecular mechanisms by which Eri1 selectively favours ssAAV transduction, we took advantage of three Eri1 mutants, each one lacking a specific functional domain of the protein (kindly provided by Dr. Zbigniew Dominski (Yang et al., 2006)). These Eri1 variants include: a mutant deleted in the SAP domain, the putative Eri1 DNA binding domain, useful to assess a possible direct interaction of Eri1 with the ssAAV DNA genome; a mutant in R105A, unable to bind the stem loop structure typical of the histone mRNAs, useful to prove a possible involvement of the histone mRNA degradation pathway during the ssAAV transduction; a mutant in M235A defective for the exoribonuclease activity, unable

to degrade both histone mRNA and endogenous small RNAs (**Figure 3.11**).

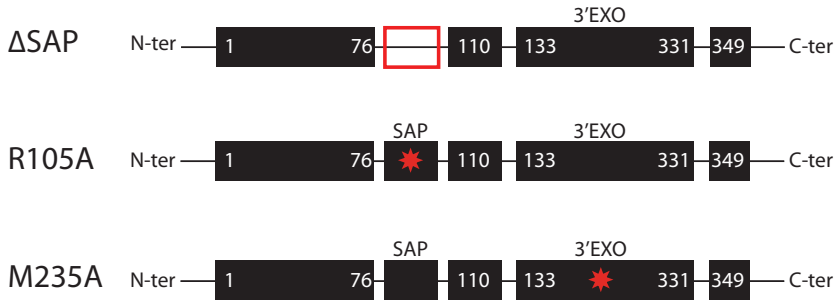

Figure 3.11 Eri1 mutants. In order to understand the molecular mechanism by which Eri1 selectively favors ssAAV transduction, we took advantage of Eri1 mutants lacking the DNA putative binding domain (ΔSAP), the histone mRNA-binding domains (R105A), or mutated in the catalytic domain of the protein (M235A).

We sub-cloned the Eri1 mutant cDNAs into a N-terminal P-Flag CMV mammalian expression vector to perform protein overexpression experiments and protein functional assays.

We transfected the three Eri1 mutants in HeLa cells and verified their expression by western blotting (**Figure 3.12**).

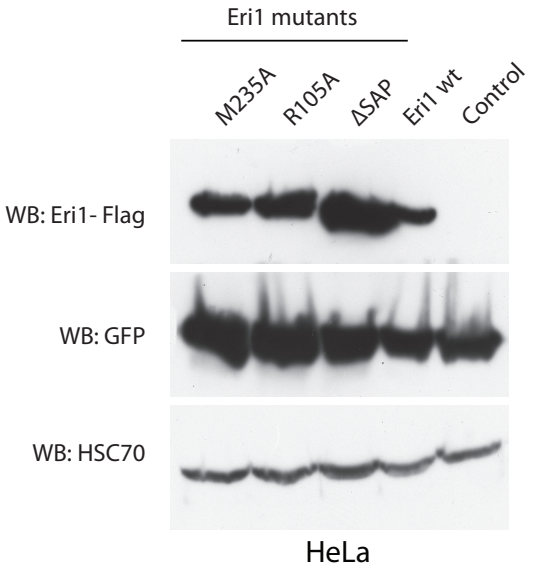

Figure 3.12. Levels of expression of Eri1 mutants. HeLa cells were simultaneously transfected with expression plasmids for the Eri1 mutants and the p-EGFP N1 plasmid (10:1 ratio). Western blot analysis was performed with an anti-Flag antibody. HSC70 was used as loading control and an anti-GFP antibody as transfection control.

The mutant Eri1 expression vectors were transfected in HeLa and, after 24 hours, cells were infected with AAV2-luc, moi 2500 vg/cell, in order to achieve a quantitative measurement of AAV infectivity. As shown in **Figure 3.13** panel A, only the wild-type Eri1 was able to induce AAV infection.

Eri1 was described as a factor able to degrade several histone mRNAs; more specifically it was deeply characterized as an exoribonuclease capable to strongly reduce the mRNA of the H2A histone. We therefore assessed the ability of the Eri1 mutants to degrade the H2A mRNA. After 24 hours from transfection, the levels of H2A mRNA were determined by real-time PCR. Our results indicate that all the mutants, at a different extent, were less efficient in histone mRNA degradation compared to wild-type Eri1 (**Figure 3.13** panel B). Taking into account the intrinsic difficulty to study histone gene expression, due to their huge number, their temporal tight regulation, considering also possible biases coming from the cellular model we used, we decided to focus on HIST1 H2A gene expression; despite this, other results indicate us that wild-type Eri1 overexpression is able to reduce significantly also HIST1 H3A and HIST1H4A histone mRNAs (data not shown). Since HU treatment has been previously described as an agent able to lead to cellular histone mRNA degradation (Sittman et al., 1983) we used this drug as a positive control in both AAV infection experiments and histone mRNA analysis. Comparing the results from the mutant overexpression experiments, we observed that there was a general negative correlation between AAV transduction and histone mRNA levels (**Figure 3.12)**. This observation suggested that Eri1 could modulate AAV infection by altering histone dosage, possibly modulating the chromatinization of the recombinant AAV genomes.

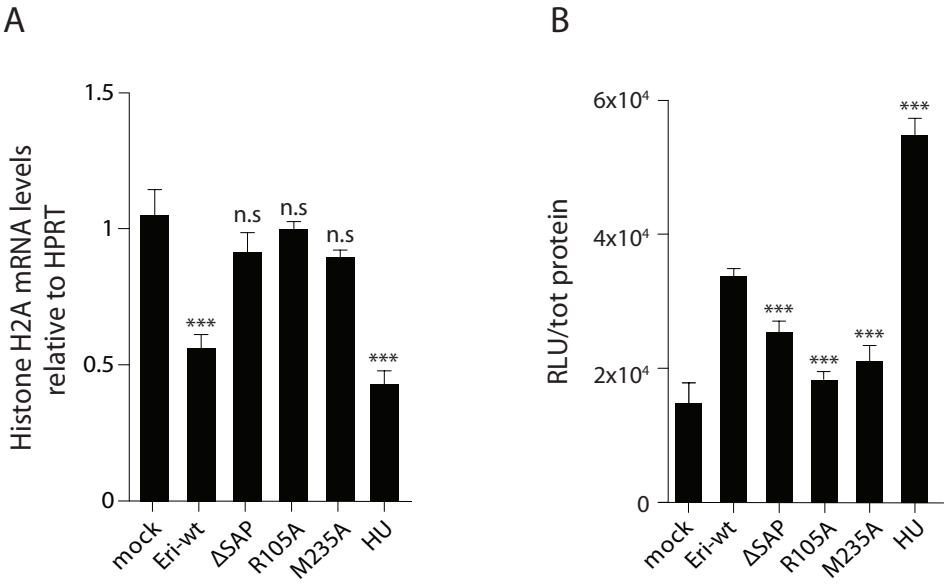

Figure 3.13. Eri1 mutants were overexpressed in HeLa cells for 24 hours before infection with an AAV2 expressing the firefly luciferase reporter gene using an moi of 2500 vg/cell. Panel A shows the levels of histone H2A mRNA normalized over untreated control; Eri1 mutants are not able to reduce H2A mRNA. Panel B shows the effect on AAV transduction of Eri1 mutants compared to wild type protein, measured as luciferase activity. Statistical significance was computed comparing treated samples over mock (Panel A) or wild type Eri1 (Panel B) using one-way ANOVA test followed by Tukey post-hoc test. The graphs show mean ± s.e.m. of three different experiments. Code for statistical significance: ** *P*=0.01, *** *P*=0.001, n.s. not significant.

3.3.4 Hydroxyurea requires Eri1 to increase ssAAV transduction

Hydroxyurea, a drug markedly increasing AAV transduction, also triggers the degradation of several classes of histone mRNAs through a molecular mechanism that is not completely understood yet (Sittman et al., 1983). To verify whether HU requires Eri1 activity to promote the enhancement of AAV transduction, we silenced Eri1 in HeLa cells before HU treatment and AAV2-Luc infection (see **Figure 3.14** panel A for a scheme of the experiment). As expected, HU treatment alone was able to increase AAV transduction but, notably, this effect was totally abolished if Eri1 was down-regulated (**Figure 3.14** panel B)**.** Thus, HU requires the integrity of Eri1 to exert its effect on ssAAV transduction. By RT-PCR analysis, we also observed that HU treatment induced a two fold increase of Eri1 mRNA levels

(**Figure 3.15**). Although there are many possible and described mechanisms that can explain the ability of HU to increase rAAV transduction, (e.g. augmented AAV nuclear entry, increased AAV double strand DNA conversion (Russell et al., 1995) (Johnson and Samulski, 2009) our observations underline the existence of an additional effect of HU that requires Eri1 catalytic activity.

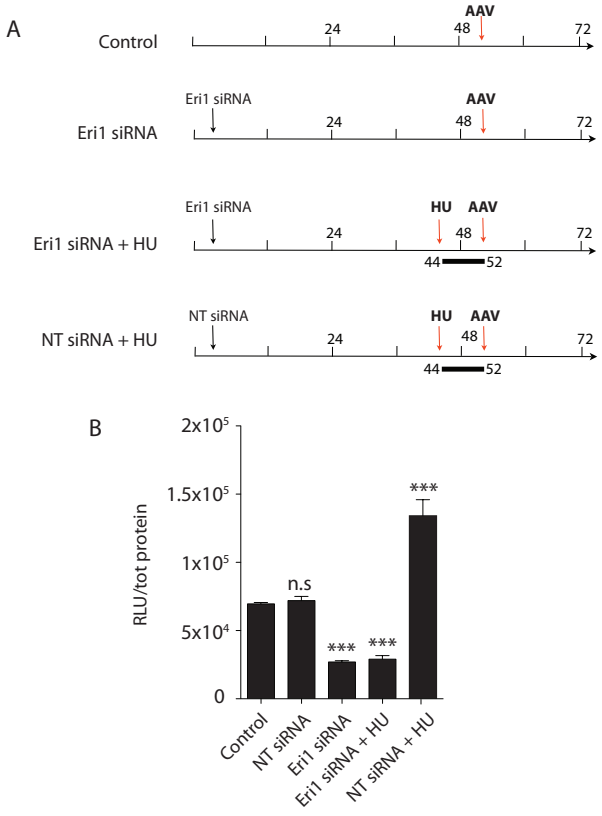

Figure 3.14. Combined effect of Eri1 knockdown and HU treatment on AAV infection of HeLa cells. Scheme of the experiment (panel A): Eri1 was silenced in HeLa cells before HU treatment; cells were been infected using an AAV2 vector expressing the firefly luciferase reporter gene. HU treatment alone was able to increase AAV infection and this effect was totally abolished when Eri1 was down-regulated (panel B). The results show mean±s.e.m. of 3 independent experiments, differences, between samples and control were evaluated by one-way anova followed by Tukey post-hoc test. Code for statistical significance:*** $P<0.001$, n.s= not significant.

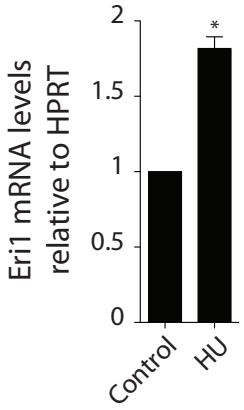

Figure 3.15. Levels of Eri1 mRNA in HeLa cells treated with HU. HeLa cells were treated with HU for 8 hours. The results are normalized over HPRT expression and show mean±s.e.m. of at least 3 independent experiments. Difference between HU treated sample and control were assessed by t-tests. Code for statistical significance (t-test) :* $P<0.05$.

3.3.5 rAAV chromatinization affects viral transduction

Although previous works have demonstrated that episomal rAAV genomes are assembled in a chromatin-like structures, the mechanism by which chromatinization occurs on AAV genomes is not elucidated (Marcus-Sekura and Carter, 1983) (Penaud-Budloo et al., 2008). Some authors previously reported that AAV genomes, once inside the nucleus of the target cells, are covered by histones, and that HDAC inhibitors could enhance the efficiency of AAV transduction (Okada et al., 2006). With the ultimate goal of studying the impact of AAV genome chromatinization in the establishment of successful viral transduction, we analyzed our primary siRNA screening data as far the HDAC genes were specifically concerned. We observed that, following down-regulation of all the six HDAC proteins, In all cases, AAV transduction increased from 2 up to 15 folds compared to the control (**Figure 3.16**). These observations further underline the correlation between viral chromatin status and AAV transduction.

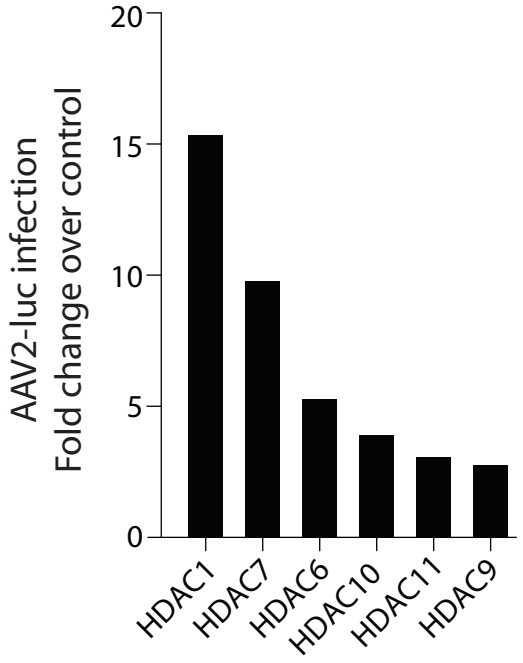

Figure 3.16. Levels of AAV transduction after HDAC knock down. HeLa cells were silenced for 48 hours and then infected with ssAAV2-luc for 24 hours. The measurement of firefly activity has been use to assess AAV infectivity and then the values were normalized over Nt-siRNA control. Bars represent the mean of the duplicate samples from the primary high throughput screening on AAV transduction.

To further explore this issue, we reconsidered the effect of the siRNA against CAF-1, one of the top-10 siRNAs increasing AAV transduction selected in the high throughput screening. CAF-1 is described as the main replication-dependent chromatin assembly factor in eukaryotic cells (Marheineke and Krude, 1998). We observed that its down-regulation in HeLa cells increased ssAAV transduction over 15 folds compared to control (**Figure 3.17**). However, when we co-silenced simultaneously Eri1 and CAF-1 the positive effect of CAF-1 siRNA on AAV infection was totally abolished (**Figure 3.18**). These results are consistent with the possibility that CAF-1 might participate in chromatin assembly during the processing of the ssAAV genome to a transcription competent ds molecule and, importantly, emphasizes the notion that rAAV chromatinization could be inhibitory for viral transduction.

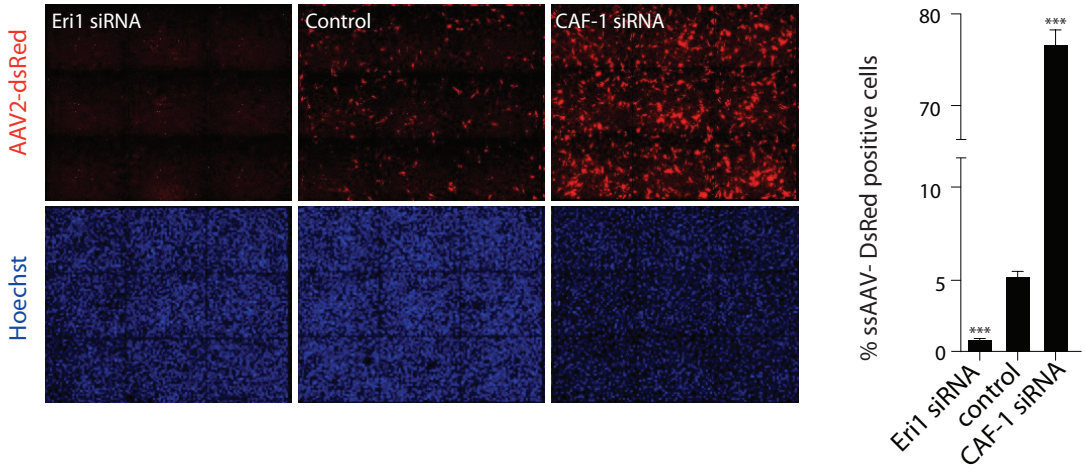

Figure 3.17. Effect of CAF-1 knock down on AAV transduction. HeLa cells were silenced for 48 hours using Eri1 and CAF-1 siRNAs. Shown are the mean±s.e.m. of 3 independent experiments. Differences, between siRNA treated samples and control were evaluated by one-way ANOVA analysis followed by Tukey post-hoc test. Code for statistical significance: *** P<0.001, n.s= not significant..

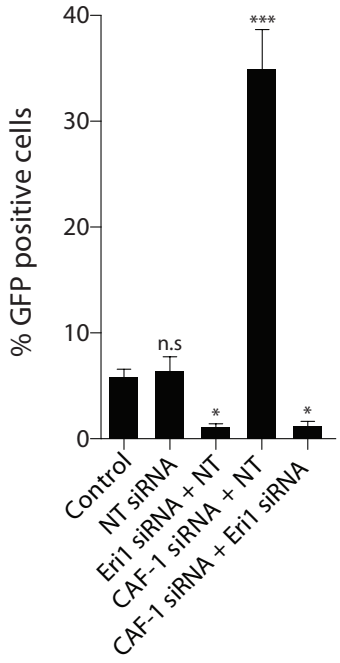

Figure 3.18. Effect of the simultaneous knock down of Eri1 and CAF-1 on AAV transduction. Eri1 and CAF-1 were simultaneously silenced in HeLa cells. After the knock-down, cells were infected with AAV2-EGFP. Differences between siRNA treated samples and control were evaluated by using one-way ANOVA test followed by post-hoc test. Graphs show the mean±s.e.m. of 3 independent experiments. Code for statistical significance : * P<0.05, *** P<0.001, n.s. not significant.

3.3.6 ssAAV and scAAV chromatin immunoprecipitation after Eri1 overexpression or HU treatment

To directly assess the molecular interaction of histone proteins with AAV genomes, we performed chromatin immunoprecipitation (ChIP) studies using specific antibodies to histone H3 and H4, as well as to the variant H3.3, considered a mark of open-chromatin (Chow et al., 2005) and pan acetylated H3 (Ac-H3), commonly associated with transcriptional activity (Cheung et al., 2000). We also performed ChiP experiments using antibodies against some DDR-related proteins (MRE11 and NBS1), inhibitory on AAV transduction (Cervelli et al.) (Lovric et al.), against H2AX, a DNA-damage related histone variant (Kuo and Yang, 2008) and against CAF-1 in order to asses its association with the AAV genomes.

Cross-linked and sonicated chromatin from untreated HEK293T and from cells infected simultaneously with ssAAV2-DsRed and scAAV2-EGFP at a moi of $1x10^4$ viral particles per cell, with or without Eri1 overexpression or HU treatment, was immunoprecipitated with each antibody. The amount of cross-linked DNA specific for rAAV was then assessed by real-time PCR using specific primers for ssAAV2-DsRed and scAAV2-EGFP genomes.

The overexpression of Eri1 determined an over 10-fold, selective reduction of ssAAV genome association with H3 and H4 proteins, while changes were negligible for scAAV AAV. After Eri1 overexpression or HU treatments, we also measured a decreased of H3 trimethyl K9 association with the AAV genome, a histone mark related to transcriptional repression. Moreover, we observed a different chromatin composition pattern on the self-complementary AAV genome, which showed enrichment for the histone variant H3.3 compared to ssAAV (**Figure 3.19**). Since H3.3 is mark of open-chromatin and it can be loaded onto DNA in a replication-independent manner, this could explain its presence on the scAAV genome. Increase of ssAAV2 transduction by Eri1 overexpression also caused a significant decrease in the association, with the viral DNA, of proteins of the cellular DNA damage response, such as NBS1 and MRE11.

After these treatments, we also measured a decrease in the association with the

AAV genome of some molecular signatures typical of the DDR, such as phosphorylated histone H2AX Eri1 overexpression or HU treatment also lead to a decrease of CAF-1 associated with the ssAAV genome (**Figure 3.19**).

Taken together, these results suggest that Eri1 regulates rAAV transduction through cellular histone dosage modulation and, in particular, that it increases cell permissivity to ssAAV transduction by relieving the inhibition that chromatinization and cellular DDR proteins impose on the incoming viral genomes.

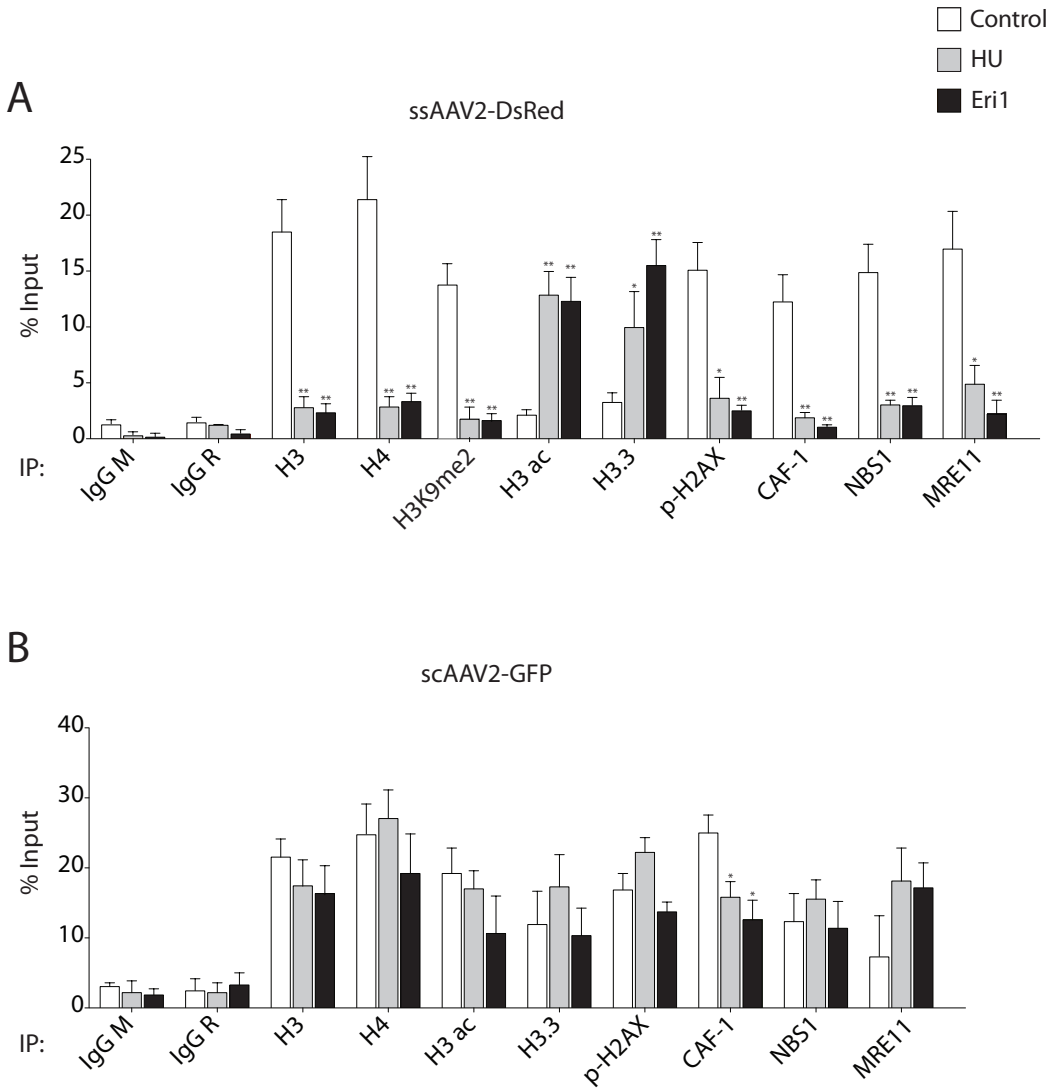

Figure 3.19. Results of chromatin immunoprecipitation experiments. ChIP experiments showed that the overexpression of Eri1 or HU treatment determined an over 10-fold, selective reduction of ssAAV genome association with H3 and H4 (panel A), while changes were negligible for scAAV DNA and for selected cellular genes (panel B). A different chromatin composition pattern was observed on the self-complementary AAV genome, which was enriched in the histone variant H3.3 compared to ssAAV (panel B). Eri1 overexpression, similar to HU treatment, increased AAV association with acetylated H3 and decreased that with H3 tri-methyl K9; a reduction in the DNA-damage related markers p-H2AX and NBS1 was also noticed. Differences between Eri1 or HU treated samples and control were assessed by using one-way ANOVA followed by Tukeys post-hoc test. Results represent the mean and s.e.m. from at least three independent chromatin immunoprecipitation experiments. Code for statistical significance : * $P<0.05$; ** $P<0.01$.

Summary Results II

The findings obtained in this chapter allowed shedding light on cellular factors involved in single-stranded (ss) AAV genome processing.

Starting from the data of high-throughput screening on AAV transduction we compared the effect of individual siRNAs against approximately 1,500 genes on transduction of HeLa cells with a standard, ssAAV2 vector expressing the Ds-Red monomer and a self-complementary (sc) AAV2 vectors expressing EGFP respectively. Notably, this analysis highlighted a previously unrecognized essential and selective role of ERI-1, a 3'-exoribonuclease known to degrade endogenous miRNAs and histone mRNAs, for ssAAV transduction. To understand the molecular mechanism by which ERI-1 selectively favors ssAAV transduction, we took advantage of ERI-1 mutants lacking the DNA- or the histone mRNA-binding domains, or mutated in the catalytic domain of the protein. We determined that ERI-1 affects ssAAV transduction neither via degradation of endogenous microRNAs nor by direct interaction with the AAV genome. In contrast, we observed that AAV transduction negatively correlated with histone mRNA levels. Interestingly, hydroxyurea, a drug markedly increasing AAV transduction, also determined histone mRNA degradation and required integrity of ERI-1 for its effect on AAV. By chromatin immunoprecipitation studies aimed at assessing the extent of chromatinization of the AAV genome, we concluded that the overexpression of ERI-1 determined an over 10-fold, selective reduction on ssAAV genome association with H3 and H4, while changes were negligible for scAAV DNA and for selected cellular genes. Consistent with chromatin exerting a repressive role on ssAAV transduction, we also observed that the downregulation of the main replication-dependent histone chaperone CAF-1 induced an over 20-fold increase in transduction. In line with our previous findings, we noticed that increase of ssAAV2 transduction by ERI-1 overexpression also caused a significant decrease in the association, with the viral DNA, of proteins of the cellular DNA damage response (DDR; e.g. Nbs1 and Mre11).

4. Discussion

This PhD thesis aims to characterize some molecular mechanisms involved in the cellular regulation of rAAV transduction. Starting from the data obtained from a high-throughput screening on rAAV transduction, performed using a genome-wide siRNA library, here we characterize the effect of some cellular factors involved in rAAV infection. In particular, we demonstrate that the activation of a cellular S-phase checkpoint is the prevalent common signature of the top-10 siRNA able to increase AAV transduction. This is in line with our previous observations that the activation of DNA damage response correlates with the efficiency of AAV in vitro.
The second part of this thesis highlights a previously undervalued role of the AAV genome chromatin state as a determinant of cellular permissivity to transduction. In particular, we describe and discuss the action of Eri1, a cellular exoribonuclease that modulate rAAV transduction exerting its role through the regulation of the cellular histone dosage.
A unifying hypothesis that links DNA damage and S-phase checkpoint activation with the rAAV chromatinization process is presented in the model described at the end of this discussion section.

4.1 The activation of cellular S-phase checkpoint positively correlates with AAV transduction

Long standing evidence indicates that AAV genome can be recognized inside the host cell by the DNA damage response (DDR) machinery and that genotoxic damage increases cellular permissivity to AAV (Zentilin et al., 2001) (Russell et al., 1995). In addition, different laboratories, including our own, have previously shown that proteins of the DDR, namely those of the MRN (MRE11-RAD50-NBS1) complex, inhibit AAV transduction in both cell culture (Cervelli et al., 2008) and

primary cells *in vivo* (Lovric et al., 2012). To systematically identify the host cell factors involved in the internalization, intracellular trafficking, processing of AAV genome and, eventually, AAV gene expression, either positively or negatively, we performed a high-throughput screening using a genome-wide siRNA library (18175 human gene targets). Consistent with our previous results, among the genes that restrict transduction by AAV vectors, this genome-wide screening, identified members of the MRN complex and other genes involved in the cellular DDR, as well as genes belonging to the ubiquitin-proteasome system.

Following these findings, we decided to investigate whether the top ten siRNAs of our primary screening were able to induce cellular DNA damage in the absence of viral infection. We first analyzed the phosphorylation of histone H2AX at Serine 139 (γ-H2AX), a hallmark of cellular DNA damage (Kuo and Yang, 2008), in HeLa cells treated with the selected siRNAs. The down-regulation of all the top-10 genes was able to increases γ-H2AX phosphorylation at different extents, with SETD8, CASP8AP2 and BOMB being the most effective. To further understand the contribution of DNA damage on rAAV transduction efficiency, we devised an experimental strategy exploiting short DNA oligonucleotides as decoys of the DDR response proteins, inhibitory of rAAV transduction. The rationale of this approach was based on the demonstration that small DNA oligonucleotides transfected into cells mimic DNA double-strand breaks and acted by disorganizing the damage signaling and DNA repair machinery. A similar approach was successfully used to inhibit the DNA repair system in cancer cells and to increase the efficacy of chemotherapy in colon or rectal cancer (Quanz et al., 2009). All the transfected oligonucleotides were able to promote phosphorylation of γ-H2AX histone in HeLa cells comparably to the effect exerted by most of the top-10 siRNAs; however, contrary to the top-10 siRNAs or genotoxic agents such as hydroxyurea, the oligonucleotide treatment was unable to increase AAV transduction. We showed that the synthetic oligonucleotides tested, although recognized as damaged DNA, were not able to trigger completely the DDR signaling cascade, and that the sole activation of γ-H2AX was not sufficient to enhance cell permissivity to AAV vector

transduction. On the other hand, the down-regulation of SETD8, the most potent siRNA at inducing AAV transduction, appeared not only to cause phosphorylation of γ-H2AX, but also of NBS1, ATM and Chk1. Further analysis, using all top 10 siRNA, revealed that at least 6 of them (SETD8, CASP8AP2, NPAT, CAF-1, BOMB and RTBDN) induced a remarkable aberration of the cell cycle profile and phosphorylation of Chk-1, a marker that indicates the activation of a cell cycle checkpoint (Martinho et al., 1998). We demonstrated that induction of DNA damage in terms of γ-H2AX activation on its own is not sufficient to explain the molecular mechanism of the siRNAs action. On the other hand, the phosphorylation of Chk1, one of the downstream effectors of the DDR signaling cascade, following cell treatment with the top 10 siRNAs, appears to be the prevalent, although not indispensable, common signature that correlates with enhanced AAV transduction. Taken together, these results indicate that several of the siRNAs inducing cellular permissivity to AAV do so by inducing DNA damage and checkpoint activation.

4.2 Eri1 selectively favours ssAAV transduction

The results of the high throughput screening allowed us to identifying not only siRNAs that enhanced but also 535 siRNAs that decreased AAV transduction without affecting cell viability. The targets of these siRNAs apparently comprise factors that are required for AAV transduction. Considering that the single-strand to double-strand conversion of the AAV vector genome inside the host cell potentially represents a limiting step for a successful gene transfer, we decided to specifically focus our study on factors involved in AAV genome processing. With this concept in mind, we compared, in secondary screenings, the effect of individual siRNAs against the approximately 500 genes required for AAV infection, on the transduction efficiency of a standard ssAAV2 vector expressing the Ds-Red monomer and a scAAV2 vectors expressing EGFP. Among other genes, the results

of our screening revealed that Eri1, a 3'-exoribonuclease known to degrade endogenous miRNAs and histone mRNAs (Kennedy et al., 2004) (Yang et al., 2006), was essential for ssAAV, but largely dispensable for scAAV transduction. The knockdown of Eri1 decreased ssAAV infection about 5 fold over control whereas changes in the scAAV transduction were negligible.

Eri1 is required for replication-dependent degradation of histone mRNA, but it is also involved in microRNA homeostasis and maturation of ribosomal 5.8S RNA (Gabel and Ruvkun, 2008; Thomas et al., 2012). To discriminate the exact molecular mechanism by which Eri1 selectively favours ssAAV transduction, we took advantage of Eri1 mutants lacking the DNA- or the histone mRNA-binding domains, or mutated in the catalytic domain of the protein. Our analysis clearly determined that Eri1 does not affect ssAAV transduction via degradation of endogenous microRNAs, nor by direct interaction with the AAV genome, since the overexpression of mutants lacking the putative DNA-binding domains (ΔSAP), or mutated in the catalytic domain (M235A) of the protein were not able to induce AAV transduction. In contrast, we observed that a defect in the histone mRNA degradation activity of Eri1 negatively correlates with AAV transduction. Taken together, these data suggest that Eri1 may exert its action on AAV transduction through the modulation of the cellular histone dosage and consequently influencing the dynamics of chromatin remodeling on AAV genome.

4.3 rAAV chromatinization influences viral transduction

It is not a novelty that chromatin dynamics and epigenetic modifications play a pivotal role in the biology of many viruses. Both AAV and another parvovirus, MVM (Minute Virus of Mice), have been previously described as organized in a chromatin structure within hours after infection in cell culture (Ben-Asher et al., 1982) (Marcus-Sekura and Carter, 1983). Moreover, R.O. Snyder and colleagues demonstrated, in non -human primates, that rAAV vectors reside predominantly as

episomal monomeric and concatameric circles in transduced skeletal muscle and that episomal AAV genomes assimilate into chromatin with a typical nucleosomal pattern (Penaud-Budloo et al., 2008). The same laboratory also found that vector genomes and gene expression persist for years in quiescent tissues, such as muscle, and suggested that the chromatin structure of AAV DNA was important for episomal maintenance and transgene expression (Penaud-Budloo et al., 2008).
In this respect, from an analysis of the data of the high-throughput screening, it is interesting to note that all the siRNAs directed against cellular histone deacetylases (HDACs) enhanced AAV transduction; the fact that HDACs are inhibitory toward AAV represents a possible indication that the chromatin state of the vector genome is crucial for an efficient viral transduction. The HDAC knockdown was able, in HeLa cells, to increase AAV infection at different extents, from 2.5 folds up to 15. These findings highlight the importance of chromatin epigenetic modifications in the efficient AAV-mediated transgene expression, and confirm previous data demonstrating that HDAC inhibitors enhanced rAAV transduction, probably by increasing the acetylation of the histones associated with AAV genome (Okada et al., 2006).

4.4 Histone metabolism and AAV infection

Eri1 plays a pivotal role in the modulation of histone metabolism; thanks to its exoribonuclase activity it can trigger the specific degradation of several classes of histone mRNAs being able to selectively recognize a particular stem-loop structure present only in the 3′ of histone mRNA (Hoefig et al., 2013). Replication-dependent histone transcripts are characterized by the absence of introns and by the presence of a stem-loop structure at the 3′ end of a very short 3′ untranslated region (UTR). These features, together with a need for active translation, are a prerequisite for their rapid decay. It has been demonstrated that Lsm1, a factor belonging to the histone mRNA processing complex, cooperates with Eri1

exoribonuclease promoting genomic stability through the control of histone mRNA decay in yeast (Herrero and Moreno, 2011). Interestingly, our high-throughput screening revealed that the silencing of both Lsm1 and Lsm7, factors cooperating with Eri1 to degrade histone mRNA, were able to decrease ssAAV infection from 3.3 to 6.7 folds compared to the control. These data provided another evidence supporting the concept that Eri1 modulates AAV infection acting through the histone mRNA degradation pathway.

Histone biosynthesis is so tightly synchronized with DNA synthesis that pools of free histones are virtually absent in proliferating cells because they are synthetized at levels matching the actual requirement for chromatin assembly; only a little variation on the stoichiometric ratio between DNA and histones could be dramatically toxic for the cells (Osley, 1991) (Singh et al., 2010).

Cellular histone dosage is tightly regulated at a transcriptional level. The regulation of the cyclin E-Cdk2 substrate NPAT, which is essential for both histone gene expression and S phase entry, provides a mechanism coordinating histone and DNA synthesis in mammalian cells (Zhao, 2004). Interestingly, the siRNA against NPAT, a master regulator of the histone gene transcription, is one of the top-10 siRNAs able to increase AAV infection identified in our screening.

4.5 DNA damage induced by hydroxyurea requires the integrity of Eri1 to increase AAV transduction

DNA damage induces a down-regulation of histone gene expression through the G1 checkpoint pathway and also triggers histone degradation at the mRNA level (Su et al., 2004) (Muller et al., 2007) (Levine et al., 1987). The mRNA levels of mammalian replication-dependent histones, both linker histone H1 and the four core-histones (H2a, H2b, H3, H4), are down-regulated in a coordinated manner in parallel with the inhibition of DNA synthesis upon DNA damage (Su et al., 2004). It is well established that hydroxyurea, a drug known to increase AAV transduction,

is also able to trigger the degradation of histone mRNAs (Hoefig et al., 2013). Taken together this evidence suggested us that hydroxyurea could exert its effect on AAV transduction by acting on the histone mRNA degradation pathway. Our experiments showed that HU requires, indeed, the integrity of Eri1 to exert its inducing effect on ssAAV transduction, since its enhancing action is totally abolished upon knocking down Eri1. Hydroxyurea may use different mechanisms to modulate AAV transduction. We previously hypothesized that HU, like other genotoxic treatments, contributes to divert inhibitory proteins of the DDR machinery away from the rAAV genomes (Cervelli et al., 2008). Samulski and colleagues showed that HU enhances AAV transduction also by increasing the AAV nucleolar trafficking (Johnson and Samulski, 2009). In the present settings, we observed that treatment of HeLa cells with HU caused a two fold increase of Eri1 mRNA level suggesting an additional molecular mechanism for the positive effect on rAAV transduction that include increased Eri1 expression and augmented histone degradation.

4.6 Dynamics of cellular protein associations onto the AAV DNA

The findings of the present work together with our previous results support a model according to which, upon entering the nucleus, recombinant ssAAV genomes, by virtue of both their ssDNA nature and the presence of the viral ITRs, are recognized by cellular DDR proteins, including MRN and MDC1. It is conceivable to hypothesize that the DNA damage response evoked by the presence of single stranded, hairpinned DNA genomes or during the conversion of from ss- to ds- viral DNA contributes to recruit histone types that are specific for closed heterochromatin, as it was recently described (Ayrapetov et al., 2014).

Our results show that the histone chaperone CAF-1 binds the AAV genome and exerts a negative effect on the efficiency of transgene expression. Multiple published evidence indicate that CAF-1 plays a role in setting up a repressed

chromatin state, illustrating that the propagation of silenced chromatin is intimately linked to the histone deposition process. Moreover, it was shown that the loss of CAF-1 function causes heterochromatin abnormalities and loss of viability during development in mouse, Xenopus and Drosophila (Quivy et al., 2001) (Moggs et al., 2000). It is possible that a mechanism that contributes to repress AAV transduction at a chromatin level can represent an evolutionary conserved innate immunity defense of the host cell against invading viruses (Lilley et al., 2010) (Arbuckle and Kristie, 2014).

On the other hand, scAAV genomes, proficient for self-annealing, can skip the double-strand conversion process together with a chromatinization process that is dependent on DNA synthesis. Moreover, it is unlikely that scAAV genomes interact with the same cellular DDR pathway as ssAAV and this may lead to a different chromatin molecular signature on their DNA (Cataldi and McCarty, 2010). In this respect, ChIP experiments showed higher association of H3.3 histone variant, a marker of open chromatin, with scAAV than ssAAV. It is known that H3.3 can be loaded onto DNA in a replication-independent manner (Chow et al., 2005) and that it constitutes the predominant form of histone H3 in non-dividing cells (Wunsch and Lough, 1987) (Pina and Suau, 1987). Interestingly, previous reports have described histone H3.3 associated also with the double stranded DNA of helper dependent Adenovirus (Ross et al., 2011).

While the H3.3 variant is prevalent on scAAV genomes, we observed that the H3 canonical H3 form also immunoprecipitated with viral DNA (Figure 4.1). This finding is not surprising, since histone H3 can be loaded onto the double stranded AAV genome following intra-molecular and intermolecular recombination events that involve cellular DNA polymerases and topoisomerases (Choi et al., 2005) and CAF-1 as histone chaperone. Nevertheless, upon CAF-1 depletion, the ssAAV transgene expression increases two fold relative to scAAV infection, indicating that the siRNA against CAF-1 differentially increases ssAAV with respect to scAAV transduction.

Changes in cellular histone dosage, mediated by Eri1, influence chromatin

assembly and composition on rAAV genomes. Han and Grunstein showed that nucleosome loss, through histone depletion, resulted in the increased transcription of numerous genes in yeast (Kim et al., 1988) and this provided the first *in vivo* evidence that nucleosomes can repress gene activity. Partial histone depletion can lead to an increase of homologous recombination and defects in DNA repair in eukaryotic cells (Prado and Aguilera, 2005). Consistent with the proposed model, we observed, by ChIP experiments, that the overexpression of Eri1 determined over 10-fold selective reduction of H3 and H4 histones associated with ssAAV genome paralleled by increased loading of the variant H3.3, while, in similar conditions, changes in histone composition were negligible for scAAV DNA. Conceivably, this double-stranded genome, immediately ready for transcription, presents an "open chromatin pattern", independent from CAF-1-mediated nucleosome assembly

Collectively, these results indicate that Eri1 is an essential factor mediating cell permissivity to ssAAV transduction by relieving the inhibition that chromatinization and cellular DDR proteins impose on the incoming viral genomes. This information can be exploited for the development of more effective AAV-mediate gene delivery strategies.

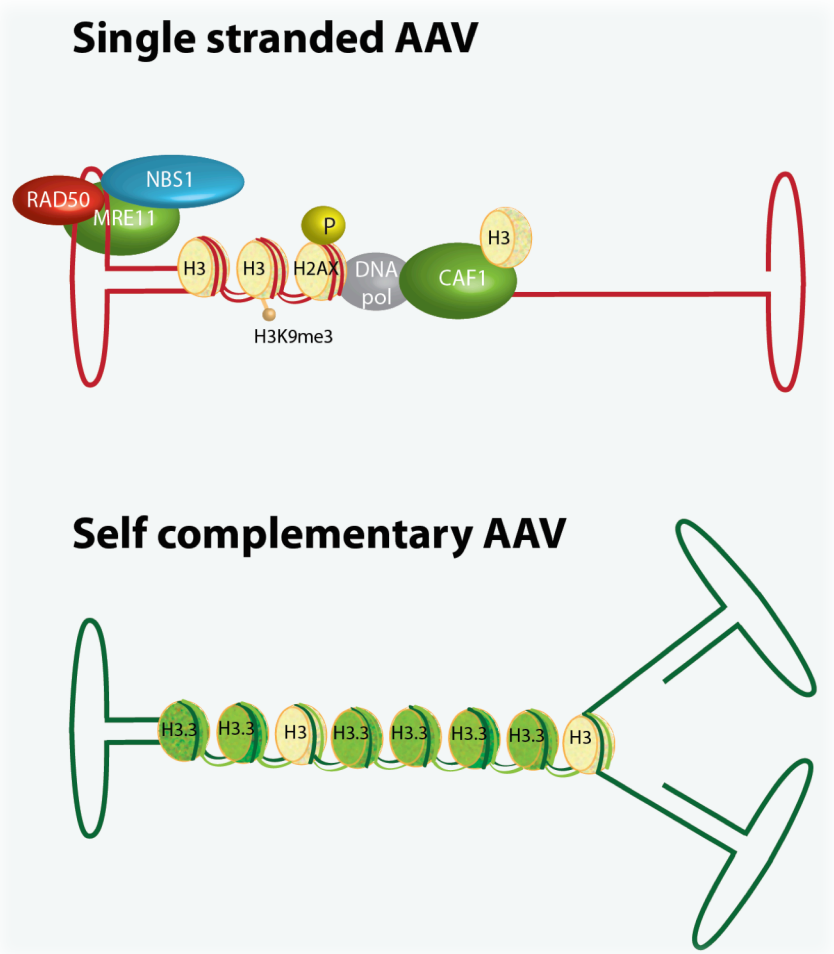

Figure 4.1 A model to explain cellular permissivity to ssAAV and scAAV.
ssAAV is recognized by the host cell as damaged DNA. This event generates a repressive chromatin environment on ssAAV during the conversion to dsDNA, which is mediated by CAF-1. scAAV presents an "open chromatin pattern" as defined by its interaction with the histone H3.3 variant. Both hydroxyurea treatment and Eri1 overexpression lead to histone depletion by degrading histone mRNAs, thus causing chromatin relaxation. These results indicate AAV chromatinization is essential to mediate cell permissivity to AAV transduction.

5. Materials and Methods

Cell cultures

HeLa, HEK293T, T98G, U2OS were purchased from the American Type Culture Collection (ATCC); MRC5 and AT5 cells were obtained in 2001 from F. d'Adda di Fagagna (The Wellcome/CRC Institute, Cambridge, United Kingdom). Huh7 cells were kindly obtained from Alessandro Marcello (ICGEB of Trieste).

The cells were cultured in Dulbecco's modified Eagle's medium (DMEM) supplemented with 10% fetal bovine serum (Life Technologies) and antibiotics, in a 5% CO2, humidified atmosphere, at 37°C.

DNA transfections

DNA oligonucleotides

HeLa cells were plated in 96 multi-well plates at a final concentration of $1x10^4$ cells per well. After 24 hours, cells were transfected with 50 ng of each DNA oligonucleotide used in this study, mixed with 0.12 µl Fugene lipofectamine (Promega) according to the manufacturer's recommendations. To obtain double-stranded oligonugleotides, an equal volume of both complementary oligo sequences was mixed at equimolar concentration in a 1.5 ml microfuge tube, heated to 90–95 °C for 3–5 min and then slowly cooled down in about 45–60 min to room temperature. Oligonucleotides were purchased from Integrated DNA Technologies (IDT, Coralville, Iowa, USA).

Sequences of used oligonucleotides:

20 bp, ACGAAGTCGCGAGACTGACG.

30 bp, CGTTTATCGCGAGCTGGTAGTACCGTAGAT.

50 bp, CGAGCTGAAGTAATTGGCTAGCTAGCTAGTTATCGATCGTACGTATTCA.

60 bp,

ACTGTATCGAGTCGTCGATCGAGCTAGCGTCAGCTGGCGTAAACTCCCGACTTAGGTC
G.

ITR,

TGCGCGCTCGCTCGCTCACTGAGGCCGCCCGGGCAAAGCCCGGGCGTCGGGCGACCT
TTGGTCGCCCGGCCTCAGTG.

Plasmids

The plasmids that express Eri1 fused with the green fluorescent protein at its C-terminus as well as the Eri1 mutants ΔSAP, 105, and 235 were kindly provided by Z. Dominski (University of University of North Carolina , Chapel Hill, NC). Eri1 mutant cDNAs were subcloned by PCR into two different mammalian expression plasmids:

1) N-Terminal p-FLAG-CMV (Sigma-Aldrich) (Cloning sites: NotI ,SalI)

Forward primer : ATAAGAATGCGGCCGCAGAGGATCCACAGAGTAA.

Reverse primer: TGCGGTCGACTTATTACTTTCTAAAATGTGGCATT .

2) p-EGFP N1 (Clontech) (Cloning sites: XhoI, PstI)

Forward primer: CCGCTCGAGATGGAGGATCCACAGAGTAA.

Reverse primer: AACTGCAGGCGACTTTCTAAAATGTGGCATT.

Eri1 wild type cDNA was also subclonend into the XhoI and AgeI sites into the p-DsRed N1 monomer vector (Clonthech)

Production of rAAV stocks

The rAAV vectors used in this study, AAV2-EGFP, AAV2-DsRED, AAV2-Luc and AAV2sc-EGFP were prepared by the AAV Vector Unit at the International Centre for Genetic Engineering and Biotechnology Trieste (http://www.icgeb.org/avu-core-

facility.html), as described previously (Arsic et al., 2004) with a few modifications. Briefly, infectious recombinant AAV vector particles were generated in HEK293T cells culture in roller bottles by dual plasmid co-transfection procedure with pDG as packaging helper plasmid (kindly provided by J. A. Kleinschmidt, DKFZ, Germany). Viral stocks were obtained by PEG precipitation and $CsCl_2$ gradient centrifugation (Ayuso et al. 2009). The physical titer of recombinant AAVs was determined by quantifying vector genomes (vg) packaged into viral particles, by real-time PCR against a standard curve of a plasmid containing the vector genome (Zentilin et al., 2001); values obtained were in the range of $1x10^{12}$ to $1x10^{13}$ vg per milliliter.

All the plasmids containing the AAV backbone, with the inverted terminal repeats, were grown in XL-10 Gold E. coli strain (Stratagene-Agilent Technologies, Santa Clara, CA, USA)

Immunofluorescence

For the AAV transduction experiments with ssAAV2-DsRed or scAAV2-EGFP, cells were cells were grown on 96-well plates or on 4-well chamber slides (Lab.Tek). At the indicated time points after AAV infection, plasmid transfection, or chemical treatments, cells were washed twice with PBS and fixed with 2% paraformaldehyde (Sigma in PBS for 15 min at room temperature. Cells were permeabilized with 0.1% Triton X-100 in PBS for 20 min followed by 100% acetone at –20°C for 20 sec and blocked with 2% BSA and 0.15% glycine in PBS. Plates were incubated with the indicated primary antibody in blocking solution overnight at 4°C. The following antibodies were used: rabbit anti phospho-NBS1 p-Ser343 NB100-92610 (Novus Biologicals CO, USA) (1:100), anti-phosoho-histone-H2A.X Ser139 05-636 (Merck Millipore MA, USA) (1:200). After washing, samples were stained with secondary anti-rabbit or anti-mouse IgG conjugated with Alexa-Flour 488 or Alexa-Flour 594 (Molecular Probes, Eugene, OR, USA), dilution 1:1000, for 1

hour at room temperature. Samples were washed with PBS + 0.1% Tween and mounted in Vectashield Mounting Medium containing 4'-6'-diamino-2-phenylidole (DAPI) (Vector Laboratories, Burlingame, CA, USA) or with Hoechst 33258 (Life Technologies).

Acquisition of images from 96 multiwell plates was performed using ImagineXpress Micro automated high-content screening fluorescence microscope (Molecular Devices CA, USA) at 10X magnification; a total of 9 imagines were acquired per well, corresponding to approximately 10.000 -15.000 cells per condition. Imagine analysis was performed using the "Multi-Wavelenght Cell Scoring" application module implemented in MetaXpress software (Molecular Devices).

RNA interference

Cells were reverse-transfected in antibiotic-free 1g/l glucose 10% fetal bovine serum Dulbecco's modified eagle medium using Lipofectamine® RNAiMAX (Life technologies), according to the manufacturer's recommendations.

Dharmacon SMART - pool® (four siRNAs per gene) against SETD8 (M-031917-00-0005), CASP82AP2 (M-012413-01-0005), SOX15 (M-012354-00-0005), TROAP (M-019980-01-0005), NPAT (M-019599-02-0005), PHC3 (M-015805-01-0005), SF3B1 (M-020061-02-0005), CAF-1, RTBDN (M-014723-01-0005), BOMB (M-016585-01-0005), CORF146 (M-018430-00-0005), Eri1 (M-021497-01-0005), RDBP (M-011761-01-0005), BCCIP (M-013030-01-0005), MSH5 (M-011337-01-0005), SCGB1D1 (M-012290-00-0005), PIK4CA (M-006776-04-0005) were used at the final concentration of 50 nanomolar (Dharmacon, Lafayette, CO, USA).

Western blotting

Total cell lysates were prepared from cells treated with siRNAs. For the immunoblotting, the cells were scraped at 4°C in HNNG buffer (15 mM Hepes pH 7.5, 250 mM NaCl, 1% NP-40, 5% glycerol, 1 mM PMSF) supplemented with 25 mM NaF, 10 mM β-glycerophosphate, 0.2 mM sodium orthovanadate and protease inhibitors cocktail tablet (Roche). The samples were heated to 90°C for 5 min before loading. Protein concentration was determined by the colorimetric BCA protein assay reading at 562 nm absorbance (Thermo Fisher Scientific, Madison, WI, USA) using atomatize Envision 2014 Multilabel Reader (PerkinElmer, Inc USA). Fifteen µg of proteins were resolved on 8% to 12% SDS-PAGE minigels, and transferred onto reinforced nitrocellulose membranes (Optitran BA-S 83, Whatman GE Healthcare, Life Sciences).

Before immunoblotting with the primary antibodies for phospho-H2AX and phospho-ATM, membranes were blocked in 5% Bovine serum albumin (BSA) in TBST (50 mM Tris-HCl pH 7.4, 200 mM NaCl, 0.04 % Tween 20) at room temperature for 2 hours. Immunoblots with the primary antibody for p-NBS1 were blocked over-night in 5% non-fat dry milk; immunoblots with the primary antibodies for NBS1, P-Chk1, ATM, Chk1, α-tubulin and anti- HSP70 were blocked in 5% non-fat dry milk for two hours at room temperature for 2 hours.

Primary antibodies detection was achieved with horseradish peroxidase-conjugated anti-rabbit or anti-mouse secondary antibodies (Santa Cruz CA, USA Biotechnology), diluted 1:3000, and exposure to X-ray film (Kodak) after incubation with ECL chemiluminescence solution (ECL™ Prime, GE Healthcare Amersham™).

The following antibodies were used in this study: mouse anti-α-tubulin and anti-HSP70 (diluted 1:10,000 in 5% non-fat dry milk) (Sigma Aldrich), mouse anti-Phospho-ATM p-Ser1981 (diluted 1: 500 in 5% BSA) mAb 4526 (Cell Signaling, MA, USA), rabbit anti-ATM total D2E2 (diluted 1:500 in 5% BSA) (Cell Signaling, MA, USA), rabbit anti phospho-NBS1 p-Ser343 (diluted 1:500 in 5% non-fat dry milk) NB100-92610 (Novus Biologicals CO, USA), rabbit NBS1 total (diluted 1:3000 in

non-fat dry milk) NB-100143 (Novus Biologicals CO, USA), rabbit p-Chk1 p-Ser345 (diluted 1:500 in 5% BSA) 133D3 (Cell Signaling, MA, USA), mouse Chk1 total (diluted 1:1000 in non-fat dry milk) 2D1G5 (Cell Signaling, MA, USA), mouse anti-phosoho-histone-H2A.X Ser139 (diluted 1:500 in 5% BSA) 05-636 (Merck Millipore MA, USA). Hydroxyurea (HU, Sigma) was used a positive control in all these experiments; where indicated, cells were incubated overnight with 1 mM HU.

Gene expression analysis

Total RNA from tissues and cells was isolated using TRIzol solution (Invitrogen). Total RNA was reverse transcribed using random primers (Invitrogen) and M-MLV reverse transcriptase (Invitrogen). Real-time quantitative PCR (qPCR) analysis was performed using the iQ™Supermix (BioRad) and TaqMan® Gene Expression Assays (Applied Biosystems) specific for the following transcripts of human origin: Eri1(# 4351372), H2A.Z (# 4331182) HPRT (# 4331182), GAPDH (# 4331182).
The amplification reactions were run in duplicates on the CFX96 Real-Time PCR Detection System/C1000 Thermal Cycler (BioRad) for 40 cycles using universal cycling conditions (95°C for 10 min, followed by 40 cycles of 95°C for 15 sec and 60°C for 1 min), according to the manufacturer's recommendations. Results were normalized to HPRT or GAPDH housekeeping genes.

Chromatin immunoprecipitation (ChIP)

Aproximatly $20x10^6$ HEK293T cells were co-transduced with self-complemetary AAV2-EGFP and single strand AAV2 DsRed at an moi of 10^4 vgp/cell each. Where indicated, cells were pre-treated with 1 mM HU overnight or transfected with an expression plasmid for Eri1 48 hours before infection. At 24 hours after infection, cells were washed with PBS and subsequently fixed by adding fixing solution (11%

formaldehyde, 100 mM NaCl, 1 mM EDTA, 0.5 mM EGTA pH 8.0, 50 mM Tris-HCl pH 8.0) directly to the aderent cells at 1% final concentration. Cross-linking reaction was allowed to proceed for 10 min at 37°C and was stopped by the addition of glycine at a final concentration of 0.125 M. Fixed cells were scraped and collected in 50 ml falcon tubes. The cells were washed once in ice-cold PBS, once in buffer B1 (0.25% Triton X-100, 10 mM EDTA, 0.5 mM EGTA, 10 mM Tris-HCl pH 8.0) and once in buffer B2 (1 mM EDTA, 0.5 mM EGTA, 200 mM NaCl, 10 mM Tris-HCl pH 8.0, 4% NP-40). Cells were digested with 1.5 unit of MNase per 10^6 cells lysate (S7 nuclease, Roche Applied Science) for 15 min at 37°C and the reaction was stopped by adding EDTA, 3 mM final concentration. Cells were pelleted by centrifugation at 700 x g per xx min and resuspended in RIPA 50 buffer

(50 mM NaCl, 20 mM Tris-HCl pH 7.4, 1 mM EDTA, 0.5% NP-40, 0.5% deoxycholic acid, 0.1% sodium dodecyl sulfate (SDS), protease inhibitors). Chromatin was sonicated (45 pulses, 10 sec on and 10 sec stop) on ice and centrifuged to pellet debris. Immunoprecipitations were precleared by adding 100 µl of total Protein A/G PLUS-Agarose (Santa Cruz CA, USA) for 3 hours at 4°.

Tree µg of primary antibody per mg of total protein was used (an average 2-5 µl of pure antibody per lysate deriving from $5x10^6$ cells, depending on the antibody concentration). The primary antibody was incubated at 4°C overnight. Immune complexes were collected with 100 µl of protein A/G PLUS-Agarose (Santa Cruz CA, USA), and beads were washed two times with RIPA 150 buffer (same as RIPA 50 but with 150 mM NaCl), two times with low-salt-wash-buffer (0.1% SDS 0.1% Triton X-100 500 mM NaCl 2mM EDTA 20mM Tris-HCl pH 8.0), two times with high-salt-wash-buffer (1mM EDTA, 10mM Tris-HCl pH 8.0, 1% NP-40, 1% DOC, 0.25M LiCl). Protein-DNA complexes were washed once in TE buffer and finally resuspended in 200 µl of TE buffer and digested with 5 IU of DNase-free RNase (Roche) for 30 min at 37°C. Samples were then treated for 3 hours at 56°C with 300 g/ml proteinase K (Sigma) in 0.5% SDS, 100 mM NaCl, and were incubated overnight at 65°C to revert crosslinks. DNA was extracted with phenol-chloroform-isoamyl alcohol, ethanol precipitation and resuspended in water for real-time PCR quantification of scAAV

and dsRed AAV genome. Quantitative SYBR green PCR was performed using primer pairs that bind both ssAAV and scAAV genome under the following condition : Activation at 95°C for 2 min, 40 cycles of denaturation at 95°C for 3 sec and annealing/extension at 60°C for 30 sec, followed by melting analysis ramping at 60°C to 95°C.

Primer pairs used :

GFP forward : 5'- CAGAAGAACGGCATCAAGGT - 3'

GFP Reverse : 5' - ACTGGGTGCTCAGGTAGTGG - 3'

DsRed forward : 5' - TCCATGAACTTCGAGGACGG - 3'

DeRed Reverse : 5' - GCCCTTGAACTTCACCTTGTAG - 3'

The following antibodies were used for chromatin immunoprecipitation: anti-histone H3 total, (06-755) (Merck Millipore MA, USA), anti-histone H4 total (07-108) (Merck Millipore MA, USA), anti-histone H3.3 (09-838) (Merck Millipore MA, USA), anti-trimethyl-histone H3 (Lys9) (05-1242), Anti-acetyl-Histone H3 Antibody 06-599 (Merck Millipore MA, USA), anti-CAF-1 (04-1523) (Merck Millipore MA, USA), anti-NBS1 (NB-100143) (Novus Biologicals CO, USA), anti-histone H2AX (07-627) (Merck Millipore MA, USA), anti-phosoho-histone-H2A.X Ser139 (05-636) (Merck Millipore MA, USA).

Statistical analysis

Unless otherwise indicated, all data are presented as mean ± standard error of the mean (s.e.m.). Statistical analysis was carried out using Prism Software (GraphPad). For statistical comparison of two groups, two-tailed Student's t-test was used. Analysis of multiple data sets was performed using one-way ANOVA followed by Tukeys post-hoc test. Star code for significance: *** $P< 0.001$, ** $0.001<P<0.01$, ** $0.01<P<0.05$, n.s. not significant.

6. Bibliography

Allan, J., Cowling, G.J., Harborne, N., Cattini, P., Craigie, R., and Gould, H. (1981). Regulation of the higher-order structure of chromatin by histones H1 and H5. J Cell Biol *90*, 279-288.

Ansel, K.M., Pastor, W.A., Rath, N., Lapan, A.D., Glasmacher, E., Wolf, C., Smith, L.C., Papadopoulou, N., Lamperti, E.D., Tahiliani, M.*, et al.* (2008). Mouse Eri1 interacts with the ribosome and catalyzes 5.8S rRNA processing. Nat Struct Mol Biol *15*, 523-530.

Aravind, L., and Koonin, E.V. (2000). SAP - a putative DNA-binding motif involved in chromosomal organization. Trends Biochem Sci *25*, 112-114.

Arbuckle, J.H., and Kristie, T.M. (2014). Epigenetic repression of herpes simplex virus infection by the nucleosome remodeler CHD3. MBio *5*, e01027-01013.

Arents, G., Burlingame, R.W., Wang, B.C., Love, W.E., and Moudrianakis, E.N. (1991). The nucleosomal core histone octamer at 3.1 A resolution: a tripartite protein assembly and a left-handed superhelix. Proc Natl Acad Sci U S A *88*, 10148-10152.

Ashktorab, H., and Srivastava, A. (1989). Identification of nuclear proteins that specifically interact with adeno-associated virus type 2 inverted terminal repeat hairpin DNA. J Virol *63*, 3034-3039.

Atchison, R.W., Casto, B.C., and Hammon, W.M. (1966). Electron microscopy of adenovirus-associated virus (AAV) in cell cultures. Virology *29*, 353-357.

Ayrapetov, M.K., Gursoy-Yuzugullu, O., Xu, C., Xu, Y., and Price, B.D. (2014). DNA double-strand breaks promote methylation of histone H3 on lysine 9 and transient formation of repressive chromatin. Proc Natl Acad Sci U S A *111*, 9169-9174.

Bartlett, J.S., Wilcher, R., and Samulski, R.J. (2000). Infectious entry pathway of adeno-associated virus and adeno-associated virus vectors. J Virol *74*, 2777-2785.

Becerra, S.P., Koczot, F., Fabisch, P., and Rose, J.A. (1988). Synthesis of adeno-associated virus structural proteins requires both alternative mRNA splicing and alternative initiations from a single transcript. J Virol *62*, 2745-2754.

Ben-Asher, E., Bratosin, S., and Aloni, Y. (1982). Intracellular DNA of the parvovirus minute virus of mice is organized in a minichromosome structure. J Virol *41*, 1044-1054.

Berns, K.I., and Linden, R.M. (1995). The cryptic life style of adeno-associated virus. Bioessays *17*, 237-245.

Bish, L.T., Morine, K., Sleeper, M.M., Sanmiguel, J., Wu, D., Gao, G., Wilson, J.M., and Sweeney, H.L. (2008). Adeno-associated virus (AAV) serotype 9 provides global cardiac gene transfer superior to AAV1, AAV6, AAV7, and AAV8 in the mouse and rat. Hum Gene Ther *19*, 1359-1368.

Buch, P.K., Bainbridge, J.W., and Ali, R.R. (2008). AAV-mediated gene therapy for retinal disorders: from mouse to man. Gene Ther *15*, 849-857.

Carrier, F., Georgel, P.T., Pourquier, P., Blake, M., Kontny, H.U., Antinore, M.J., Gariboldi, M., Myers, T.G., Weinstein, J.N., Pommier, Y.*, et al.* (1999). Gadd45, a p53-responsive stress protein, modifies DNA accessibility on damaged chromatin. Mol Cell Biol *19*, 1673-1685.

Carter, B.J. (2005). Adeno-associated virus vectors in clinical trials. Hum Gene Ther *16*, 541-550.

Casto, B.C., Atchison, R.W., and Hammon, W.M. (1967). Studies on the relationship between adeno-associated virus type I (AAV-1) and adenoviruses. I. Replication of AAV-1 in certain cell cultures and its effect on helper adenovirus. Virology *32*, 52-59.

Cataldi, M.P., and McCarty, D.M. (2010). Differential effects of DNA double-strand break repair pathways on single-strand and self-complementary adeno-associated virus vector genomes. J Virol *84*, 8673-8682.

Cervelli, T., Palacios, J.A., Zentilin, L., Mano, M., Schwartz, R.A., Weitzman, M.D., and Giacca, M. (2008). Processing of recombinant AAV genomes occurs in specific

nuclear structures that overlap with foci of DNA-damage-response proteins. J Cell Sci *121*, 349-357.

Chaturvedi, P., Eng, W.K., Zhu, Y., Mattern, M.R., Mishra, R., Hurle, M.R., Zhang, X., Annan, R.S., Lu, Q., Faucette, L.F.*, et al.* (1999). Mammalian Chk2 is a downstream effector of the ATM-dependent DNA damage checkpoint pathway. Oncogene *18*, 4047-4054.

Chen, C.C., and Tyler, J. (2008). Chromatin reassembly signals the end of DNA repair. Cell Cycle *7*, 3792-3797.

Chen, Y., and Poon, R.Y. (2008). The multiple checkpoint functions of CHK1 and CHK2 in maintenance of genome stability. Front Biosci *13*, 5016-5029.

Cheng, Y., and Patel, D.J. (2004). Crystallographic structure of the nuclease domain of 3'hExo, a DEDDh family member, bound to rAMP. J Mol Biol *343*, 305-312.

Cheung, P., Allis, C.D., and Sassone-Corsi, P. (2000). Signaling to chromatin through histone modifications. Cell *103*, 263-271.

Cheutin, T., McNairn, A.J., Jenuwein, T., Gilbert, D.M., Singh, P.B., and Misteli, T. (2003). Maintenance of stable heterochromatin domains by dynamic HP1 binding. Science *299*, 721-725.

Choi, V.W., Samulski, R.J., and McCarty, D.M. (2005). Effects of adeno-associated virus DNA hairpin structure on recombination. J Virol *79*, 6801-6807.

Chow, C.M., Georgiou, A., Szutorisz, H., Maia e Silva, A., Pombo, A., Barahona, I., Dargelos, E., Canzonetta, C., and Dillon, N. (2005). Variant histone H3.3 marks promoters of transcriptionally active genes during mammalian cell division. EMBO Rep *6*, 354-360.

Christine, C.W., Starr, P.A., Larson, P.S., Eberling, J.L., Jagust, W.J., Hawkins, R.A., VanBrocklin, H.F., Wright, J.F., Bankiewicz, K.S., and Aminoff, M.J. (2009). Safety and tolerability of putaminal AADC gene therapy for Parkinson disease. Neurology *73*, 1662-1669.

Cideciyan, A.V., Hauswirth, W.W., Aleman, T.S., Kaushal, S., Schwartz, S.B., Boye, S.L., Windsor, E.A., Conlon, T.J., Sumaroka, A., Pang, J.J*., et al.* (2009). Human RPE65 gene therapy for Leber congenital amaurosis: persistence of early visual improvements and safety at 1 year. Hum Gene Ther *20*, 999-1004.

Congdon, L.M., Houston, S.I., Veerappan, C.S., Spektor, T.M., and Rice, J.C. (2010). PR-Set7-mediated monomethylation of histone H4 lysine 20 at specific genomic regions induces transcriptional repression. J Cell Biochem *110*, 609-619.

DeLisle, A.J., Graves, R.A., Marzluff, W.F., and Johnson, L.F. (1983). Regulation of histone mRNA production and stability in serum-stimulated mouse 3T6 fibroblasts. Mol Cell Biol *3*, 1920-1929.

DeRan, M., Pulvino, M., Greene, E., Su, C., and Zhao, J. (2008). Transcriptional activation of histone genes requires NPAT-dependent recruitment of TRRAP-Tip60 complex to histone promoters during the G1/S phase transition. Mol Cell Biol *28*, 435-447.

Doil, C., Mailand, N., Bekker-Jensen, S., Menard, P., Larsen, D.H., Pepperkok, R., Ellenberg, J., Panier, S., Durocher, D., Bartek, J*., et al.* (2009). RNF168 binds and amplifies ubiquitin conjugates on damaged chromosomes to allow accumulation of repair proteins. Cell *136*, 435-446.

Dominski, Z., Yang, X.C., Kaygun, H., Dadlez, M., and Marzluff, W.F. (2003). A 3' exonuclease that specifically interacts with the 3' end of histone mRNA. Mol Cell *12*, 295-305.

Duchaine, T.F., Wohlschlegel, J.A., Kennedy, S., Bei, Y., Conte, D., Jr., Pang, K., Brownell, D.R., Harding, S., Mitani, S., Ruvkun, G*., et al.* (2006). Functional proteomics reveals the biochemical niche of C. elegans DCR-1 in multiple small-RNA-mediated pathways. Cell *124*, 343-354.

Dulev, S., Tkach, J., Lin, S., and Batada, N.N. (2014). SET8 methyltransferase activity during the DNA double-strand break response is required for recruitment of 53BP1. EMBO Rep.

Dutheil, N., Shi, F., Dupressoir, T., and Linden, R.M. (2000). Adeno-associated virus site-specifically integrates into a muscle-specific DNA region. Proc Natl Acad Sci U S A *97*, 4862-4866.

Faber, A.W., Van Dijk, M., Raue, H.A., and Vos, J.C. (2002). Ngl2p is a Ccr4p-like RNA nuclease essential for the final step in 3'-end processing of 5.8S rRNA in Saccharomyces cerevisiae. RNA *8*, 1095-1101.

Faucher, D., and Wellinger, R.J. (2010). Methylated H3K4, a transcription-associated histone modification, is involved in the DNA damage response pathway. PLoS Genet *6*.

Ferrari, F.K., Samulski, T., Shenk, T., and Samulski, R.J. (1996). Second-strand synthesis is a rate-limiting step for efficient transduction by recombinant adeno-associated virus vectors. J Virol *70*, 3227-3234.

Ferrari, K.J., and Pasini, D. (2013). Regulation and function of DNA and histone methylations. Curr Pharm Des *19*, 719-733.

Fragkos, M., Breuleux, M., Clement, N., and Beard, P. (2008). Recombinant adeno-associated viral vectors are deficient in provoking a DNA damage response. J Virol *82*, 7379-7387.

Fu, H., Muenzer, J., Samulski, R.J., Breese, G., Sifford, J., Zeng, X., and McCarty, D.M. (2003). Self-complementary adeno-associated virus serotype 2 vector: global distribution and broad dispersion of AAV-mediated transgene expression in mouse brain. Mol Ther *8*, 911-917.

Gabel, H.W., and Ruvkun, G. (2008). The exonuclease ERI-1 has a conserved dual role in 5.8S rRNA processing and RNAi. Nat Struct Mol Biol *15*, 531-533.

Galev, E.E., Afanas'ev, B.N., Buchatskii, L.P., Kozlov Iu, V., and Baev, A.A. (1989). [Features of the organization of the densovirus genome]. Dokl Akad Nauk SSSR *307*, 996-1000.

Gao, G., Vandenberghe, L.H., and Wilson, J.M. (2005). New recombinant serotypes of AAV vectors. Curr Gene Ther *5*, 285-297.

Gao, G.P., Alvira, M.R., Wang, L., Calcedo, R., Johnston, J., and Wilson, J.M. (2002). Novel adeno-associated viruses from rhesus monkeys as vectors for human gene therapy. Proc Natl Acad Sci U S A *99*, 11854-11859.

Gao, G.P., Qu, G., Faust, L.Z., Engdahl, R.K., Xiao, W., Hughes, J.V., Zoltick, P.W., and Wilson, J.M. (1998). High-titer adeno-associated viral vectors from a Rep/Cap cell line and hybrid shuttle virus. Hum Gene Ther *9*, 2353-2362.

Girod, A., Wobus, C.E., Zadori, Z., Ried, M., Leike, K., Tijssen, P., Kleinschmidt, J.A., and Hallek, M. (2002). The VP1 capsid protein of adeno-associated virus type 2 is carrying a phospholipase A2 domain required for virus infectivity. J Gen Virol *83*, 973-978.

Grimm, D., Kay, M.A., and Kleinschmidt, J.A. (2003). Helper virus-free, optically controllable, and two-plasmid-based production of adeno-associated virus vectors of serotypes 1 to 6. Mol Ther *7*, 839-850.

Grimm, D., Kern, A., Rittner, K., and Kleinschmidt, J.A. (1998). Novel tools for production and purification of recombinant adenoassociated virus vectors. Hum Gene Ther *9*, 2745-2760.

Guo, P., Xiao, X., El-Gohary, Y., Paredes, J., Prasadan, K., Shiota, C., Wiersch, J., Welsh, C., and Gittes, G.K. (2013). A simplified purification method for AAV variant by polyethylene glycol aqueous two-phase partitioning. Bioengineered *4*, 103-106.

Hansen, J., Qing, K., and Srivastava, A. (2001). Infection of purified nuclei by adeno-associated virus 2. Mol Ther *4*, 289-296.

Hermens, W.T., ter Brake, O., Dijkhuizen, P.A., Sonnemans, M.A., Grimm, D., Kleinschmidt, J.A., and Verhaagen, J. (1999). Purification of recombinant adeno-associated virus by iodixanol gradient ultracentrifugation allows rapid and reproducible preparation of vector stocks for gene transfer in the nervous system. Hum Gene Ther *10*, 1885-1891.

Herrero, A.B., and Moreno, S. (2011). Lsm1 promotes genomic stability by controlling histone mRNA decay. EMBO J *30*, 2008-2018.

Hershko, A., and Ciechanover, A. (1998). The ubiquitin system. Annu Rev Biochem *67*, 425-479.

High, K.H., Nathwani, A., Spencer, T., and Lillicrap, D. (2014). Current status of haemophilia gene therapy. Haemophilia *20 Suppl 4*, 43-49.

Hoefig, K.P., Rath, N., Heinz, G.A., Wolf, C., Dameris, J., Schepers, A., Kremmer, E., Ansel, K.M., and Heissmeyer, V. (2013). Eri1 degrades the stem-loop of oligouridylated histone mRNAs to induce replication-dependent decay. Nat Struct Mol Biol *20*, 73-81.

Holscher, C., Horer, M., Kleinschmidt, J.A., Zentgraf, H., Burkle, A., and Heilbronn, R. (1994). Cell lines inducibly expressing the adeno-associated virus (AAV) rep gene: requirements for productive replication of rep-negative AAV mutants. J Virol *68*, 7169-7177.

Houlard, M., Berlivet, S., Probst, A.V., Quivy, J.P., Hery, P., Almouzni, G., and Gerard, M. (2006). CAF-1 is essential for heterochromatin organization in pluripotent embryonic cells. PLoS Genet *2*, e181.

Huertas, P. (2010). DNA resection in eukaryotes: deciding how to fix the break. Nat Struct Mol Biol *17*, 11-16.

Hummon, A.B., Pitt, J.J., Camps, J., Emons, G., Skube, S.B., Huppi, K., Jones, T.L., Beissbarth, T., Kramer, F., Grade, M.*, et al.* (2012). Systems-wide RNAi analysis of CASP8AP2/FLASH shows transcriptional deregulation of the replication-dependent histone genes and extensive effects on the transcriptome of colorectal cancer cells. Mol Cancer *11*, 1.

Huser, D., Gogol-Doring, A., Chen, W., and Heilbronn, R. (2014). Adeno-Associated Virus Type 2 Wild-Type and Vector-Mediated Genomic Integration Profiles of Human Diploid Fibroblasts Analyzed by Third-Generation PacBio DNA Sequencing. J Virol *88*, 11253-11263.

Huser, D., Gogol-Doring, A., Lutter, T., Weger, S., Winter, K., Hammer, E.M., Cathomen, T., Reinert, K., and Heilbronn, R. (2010). Integration preferences of wildtype AAV-2 for consensus rep-binding sites at numerous loci in the human genome. PLoS Pathog *6*, e1000985.

Iida, T., Kawaguchi, R., and Nakayama, J. (2006). Conserved ribonuclease, Eri1, negatively regulates heterochromatin assembly in fission yeast. Curr Biol *16*, 1459-1464.

Inagaki, K., Fuess, S., Storm, T.A., Gibson, G.A., McTiernan, C.F., Kay, M.A., and Nakai, H. (2006). Robust systemic transduction with AAV9 vectors in mice: efficient global cardiac gene transfer superior to that of AAV8. Mol Ther *14*, 45-53.

Inagaki, K., Lewis, S.M., Wu, X., Ma, C., Munroe, D.J., Fuess, S., Storm, T.A., Kay, M.A., and Nakai, H. (2007). DNA palindromes with a modest arm length of greater, similar 20 base pairs are a significant target for recombinant adeno-associated virus vector integration in the liver, muscles, and heart in mice. J Virol *81*, 11290-11303.

Ito, T. (2007). Role of histone modification in chromatin dynamics. J Biochem *141*, 609-614.

Jenuwein, T., and Allis, C.D. (2001). Translating the histone code. Science *293*, 1074-1080.

Johnson, J.S., Gentzsch, M., Zhang, L., Ribeiro, C.M., Kantor, B., Kafri, T., Pickles, R.J., and Samulski, R.J. (2011). AAV exploits subcellular stress associated with inflammation, endoplasmic reticulum expansion, and misfolded proteins in models of cystic fibrosis. PLoS Pathog *7*, e1002053.

Johnson, J.S., and Samulski, R.J. (2009). Enhancement of adeno-associated virus infection by mobilizing capsids into and out of the nucleolus. J Virol *83*, 2632-2644.

Jurvansuu, J., Raj, K., Stasiak, A., and Beard, P. (2005). Viral transport of DNA damage that mimics a stalled replication fork. J Virol *79*, 569-580.

Kennedy, S., Wang, D., and Ruvkun, G. (2004). A conserved siRNA-degrading RNase negatively regulates RNA interference in C. elegans. Nature *427*, 645-649.

Kim, U.J., Han, M., Kayne, P., and Grunstein, M. (1988). Effects of histone H4 depletion on the cell cycle and transcription of Saccharomyces cerevisiae. EMBO J *7*, 2211-2219.

Komatsu, T., and Nagata, K. (2012). Replication-uncoupled histone deposition during adenovirus DNA replication. J Virol *86*, 6701-6711.

Kornberg, R.D. (1974). Chromatin structure: a repeating unit of histones and DNA. Science *184*, 868-871.

Kouzarides, T. (2000). Acetylation: a regulatory modification to rival phosphorylation? EMBO J *19*, 1176-1179.

Kronenberg, S., Kleinschmidt, J.A., and Bottcher, B. (2001). Electron cryo-microscopy and image reconstruction of adeno-associated virus type 2 empty capsids. EMBO Rep *2*, 997-1002.

Kuo, L.J., and Yang, L.X. (2008). Gamma-H2AX - a novel biomarker for DNA double-strand breaks. In Vivo *22*, 305-309.

Laughlin, C.A., Tratschin, J.D., Coon, H., and Carter, B.J. (1983). Cloning of infectious adeno-associated virus genomes in bacterial plasmids. Gene *23*, 65-73.

Leger, A., Le Guiner, C., Nickerson, M.L., McGee Im, K., Ferry, N., Moullier, P., Snyder, R.O., and Penaud-Budloo, M. (2011). Adeno-associated viral vector-mediated transgene expression is independent of DNA methylation in primate liver and skeletal muscle. PLoS One *6*, e20881.

Levine, B.J., Chodchoy, N., Marzluff, W.F., and Skoultchi, A.I. (1987). Coupling of replication type histone mRNA levels to DNA synthesis requires the stem-loop sequence at the 3' end of the mRNA. Proc Natl Acad Sci U S A *84*, 6189-6193.

Lilley, C.E., Chaurushiya, M.S., and Weitzman, M.D. (2010). Chromatin at the intersection of viral infection and DNA damage. Biochim Biophys Acta *1799*, 319-327.

Lovric, J., Mano, M., Zentilin, L., Eulalio, A., Zacchigna, S., and Giacca, M. (2012). Terminal differentiation of cardiac and skeletal myocytes induces permissivity to AAV transduction by relieving inhibition imposed by DNA damage response proteins. Mol Ther *20*, 2087-2097.

Luger, K., Mader, A.W., Richmond, R.K., Sargent, D.F., and Richmond, T.J. (1997). Crystal structure of the nucleosome core particle at 2.8 A resolution. Nature *389*, 251-260.

Lukas, J., and Bartek, J. (2009). DNA repair: New tales of an old tail. Nature *458*, 581-583.

Lyon, A.R., Bannister, M.L., Collins, T., Pearce, E., Sepehripour, A.H., Dubb, S.S., Garcia, E., O'Gara, P., Liang, L., Kohlbrenner, E.*, et al.* (2011). SERCA2a gene transfer decreases sarcoplasmic reticulum calcium leak and reduces ventricular

arrhythmias in a model of chronic heart failure. Circ Arrhythm Electrophysiol *4*, 362-372.

Mandel, R.J. (2010). CERE-110, an adeno-associated virus-based gene delivery vector expressing human nerve growth factor for the treatment of Alzheimer's disease. Curr Opin Mol Ther *12*, 240-247.

Marcello, A., Massimi, P., Banks, L., and Giacca, M. (2000). Adeno-associated virus type 2 rep protein inhibits human papillomavirus type 16 E2 recruitment of the transcriptional coactivator p300. J Virol *74*, 9090-9098.

Marcus, C.J., Laughlin, C.A., and Carter, B.J. (1981). Adeno-associated virus RNA transcription in vivo. Eur J Biochem *121*, 147-154.

Marcus-Sekura, C.J., and Carter, B.J. (1983). Chromatin-like structure of adeno-associated virus DNA in infected cells. J Virol *48*, 79-87.

Marheineke, K., and Krude, T. (1998). Nucleosome assembly activity and intracellular localization of human CAF-1 changes during the cell division cycle. J Biol Chem *273*, 15279-15286.

Martinho, R.G., Lindsay, H.D., Flaggs, G., DeMaggio, A.J., Hoekstra, M.F., Carr, A.M., and Bentley, N.J. (1998). Analysis of Rad3 and Chk1 protein kinases defines different checkpoint responses. EMBO J *17*, 7239-7249.

Marzluff, W.F., Gongidi, P., Woods, K.R., Jin, J., and Maltais, L.J. (2002). The human and mouse replication-dependent histone genes. Genomics *80*, 487-498.

Marzluff, W.F., Wagner, E.J., and Duronio, R.J. (2008). Metabolism and regulation of canonical histone mRNAs: life without a poly(A) tail. Nat Rev Genet *9*, 843-854.

McCarty, D.M., Fu, H., Monahan, P.E., Toulson, C.E., Naik, P., and Samulski, R.J. (2003). Adeno-associated virus terminal repeat (TR) mutant generates self-complementary vectors to overcome the rate-limiting step to transduction in vivo. Gene Ther *10*, 2112-2118.

McCarty, D.M., Monahan, P.E., and Samulski, R.J. (2001). Self-complementary recombinant adeno-associated virus (scAAV) vectors promote efficient transduction independently of DNA synthesis. Gene Ther *8*, 1248-1254.

McPherson, R.A., Rosenthal, L.J., and Rose, J.A. (1985). Human cytomegalovirus completely helps adeno-associated virus replication. Virology *147*, 217-222.

Mendelson, E., Trempe, J.P., and Carter, B.J. (1986). Identification of the trans-acting Rep proteins of adeno-associated virus by antibodies to a synthetic oligopeptide. J Virol *60*, 823-832.

Mietzsch, M., Grasse, S., Zurawski, C., Weger, S., Bennett, A., Agbandje-McKenna, M., Muzyczka, N., Zolotukhin, S., and Heilbronn, R. (2014). OneBac: platform for scalable and high-titer production of adeno-associated virus serotype 1-12 vectors for gene therapy. Hum Gene Ther *25*, 212-222.

Miller, D.G., Trobridge, G.D., Petek, L.M., Jacobs, M.A., Kaul, R., and Russell, D.W. (2005). Large-scale analysis of adeno-associated virus vector integration sites in normal human cells. J Virol *79*, 11434-11442.

Mizukami, H., Mimuro, J., Ogura, T., Okada, T., Urabe, M., Kume, A., Sakata, Y., and Ozawa, K. (2006). Adipose tissue as a novel target for in vivo gene transfer by adeno-associated viral vectors. Hum Gene Ther *17*, 921-928.

Mizukami, H., Young, N.S., and Brown, K.E. (1996). Adeno-associated virus type 2 binds to a 150-kilodalton cell membrane glycoprotein. Virology *217*, 124-130.

Moggs, J.G., Grandi, P., Quivy, J.P., Jonsson, Z.O., Hubscher, U., Becker, P.B., and Almouzni, G. (2000). A CAF-1-PCNA-mediated chromatin assembly pathway triggered by sensing DNA damage. Mol Cell Biol *20*, 1206-1218.

Mowry, K.L., and Steitz, J.A. (1987). Identification of the human U7 snRNP as one of several factors involved in the 3' end maturation of histone premessenger RNA's. Science *238*, 1682-1687.

Muller, B., Blackburn, J., Feijoo, C., Zhao, X., and Smythe, C. (2007). DNA-activated protein kinase functions in a newly observed S phase checkpoint that links histone mRNA abundance with DNA replication. J Cell Biol *179*, 1385-1398.

Muramatsu, S., Fujimoto, K., Kato, S., Mizukami, H., Asari, S., Ikeguchi, K., Kawakami, T., Urabe, M., Kume, A., Sato, T.*, et al.* (2010). A phase I study of aromatic L-amino acid decarboxylase gene therapy for Parkinson's disease. Mol Ther *18*, 1731-1735.

Murphy, J.C., Fischle, W., Verdin, E., and Sinclair, J.H. (2002). Control of cytomegalovirus lytic gene expression by histone acetylation. EMBO J *21*, 1112-1120.

Murr, R., Loizou, J.I., Yang, Y.G., Cuenin, C., Li, H., Wang, Z.Q., and Herceg, Z. (2006). Histone acetylation by Trrap-Tip60 modulates loading of repair proteins and repair of DNA double-strand breaks. Nat Cell Biol *8*, 91-99.

Murray, K. (1964). The Occurrence of Epsilon-N-Methyl Lysine in Histones. Biochemistry *3*, 10-15.

Nakai, H., Storm, T.A., and Kay, M.A. (2000). Recruitment of single-stranded recombinant adeno-associated virus vector genomes and intermolecular recombination are responsible for stable transduction of liver in vivo. J Virol *74*, 9451-9463.

Nicolson, S.C., and Samulski, R.J. (2014). Recombinant adeno-associated virus utilizes host cell nuclear import machinery to enter the nucleus. J Virol *88*, 4132-4144.

Nonnenmacher, M., and Weber, T. (2012). Intracellular transport of recombinant adeno-associated virus vectors. Gene Ther *19*, 649-658.

Ogiwara, H., Ui, A., Otsuka, A., Satoh, H., Yokomi, I., Nakajima, S., Yasui, A., Yokota, J., and Kohno, T. (2011). Histone acetylation by CBP and p300 at double-strand break sites facilitates SWI/SNF chromatin remodeling and the recruitment of non-homologous end joining factors. Oncogene *30*, 2135-2146.

Ohashi, K., Nakai, H., Couto, L.B., and Kay, M.A. (2005). Modified infusion procedures affect recombinant adeno-associated virus vector type 2 transduction in the liver. Hum Gene Ther *16*, 299-306.

Okada, T., Uchibori, R., Iwata-Okada, M., Takahashi, M., Nomoto, T., Nonaka-Sarukawa, M., Ito, T., Liu, Y., Mizukami, H., Kume, A.*, et al.* (2006). A histone

deacetylase inhibitor enhances recombinant adeno-associated virus-mediated gene expression in tumor cells. Mol Ther *13*, 738-746.

Osley, M.A. (1991). The regulation of histone synthesis in the cell cycle. Annu Rev Biochem *60*, 827-861.

Pai, C.C., Deegan, R.S., Subramanian, L., Gal, C., Sarkar, S., Blaikley, E.J., Walker, C., Hulme, L., Bernhard, E., Codlin, S.*, et al.* (2014). A histone H3K36 chromatin switch coordinates DNA double-strand break repair pathway choice. Nat Commun *5*, 4091.

Paull, T.T., and Lee, J.H. (2005). The Mre11/Rad50/Nbs1 complex and its role as a DNA double-strand break sensor for ATM. Cell Cycle *4*, 737-740.

Pei, H., Zhang, L., Luo, K., Qin, Y., Chesi, M., Fei, F., Bergsagel, P.L., Wang, L., You, Z., and Lou, Z. (2011). MMSET regulates histone H4K20 methylation and 53BP1 accumulation at DNA damage sites. Nature *470*, 124-128.

Penaud-Budloo, M., Le Guiner, C., Nowrouzi, A., Toromanoff, A., Cherel, Y., Chenuaud, P., Schmidt, M., von Kalle, C., Rolling, F., Moullier, P.*, et al.* (2008). Adeno-associated virus vector genomes persist as episomal chromatin in primate muscle. J Virol *82*, 7875-7885.

Petersen-Jones, S.M., Bartoe, J.T., Fischer, A.J., Scott, M., Boye, S.L., Chiodo, V., and Hauswirth, W.W. (2009). AAV retinal transduction in a large animal model species: comparison of a self-complementary AAV2/5 with a single-stranded AAV2/5 vector. Mol Vis *15*, 1835-1842.

Pina, B., and Suau, P. (1987). Changes in histones H2A and H3 variant composition in differentiating and mature rat brain cortical neurons. Dev Biol *123*, 51-58.

Polo, S.E., Roche, D., and Almouzni, G. (2006). New histone incorporation marks sites of UV repair in human cells. Cell *127*, 481-493.

Povirk, L.F. (2012). Processing of damaged DNA ends for double-strand break repair in mammalian cells. ISRN Mol Biol *2012*.

Prado, F., and Aguilera, A. (2005). Partial depletion of histone H4 increases homologous recombination-mediated genetic instability. Mol Cell Biol *25*, 1526-1536.

Qing, Y., Yamazoe, M., Hirota, K., Dejsuphong, D., Sakai, W., Yamamoto, K.N., Bishop, D.K., Wu, X., and Takeda, S. (2011). The epistatic relationship between BRCA2 and the other RAD51 mediators in homologous recombination. PLoS Genet *7*, e1002148.

Quanz, M., Berthault, N., Roulin, C., Roy, M., Herbette, A., Agrario, C., Alberti, C., Josserand, V., Coll, J.L., Sastre-Garau, X.*, et al.* (2009). Small-molecule drugs mimicking DNA damage: a new strategy for sensitizing tumors to radiotherapy. Clin Cancer Res *15*, 1308-1316.

Quivy, J.P., Grandi, P., and Almouzni, G. (2001). Dimerization of the largest subunit of chromatin assembly factor 1: importance in vitro and during Xenopus early development. EMBO J *20*, 2015-2027.

Quivy, V., Adam, E., Collette, Y., Demonte, D., Chariot, A., Vanhulle, C., Berkhout, B., Castellano, R., de Launoit, Y., Burny, A.*, et al.* (2002). Synergistic activation of human immunodeficiency virus type 1 promoter activity by NF-kappaB and inhibitors of deacetylases: potential perspectives for the development of therapeutic strategies. J Virol *76*, 11091-11103.

Riu, E., Chen, Z.Y., Xu, H., He, C.Y., and Kay, M.A. (2007). Histone modifications are associated with the persistence or silencing of vector-mediated transgene expression in vivo. Mol Ther *15*, 1348-1355.

Rodino-Klapac, L.R., Chicoine, L.G., Kaspar, B.K., and Mendell, J.R. (2007). Gene therapy for duchenne muscular dystrophy: expectations and challenges. Arch Neurol *64*, 1236-1241.

Rogakou, E.P., Boon, C., Redon, C., and Bonner, W.M. (1999). Megabase chromatin domains involved in DNA double-strand breaks in vivo. J Cell Biol *146*, 905-916.

Rogakou, E.P., Pilch, D.R., Orr, A.H., Ivanova, V.S., and Bonner, W.M. (1998). DNA double-stranded breaks induce histone H2AX phosphorylation on serine 139. J Biol Chem *273*, 5858-5868.

Ross, P.J., Kennedy, M.A., Christou, C., Risco Quiroz, M., Poulin, K.L., and Parks, R.J. (2011). Assembly of helper-dependent adenovirus DNA into chromatin promotes efficient gene expression. J Virol *85*, 3950-3958.

Russell, D.W., Alexander, I.E., and Miller, A.D. (1995). DNA synthesis and topoisomerase inhibitors increase transduction by adeno-associated virus vectors. Proc Natl Acad Sci U S A *92*, 5719-5723.

Salmon, F., Grosios, K., and Petry, H. (2014). Safety profile of recombinant adeno-associated viral vectors: focus on alipogene tiparvovec (Glybera(R)). Expert Rev Clin Pharmacol *7*, 53-65.

Samulski, R.J., Berns, K.I., Tan, M., and Muzyczka, N. (1982). Cloning of adeno-associated virus into pBR322: rescue of intact virus from the recombinant plasmid in human cells. Proc Natl Acad Sci U S A *79*, 2077-2081.

Sartori, A.A., Lukas, C., Coates, J., Mistrik, M., Fu, S., Bartek, J., Baer, R., Lukas, J., and Jackson, S.P. (2007). Human CtIP promotes DNA end resection. Nature *450*, 509-514.

Schaffner, W., Kunz, G., Daetwyler, H., Telford, J., Smith, H.O., and Birnstiel, M.L. (1978). Genes and spacers of cloned sea urchin histone DNA analyzed by sequencing. Cell *14*, 655-671.

Schneiderman, J.I., Orsi, G.A., Hughes, K.T., Loppin, B., and Ahmad, K. (2012). Nucleosome-depleted chromatin gaps recruit assembly factors for the H3.3 histone variant. Proc Natl Acad Sci U S A *109*, 19721-19726.

Schwartz, R.A., Carson, C.T., Schuberth, C., and Weitzman, M.D. (2009). Adeno-associated virus replication induces a DNA damage response coordinated by DNA-dependent protein kinase. J Virol *83*, 6269-6278.

Schwartz, R.A., Palacios, J.A., Cassell, G.D., Adam, S., Giacca, M., and Weitzman, M.D. (2007). The Mre11/Rad50/Nbs1 complex limits adeno-associated virus transduction and replication. J Virol *81*, 12936-12945.

Seisenberger, G., Ried, M.U., Endress, T., Buning, H., Hallek, M., and Brauchle, C. (2001). Real-time single-molecule imaging of the infection pathway of an adeno-associated virus. Science *294*, 1929-1932.

Senapathy, P., and Carter, B.J. (1984). Molecular cloning of adeno-associated virus variant genomes and generation of infectious virus by recombination in mammalian cells. J Biol Chem *259*, 4661-4666.

Senapathy, P., Tratschin, J.D., and Carter, B.J. (1984). Replication of adeno-associated virus DNA. Complementation of naturally occurring rep- mutants by a wild-type genome or an ori- mutant and correction of terminal palindrome deletions. J Mol Biol *179*, 1-20.

Sheridan, C. (2011). Gene therapy finds its niche. Nat Biotechnol *29*, 121-128.

Shrader, T.E., and Crothers, D.M. (1990). Effects of DNA sequence and histone-histone interactions on nucleosome placement. J Mol Biol *216*, 69-84.

Siegl, G., Bates, R.C., Berns, K.I., Carter, B.J., Kelly, D.C., Kurstak, E., and Tattersall, P. (1985). Characteristics and taxonomy of Parvoviridae. Intervirology *23*, 61-73.

Simonelli, F., Maguire, A.M., Testa, F., Pierce, E.A., Mingozzi, F., Bennicelli, J.L., Rossi, S., Marshall, K., Banfi, S., Surace, E.M.*, et al.* (2010). Gene therapy for Leber's congenital amaurosis is safe and effective through 1.5 years after vector administration. Mol Ther *18*, 643-650.

Singh, R.K., Liang, D., Gajjalaiahvari, U.R., Kabbaj, M.H., Paik, J., and Gunjan, A. (2010). Excess histone levels mediate cytotoxicity via multiple mechanisms. Cell Cycle *9*, 4236-4244.

Sittman, D.B., Graves, R.A., and Marzluff, W.F. (1983). Histone mRNA concentrations are regulated at the level of transcription and mRNA degradation. Proc Natl Acad Sci U S A *80*, 1849-1853.

Smith, S., and Stillman, B. (1991). Stepwise assembly of chromatin during DNA replication in vitro. EMBO J *10*, 971-980.

Sonntag, F., Bleker, S., Leuchs, B., Fischer, R., and Kleinschmidt, J.A. (2006). Adeno-associated virus type 2 capsids with externalized VP1/VP2 trafficking domains are generated prior to passage through the cytoplasm and are maintained until uncoating occurs in the nucleus. J Virol *80*, 11040-11054.

Sonntag, F., Schmidt, K., and Kleinschmidt, J.A. (2010). A viral assembly factor promotes AAV2 capsid formation in the nucleolus. Proc Natl Acad Sci U S A *107*, 10220-10225.

Su, C., Gao, G., Schneider, S., Helt, C., Weiss, C., O'Reilly, M.A., Bohmann, D., and Zhao, J. (2004). DNA damage induces downregulation of histone gene expression through the G1 checkpoint pathway. EMBO J *23*, 1133-1143.

Summerford, C., Bartlett, J.S., and Samulski, R.J. (1999). AlphaVbeta5 integrin: a co-receptor for adeno-associated virus type 2 infection. Nat Med *5*, 78-82.

Summerford, C., and Samulski, R.J. (1998). Membrane-associated heparan sulfate proteoglycan is a receptor for adeno-associated virus type 2 virions. J Virol *72*, 1438-1445.

Symington, L.S., and Gautier, J. (2011). Double-strand break end resection and repair pathway choice. Annu Rev Genet *45*, 247-271.

Tagami, H., Ray-Gallet, D., Almouzni, G., and Nakatani, Y. (2004). Histone H3.1 and H3.3 complexes mediate nucleosome assembly pathways dependent or independent of DNA synthesis. Cell *116*, 51-61.

Tan, D., Marzluff, W.F., Dominski, Z., and Tong, L. (2013). Structure of histone mRNA stem-loop, human stem-loop binding protein, and 3'hExo ternary complex. Science *339*, 318-321.

Teif, V.B., and Rippe, K. (2009). Predicting nucleosome positions on the DNA: combining intrinsic sequence preferences and remodeler activities. Nucleic Acids Res *37*, 5641-5655.

Thomas, M.F., Abdul-Wajid, S., Panduro, M., Babiarz, J.E., Rajaram, M., Woodruff, P., Lanier, L.L., Heissmeyer, V., and Ansel, K.M. (2012). Eri1 regulates microRNA homeostasis and mouse lymphocyte development and antiviral function. Blood *120*, 130-142.

Trempe, J.P., and Carter, B.J. (1988). Regulation of adeno-associated virus gene expression in 293 cells: control of mRNA abundance and translation. J Virol *62*, 68-74.

Trievel, R.C., Beach, B.M., Dirk, L.M., Houtz, R.L., and Hurley, J.H. (2002). Structure and catalytic mechanism of a SET domain protein methyltransferase. Cell *111*, 91-103.

Walworth, N.C., and Bernards, R. (1996). rad-dependent response of the chk1-encoded protein kinase at the DNA damage checkpoint. Science *271*, 353-356.

Wu, Z., Sun, J., Zhang, T., Yin, C., Yin, F., Van Dyke, T., Samulski, R.J., and Monahan, P.E. (2008). Optimization of self-complementary AAV vectors for liver-directed expression results in sustained correction of hemophilia B at low vector dose. Mol Ther *16*, 280-289.

Wunsch, A.M., and Lough, J. (1987). Modulation of histone H3 variant synthesis during the myoblast-myotube transition of chicken myogenesis. Dev Biol *119*, 94-99.

Xiao, W., Warrington, K.H., Jr., Hearing, P., Hughes, J., and Muzyczka, N. (2002). Adenovirus-facilitated nuclear translocation of adeno-associated virus type 2. J Virol *76*, 11505-11517.

Yakobson, B., Hrynko, T.A., Peak, M.J., and Winocour, E. (1989). Replication of adeno-associated virus in cells irradiated with UV light at 254 nm. J Virol *63*, 1023-1030.

Yalkinoglu, A.O., Heilbronn, R., Burkle, A., Schlehofer, J.R., and zur Hausen, H. (1988). DNA amplification of adeno-associated virus as a response to cellular genotoxic stress. Cancer Res *48*, 3123-3129.

Yan, Z., Zak, R., Luxton, G.W., Ritchie, T.C., Bantel-Schaal, U., and Engelhardt, J.F. (2002). Ubiquitination of both adeno-associated virus type 2 and 5 capsid proteins affects the transduction efficiency of recombinant vectors. J Virol *76*, 2043-2053.

Yan, Z., Zak, R., Zhang, Y., Ding, W., Godwin, S., Munson, K., Peluso, R., and Engelhardt, J.F. (2004). Distinct classes of proteasome-modulating agents cooperatively augment recombinant adeno-associated virus type 2 and type 5-mediated transduction from the apical surfaces of human airway epithelia. J Virol *78*, 2863-2874.

Yang, X.C., Purdy, M., Marzluff, W.F., and Dominski, Z. (2006). Characterization of 3'hExo, a 3' exonuclease specifically interacting with the 3' end of histone mRNA. J Biol Chem *281*, 30447-30454.

Ylisastigui, L., Coull, J.J., Rucker, V.C., Melander, C., Bosch, R.J., Brodie, S.J., Corey, L., Sodora, D.L., Dervan, P.B., and Margolis, D.M. (2004). Polyamides reveal a role for repression in latency within resting T cells of HIV-infected donors. J Infect Dis *190*, 1429-1437.

Zabner, J., Seiler, M., Walters, R., Kotin, R.M., Fulgeras, W., Davidson, B.L., and Chiorini, J.A. (2000). Adeno-associated virus type 5 (AAV5) but not AAV2 binds to the apical surfaces of airway epithelia and facilitates gene transfer. J Virol *74*, 3852-3858.

Zentilin, L., Marcello, A., and Giacca, M. (2001). Involvement of cellular double-stranded DNA break binding proteins in processing of the recombinant adeno-associated virus genome. J Virol *75*, 12279-12287.

Zhao, G.Y., Sonoda, E., Barber, L.J., Oka, H., Murakawa, Y., Yamada, K., Ikura, T., Wang, X., Kobayashi, M., Yamamoto, K.*, et al.* (2007). A critical role for the ubiquitin-conjugating enzyme Ubc13 in initiating homologous recombination. Mol Cell *25*, 663-675.

Zhao, J. (2004). Coordination of DNA synthesis and histone gene expression during normal cell cycle progression and after DNA damage. Cell Cycle *3*, 695-697.

Zhou, M., Deng, L., Lacoste, V., Park, H.U., Pumfery, A., Kashanchi, F., Brady, J.N., and Kumar, A. (2004). Coordination of transcription factor phosphorylation and histone methylation by the P-TEFb kinase during human immunodeficiency virus type 1 transcription. J Virol *78*, 13522-13533.

Zhou, X., Zeng, X., Fan, Z., Li, C., McCown, T., Samulski, R.J., and Xiao, X. (2008). Adeno-associated virus of a single-polarity DNA genome is capable of transduction in vivo. Mol Ther *16*, 494-499.

Ziv, Y., Bielopolski, D., Galanty, Y., Lukas, C., Taya, Y., Schultz, D.C., Lukas, J., Bekker-Jensen, S., Bartek, J., and Shiloh, Y. (2006). Chromatin relaxation in response to DNA double-strand breaks is modulated by a novel ATM- and KAP-1 dependent pathway. Nat Cell Biol *8*, 870-876.

Zolotukhin, S., Potter, M., Zolotukhin, I., Sakai, Y., Loiler, S., Fraites, T.J., Jr., Chiodo, V.A., Phillipsberg, T., Muzyczka, N., Hauswirth, W.W*., et al*. (2002). Production and purification of serotype 1, 2, and 5 recombinant adeno-associated viral vectors. Methods *28*, 158-167.

Zuo, Y., and Deutscher, M.P. (2001). Exoribonuclease superfamilies: structural analysis and phylogenetic distribution. Nucleic Acids Res *29*, 1017-1026.

7. Ringraziamenti

E' mia intenzione esprimere un sentimento di profonda riconoscenza e gratitudine nei confronti di tutte quelle persone che hanno contribuito direttamente ed indirettamente alla mia crescita scientifica e personale. Durante questo dottorato ho capito che non avrei cambiato il mondo con la mia ricerca, almeno non quanto avrei voluto quando mi presentai, all'esame di ammissione della Normale di Pisa, da semplice laureato in Biologia Molecolare. Ho ricevuto un grande dono in questi sei anni : una maggiore consapevolezza della complessità del mondo scientifico ed una conseguente voglia di mettermi in gioco con gli strumenti acquisiti. Prodotti che non hanno ne un prezzo ne un "impact factor". Ringrazio in primis la mia famiglia che ha sempre creduto in me. Mia madre che, oltre ad avermi insegnato a parlare in italiano, ha saputo, con estrema sensibilità e pazienza, accompagnarmi fino ad oggi. Ringrazio mio padre per aver stimolato in me, fin da bambino, curiosità e senso critico. Ringrazio mio cugino Joe per avermi iniziato alla carriera scientifica: è stato per me un modello ed un mentore. Ci sono poi persone che non si possono dimenticare. Ognuno di noi è parzialmente artefice non solo della propria vita ma anche del destino altrui. Nel primo anno di studi a Pisa incontrai, durante un corso, il Prof. Mauro Giacca e fui letteralmente folgorato dal suo acume scientifico. Desideravo fare ricerca sulla terapia genica e non mi feci offrire due volte la possibilità di fare scienza con lui nel suo prestigioso laboratorio. Grazie Mauro. Ringrazio Arturo Falaschi, ormai scomparso. Dolce è il ricordo del suo sorriso e vivida in me l'immagine della sua nitidezza scientifica; a lui sono grato per la fiducia che ripose in me, quando mi ammise all'esame di Perfezionamento della Normale Superiore di Pisa. E ancora, devo a lui il nullaosta che mi ha permesso di trasferirmi a Trieste. Ringrazio la mia ragazza, Laura, ed in miei migliori amici che oltre ad avermi saputo trasmettere affetto mi sono stati vicini nei momenti di maggiore difficoltà e bisogno. Un caloroso grazie a Lorena Zentilin ed a tutte le persone del laboratorio di Molecular Medicine che hanno contribuito alla mia formazione. Non posso che raccomandare a tutti di cercare di realizzare i propri

sogni: se qualcuno non dovesse riuscirci almeno non potrà mai avere il rimpianto di non averci provato.

Rudy Ippodrino